National Library of Canada
Acquisitions and Bibliographic Services Branch
395 Wellington Street
Ottawa, Ontario
K1A 0N4

Bibliothèque nationale du Canada
Direction des acquisitions et des services bibliographiques
395, rue Wellington
Ottawa (Ontario)
K1A 0N4

Your file Votre référence

Our file Notre référence

NOTICE

The quality of this microform is heavily dependent upon the quality of the original thesis submitted for microfilming. Every effort has been made to ensure the highest quality of reproduction possible.

If pages are missing, contact the university which granted the degree.

Some pages may have indistinct print especially if the original pages were typed with a poor typewriter ribbon or if the university sent us an inferior photocopy.

Reproduction in full or in part of this microform is governed by the Canadian Copyright Act, R.S.C. 1970, c. C-30, and subsequent amendments.

AVIS

La qualité de cette microforme dépend grandement de la qualité de la thèse soumise au microfilmage. Nous avons tout fait pour assurer une qualité supérieure de reproduction.

S'il manque des pages, veuillez communiquer avec l'université qui a conféré le grade.

La qualité d'impression de certaines pages peut laisser à désirer, surtout si les pages originales ont été dactylographiées à l'aide d'un ruban usé ou si l'université nous a fait parvenir une photocopie de qualité inférieure.

La reproduction, même partielle, de cette microforme est soumise à la Loi canadienne sur le droit d'auteur, SRC 1970, c. C-30, et ses amendements subséquents.

Canada

UNIVERSITY OF ALBERTA

LASER IONIZATION METHODS FOR LIQUID CHROMATOGRAPHY DETECTION

BY

XI-JIAN GUO

A thesis submitted to the Faculty of Graduate Studies and Research in partial fulfillment of the requirements for the degree of Master of Science.

DEPARTMENT OF CHEMISTRY

EDMONTON, ALBERTA

Fall 1994

National Library of Canada

Acquisitions and Bibliographic Services Branch

395 Wellington Street
Ottawa, Ontario
K1A 0N4

Bibliothèque nationale du Canada

Direction des acquisitions et des services bibliographiques

395, rue Wellington
Ottawa (Ontario)
K1A 0N4

Your file Votre référence

Our file Notre référence

The author has granted an irrevocable non-exclusive licence allowing the National Library of Canada to reproduce, loan, distribute or sell copies of his/her thesis by any means and in any form or format, making this thesis available to interested persons.

L'auteur a accordé une licence irrévocable et non exclusive permettant à la Bibliothèque nationale du Canada de reproduire, prêter, distribuer ou vendre des copies de sa thèse de quelque manière et sous quelque forme que ce soit pour mettre des exemplaires de cette thèse à la disposition des personnes intéressées.

The author retains ownership of the copyright in his/her thesis. Neither the thesis nor substantial extracts from it may be printed or otherwise reproduced without his/her permission.

L'auteur conserve la propriété du droit d'auteur qui protège sa thèse. Ni la thèse ni des extraits substantiels de celle-ci ne doivent être imprimés ou autrement reproduits sans son autorisation.

ISBN 0-315-95040-4

Canada

UNIVERSITY OF ALBERTA

RELEASE FORM

NAME OF AUTHOR: XI-JIAN GUO

TITLE OF THESIS: LASER IONIZATION METHODS FOR LIQUID CHROMATOGRAPHY DETECTION

DEGREE: MASTER OF SCIENCE

YEAR THIS DEGREE GRANTED: 1994

Permission is hereby granted to the University of Alberta Library to reproduce single copies of this thesis and to lend or sell such copies for private, scholarly or scientific research purposes only.

The author reserves all other publication and other rights in association with the copyright in the thesis, and except as hereinbefore provided neither the thesis nor any substantial portion thereof may be printed or otherwise reproduced in any material form whatever without the author's written permission.

Guo Xijian

202, 10716--80 AVE,
Edmonton, Alberta,
Canada T6E 1V8

Aug. 31, 1994

UNIVERSITY OF ALBERTA

FACULTY OF GRADUATE STUDIES AND RESEARCH

The undersigned certify that they have read, and recommend to the Faculty of Graduate Studies and Research for acceptance, a thesis entitled LASER IONIZATION METHODS FOR LIQUID CHROMATOGRAPHY DETECTION submitted by XI-JIAN GUO in partial fulfillment of the requirements for the degree MASTER of SCIENCE in ANALYTICAL CHEMISTRY.

Dr. Liang Li,
Associate Professor, Chemistry

Dr. Norman Dovichi,
Professor, Chemistry

Dr. Yongsheng Feng,
Assistant Professor, Soil Science

This work is dedicated to my wife, my parents, and my sisters. Without their full support throughout the years, I would not have been able to go so far.

ABSTRACT

Multiphoton ionization (MPI) mass spectrometry has been shown to be a powerful technique for chemical detection and structural analysis. In this technique, an intense laser beam is used to ionize sample molecules and the resulting ions are usually detected by a time-of-flight mass spectrometer (TOFMS).

In the analysis of thermally labile and nonvolatile molecules in complex matrices, the combination of liquid chromatography (LC) with mass spectrometry is normally used to obtain molecular and structural information. By combining MPI technique with a TOFMS, a highly selective and sensitive detector for LC is available for the detection of thermally labile and nonvolatile compounds in complex mixtures.

This thesis consists of two parts. In Part I, interfacing conventional high performance liquid chromatography (HPLC) with time-of-flight mass spectrometry with a pulsed sample introduction (PSI) interface is reported. The construction of the PSI interface is outlined and the performance of the PSI interface in terms of its applicability, reproducibility, sensitivity is examined. The ion chromatogram obtained by using our HPLC/TOFMS system is similar to that obtained with a LC-UV detector. No significant peak distortion is introduced by the PSI interface. Various experimental parameters affecting the performance of the HPLC/TOFMS system are investigated. It is shown that the PSI-HPLC/TOFMS system can handle liquid flow rates ranging from 0.5 mL/min to 1.6 mL/min. Water and various organic solvents can be used as the mobile phase. Volatile buffers and solvent modifiers can also be used. Several other parameters affecting the system performance, including the temperature of the sample vaporizer and the capillary tube in the interface, as well as the flow rate of the makeup gas, are also investigated. In addition, the effective sample transfer efficiency of the PSI interface is

studied. Finally, several examples of real applications by the PSI-HPLC/TOFMS system are given to illustrate its capability. The advantages and limitations of the PSI interface in comparison with other interfacing techniques are briefly discussed.

In part II, the analytical applicability of laser-induced photoelectric effects in membranes is studied. Our preliminary results show that this technique can be used for analytical purposes. UV light flashes induce photovoltage transients across the Teflon membrane by ionizing absorbed molecules, such as aromatic amino acids. Important factors affecting the photovoltage amplitude are also investigated. The major drawback of the technique is its high detection limit. Future improvements are suggested to overcome the problem.

Acknowledgments

I would like to take this opportunity to thank Professor Liang Li for his guidance, inspiration and encouragement throughout this work. Without his enormous and patient efforts, this work would not have been possible.

I also wish to thank the members of my thesis committee, Professor Norman Dovichi, and Professor Yongsheng Feng, for their thorough review and proofreading of this thesis.

I must thank the members of our research group, Alan P.L. Wang, Davinder S. Nagra, and Jianyun Zhang for the many discussions and cooperation we had during the past years. It has been a great and wonderful experience for me to have worked with them.

I also thank all the personnel in the machine shop and the electronics shop for their excellent and skillful job on building the pulsed sample introduction interface as well as other technical work.

Finally, I wish acknowledge the Department of Chemistry, University of Alberta, the Natural Science and Engineering Research Council of Canada for funding this work.

Table of Contents

Part I Liquid Chromatography/Time-of-Flight Mass Spectrometry with a Pulsed Sample Introduction (PSI) Interface

Chapter

1. Introduction 1
   - 1.1. Multiphoton Ionization 2
   - 1.2. LC/MS Interfacing 7
   - 1.3. Time-of-Flight Mass Spectrometer as a LC Detector 12
2. Experimental 15
   - 2.1 Liquid Chromatography 15
   - 2.2 Pulsed Sample Introduction Interface 15
   - 2.3 Time-of-Flight Mass Spectrometer 19
   - 2.4 Data System 20
   - 2.5 Materials and Reagents 28
3. Results and Discussion 29
   - 3.1 Applicability of the PSI Interface 29
   - 3.2 Background Reduction 32
   - 3.3 Performance of the LC/TOFMS system 36
   - 3.4 Parameters affecting the LC/TOFMS Performance 38
   - 3.5 Sample Transfer Efficiency in the PSI Interface 51
   - 3.6 Applications of the LC/TOFMS System 58
4. Conclusion and Future Work 76

Part II Analytical Applicability of Laser-Induced Photoelectric Effects in Teflon Membrane

Chapter

5. Introduction 80

5.1. Laser Ionization in Solution 80

5.2. Photo-Electric Effects 81

5.3. Research Goal 85

6. Experimental 87

7. Results and Discussion 90

7.1. Teflon Membrane Generated Waveforms 90

7.2. Important Factors affecting the photovoltage in Teflon Membrane 90

8. Conclusion and Future Work 101

Bibliography 103

List of Tables

Table		Page
1.1	LC/MS interfaces	10
1.2	Characteristics of the most widely used LC/MS interfaces	11
3.1	Compounds studied by MPI mass spectrometry with the PSI interface	30
3.2	Sample transfer efficiency of the pulsed sample introduction interface	54

List of Figures

Figure		Page
1.1.	Energy level diagram in MPI transitions: (a) Nonresonant MPI, (b) Resonant two-photon ionization (R2PI), (c)Two-photon resonant ionization MPI.	4
1.2.	Ladder switching mechanism.	6
2.1.	Schematic diagram of the experimental set-up of HPLC/TOFMS with a PSI interface.	16
2.2.	Schematic of the design of the pulsed sample introduction interface. Drawing is not to scale. The dimensions of the major components are given in the text.	17
2.3.	The setup panel of the control panels of the data acquisition system.	22
2.4.	The run panel of the control panels of the data acquisition system.	24
2.5.	The analysis panel of the control panels of the data acquisition system.	26
3.1.	MPI mass spectra of (A) triphenylene, (B) 4-hydroxyl-3-methoxyphenyl-acetic acid, (C) 4-acetaminophenol, and (D) imipramine. The ionization laser beam is at 266 nm with its power density about 1 x 10^6 W/cm^2.	33
3.2.	MPI mass spectra of (A) background, (B) aniline with background, trap filled. The ionization laser beam is at 266 nm with its power density about 2 x 10^6 W/cm^2.	35
3.3.	(A) LC/UV chromatogram, and (B) total ion chromatogram of a mixture of phenanthrene (peak 1) and 9-bromophenanthrene (peak 2).	37
3.4.	Flowgrams for repeated injections of different concentrations of caffeine.	38
3.5.	Mobile phase flow rate dependence on the performance of the PSI interface. Indole-3-acetic acid (1μg per injection) is used as the test sample. Methanol is used as mobile phase.	40

3.6. Scaled peak area as a function of the water content in the methanol/water mobile phase. The flow rate is kept constant at 1 mL/min. 42

3.7. Peak area as a function of the temperature of the sample vaporizer. Indole-3-acetic acid is used as the test sample. Methanol is used as the mobile phase at a flow rate of 1 mL/min. 44

3.8. Peak area as a function of the temperature of the capillary tube. The LC conditions are the same as those used in Figure 3.7. 46

3.9. Peak area as a function of the makeup gas flow rate. The LC conditions are the same as those used in Figure 3.7. 47

3.10. Signal to noise ratio of the first peak in the ion chromatogram in Figure 3.3 (B) as a function of the repetition rate of the experiment in the PSI-LC/TOFMS. 49

3.11. MPI mass spectra of Indole-3-acetic acid at different delay time: (A) Δt=660 μs, (B) Δt=540 μs. The ionization laser beam is at 266 nm with its power density about 4 x 10^6 W/cm^2. 51

3.12. A typical peak obtained by the LC/TOFMS system. The dot line is the experimental results from the injection of indole-3-acetic acid. the solid line is generated from the curve fitting program. 56

3.13. Multiphoton ionization mass spectrum of aniline obtained by using the PSI interface with a total injection of 20 pg of the sample. Methanol is used as the mobile phase at a flow rate of 1 mL/min. Laser ionization is performed at 266 nm with a laser power density of ~ 5x10^6 W/cm^2. 58

3.14. (A) LC/UV chromatogram, and (B) LC/TOFMS ion chromatogram of a mixture of indoles (10 ng each): (1) 5-hydroxytryptamine (serotonine), (2) tryptamine, (3) melatonin, and (4) tryptophol. 59

3.15. MPI mass spectra of indoles at the peaks corresponding to the ion

shown in Figure 3.14 (B): (A) 5-hydroxytryptamine (serotonine); (B) tryptamine; (C) melatonin; and (D) tryptophol. The laser ionization is performed at 266 nm with a laser power density of ~ $5x10^6$ W/cm^2. 61

3.16. (A) LC/UV chromatogram, and (B) LC/TOFMS ion chromatogram of a mixture of four dipeptides: (1) Tyr-GLy (400 ng), (2) Gly-Trp (200 ng), (3) Leu-Trp (200 ng), and (4) Trp-Leu (200 ng). 63

3.17. MPI mass spectra of (A) Tyr-Gly (MW=317), (B) Gly-Trp (MW=261), (C) Leu-Trp (MW=317), and (D) Trp-Leu (MW=317). The ionization laser beam is at 266 nm with its power density about 5 x 10^6 W/cm^2. 64

3.18. (A) LC/UV chromatogram, and (B) LC/TOFMS ion chromatogram of a mixture of seven PAHs. 67

3.19. (A) The selected ion chromatogram of acenaphthene, and (B) The selected ion chromatogram of fluorene. 69

3.20. MPI mass spectra of acenaphthene and fluorene. 70

3.21. (A) LC/UV chromatogram, and (B) LC/TOFMS ion chromatogram of instant coffee. 71

3.22. MPI mass spectra of pure caffeine, and caffeine in instant coffee. 72

3.23. The calibration curve of caffeine by LC/UV. 73

3.24. The calibration curve of caffeine by LC/TOFMS. 75

5.1. Photoelectric effects in membranes 82

5.2. A simple parallel-plate capacitor model of a bilayer membrane, in which electric charges displaced within the dielectric alter thetransmembrane voltage. Thses voltage variations are detected by an electrometer. The positive charge movements illustrated here, from point #1 to 2, and either on to 3 or back to1, produce the voltage variations illustrated, which

are also discussed in the text. 83

6.1. The schematic of the experimental set-up used to obtain photoelectric effects from the Teflon membrane. 88

7.1. Typical photovoltage waveforms induced by Tryptophan, Tyrosine, and UV light flashes on Teflon membrane. (a) 10 mM NaCl noise trace. (osilloscope was set at 1.0 mV/0.1 ms per division). (b) 10 mM tryptophan. (c) 20 mM tyrosine. 91

7.2. A log-log plot of the photovoltage amplitude (mV) vs salt concentration for the Teflon membrane with 10 mM Trp. 92

7.3. The log-log plot of the photovoltage amplitude of 10 mM Trp in 0.1 mM NaCl inside cell vs the NaCl concentration outside the membrane cell. 94

7.4. A log-log plot of the photovoltage amplitude vs Trp concentration in 10 mM NaCl. 95

7.5. The photovoltage amplitude (mV) vs laser power (mW) for 20 μM Trp in 10 mM NaCl. 97

7.6. A log-log plot of the signal intensity vs the laser intensity (mW) for 20 mM Trp in 10 mM NaCl solution. 98

7.7. A log-log plot of the signal intensity vs the laser intensity (mW) for saturated tyrosine in 10 mM NaCl solution. 99

7.8. A log-log plot of the signal intensity vs the laser intensity (mW) for 0.1M $K_4Fe(CN)_6$ in 10 mM NaCl solution. 100

List of Abbreviations

APEI - Atmosphere-Pressure Spray with Electron Ionization.

CI - Chemical Ionization.

DMA - Direct Memory Access.

DSO - Digital Storage Oscilloscopes

EI - Electron Impact.

FAB - Fast Atom Bombardment.

FD - Filed Desorption.

FTMS - Fourier-Transform Mass Spectrometer.

FWHM - Full-width at Half Maximum.

GC - Gas Chromatography.

GC/MS - Gas Chromatography/Mass Spectrometry.

GPIB - General Purpose Interface Bus.

HPLC - High Performance Liquid Chromatography.

IEV - Ion Evaporation.

IP - Ionization Potential.

LC - Liquid Chromatography.

LC/MS - Liquid Chromatography Mass Spectrometry.

LC/TOFMS - Liquid Chromatography/Time-of-Flight Mass Spectrometry.

LC/UV - Liquid Chromatography/Ultraviolet.

LD - Laser Desorption.

LDMS - Laser Desorption Mass Spectrometry.

LN_2 - Liquid Nitrogen.

MPI - Multiphoton Ionization.

MS - Mass Spectrometry.

MW - Molecular Weight.

PAHs - Polycyclic Aromatic Hydrocarbons.

PC - Personal Computer.

PSI - Pulsed Sample Interface.

RSD - Relative Standard Deviation.

R2PI - Resonant Two-Photon Ionization.

SFC - Supercritical Fluid Chromatography.

SIMS - Secondary Ion Mass Spectrometry.

SJ - Supersonic Jet.

SJS - Supersonic Jet Spectroscopy.

S/N- Signal-to-Noise.

TC - Thermocouple.

TOFMS - Time-of-Flight Mass Spectrometry.

UV - Ultraviolet.

Vis - Visible.

Part I

Liquid Chromatography/Time-of-Flight Mass Spectrometry with a Pulsed Sample Introduction (PSI) Interface

Chapter 1

Introduction

Mass spectrometry (MS) is one of the most important techniques used for chemical analysis. At present, MS is one of the most sensitive methods of molecular analysis. Moreover, it has the potential to yield information on the molecular weight as well as the structure of the analyte. The basis in MS is the production of ions, that are subsequently separated or filtered according to their mass-to-charge (m/z) ratio and detected. Thus, the development of new and more versatile ionization methods has been one of the most active areas in this field. So far, many ionization methods have been developed and used in MS. These methods include electron impact (EI), chemical ionization (CI), fast atom bombardment (FAB), plasma desorption (PD), field desorption (FD), matrix-assisted secondary ion mass spectrometry (SIMS), laser desorption (LD), laser-induced multiphoton ionization (MPI), and others.

The application of laser-induced MPI to MS has greatly enhanced its capabilities in many ways. As a matter of fact, MPI mass spectrometry has already established itself as a powerful technique for chemical detection and structural analysis [1]. In MPI, sample molecules are ionized by absorbing two or more photons from a pulsed laser beam and the resulting ions are detected by, usually, a time-of-flight mass spectrometer (TOFMS) [1-9] or a Fourier transform mass spectrometer (FTMS) [10-14]. Advantages of using MPI as an ionization source for MS include high sensitivity, high selectivity, and the ability to control the mass fragmentation patterns. Recently, the MPI technique has been extended to studies of biological chemicals [1]. In order to volatilize these nonvolatile and thermally labile molecules into the gas phase for MPI, various techniques such as LD, FAB, and pulsed rapid heating method have been developed [7-9,14-16].

However, for real sample analysis, it is often necessary to separate the complex mixture prior to sample injection into a mass spectrometer. Thus, there is a great deal of interest in combining chromatography techniques such as gas chromatography (GC), high performance liquid chromatography (HPLC), and supercritical fluid chromatography (SFC) with a mass spectrometer for on-line detection. These hyphenated techniques have become some of the most powerful tools for chemical analysis of complex mixture.

In this part, recent development of a pulsed sample introduction (PSI) interface for interfacing LC with TOFMS is reported. For the first time we show the combination of conventional LC with TOFMS for the detection of thermally labile and nonvolatile chemicals in mixture.

1.1 Multiphoton Ionization

The advent of high peak power, tunable visible and ultraviolet laser source has made multiphoton ionization processes feasible. The multiphoton ionization (MPI) technique depends upon the absorption of two or more photons by a molecule upon irradiation with an intense visible or ultraviolet light source, resulting in the production of a positive ion with the concurrent release of an electron. The cross-section of ionization is greatly enhanced, when the excitation laser frequency is tuned to a real intermediate electronic state. This technique is called resonance-enhanced multiphoton ionization (REMPI). A molecule will be ionized only if the total energy of the adsobed photons exceeds the ionization potential of the molecule. When the laser wavelength is not tuned to a real electronic state, the probability for MPI is negligible. Therefore, although ions are produced as the final product for detection in mass spectrometry, the ion current depends on the absorption cross-section of the molecule at the selected laser frequency. Thus, the intensity of the ion current as a function of laser frequency reflects the absorption-excitation spectrum of the intermediate state. The truly unique property

of MPI is that it can be used as a mean of achieving spectral selectivity of a target compound prior to mass analysis.

There are several different ways in which MPI can be induced as shown in Figure 1.1. The MPI technique that has found most extensive applications in analytical chemistry is resonant two-photon ionization (R2PI) [1-47]. In this process, one photon excites a molecule to an excited electronic state, and a second photon ionizes the molecule (see Figure 1.1 (b)). Thus, the total energy of the two photons must be greater than the ionization potential of the molecule for R2PI, although the two photons may have either the same or different frequencies. Other processes are nonresonant ionization and two-photon resonant ionization (see Figure 1.1 (a) and (c)). However, because in these processes at least one photon is nonresonant and interacts with a very short-lived virtual state ($< 10^{-15}$ sec), the efficiency for ionization is far less than that achieved in R2PI. In addition, in nonresonant MPI, the wavelength selectivity, which is unique to the MPI process, is lost. Since most organic compounds have ionization potential (IP) between 7 and 13 eV, R2PI can be achieved using near-UV pulsed laser sources. Thus, high peak power, broadly tunable Nd:YAG and excimer-pumped frequency-doubled dye lasers in the UV region serve as versatile sources for selective resonant two-photon ionization of molecules.

R2PI has several important attributes for mass spectrometry along with its potential for high selectivity. In particular, it can be used to control the fragmentation pattern obtained. This technique can provide very effeicient soft ionization of molecules yielding the molecular ion with little or no fragmentation [12, 24-27, 31-35, 38, 43]. Although the full capability of this property has not been explored, soft ionization generally appears to occur at modest laser energies ($< 10^6$ W/cm^2) for a wide range of organic species. For small aromatics such as aniline [24, 25, 27], benzene [35, 36], and naphthalene [27, 35, 38], abundant molecular ions with little or no fragmentation can be

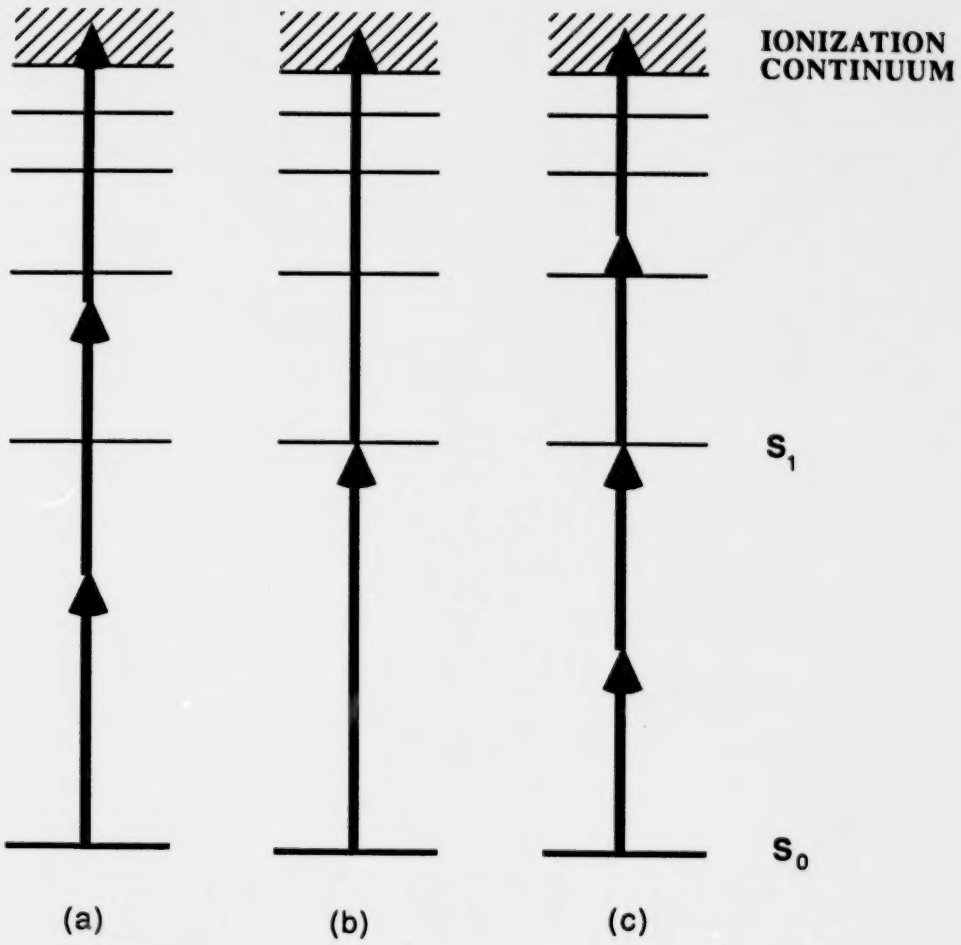

Figure 1.1 Energy level diagram in MPI transitions:

(a) Nonresonant MPI,

(b) Resonant two-photon ionization (R2PI),

(c) Two-photon resonant ionization MPI.

routinely produced. In more recent studies, relatively soft ionization has resulted from R2PI of fragile biological and thermally labile molecules [12, 27, 38]. The ability to generate only molecular ion can simplify the mass spectrum considerably and raises the possibility of identification according to molecular weight.

R2PI is also capable of providing extensive fragmentation either by increasing the laser power density or by varying the laser frequency chosen for ionization. Zandee and co-workers [31-34], for example, have reported that C^+ is the predominant ion from resonance-enhanced multiphoton ionization of benzene when a laser power density of about 10^9 W/cm^2 is used at a wavelength of 391.4 nm. As the laser power density is varied, the fragmentation pattern will correspondingly alter where different ratios of carbon fragments including $C_6H_n^+$, $C_5H_n^+$, $C_4H_n^+$, $C_3H_n^+$, $C_2H_n^+$ and CH_n^+ will be observed. Similar results have been observed in MPI as a function of laser power in the near UV (300-260 nm) by many other researchers [25-27, 36-40]. Several mechanisms have been put forward [41-44] to explain the fragmentation process in MPI. Generally accepted is the "ladder switching model," which is supported by experimental results and theoretical studies [45-47]. As shown in Figure 1.2, the neutral molecule absorbs two photons on its "absorption ladder" and is ionized. Here the internal energy is only slightly higher than the ionization energy. The molecule ion then absorbs one or several more photons, thereby starting the first fragmentation reaction. The system then switches from the molecule absorption ladder to a fragment ion, which can absorb further photons on its absorption ladder, including further fragmentation reactions. This absorption-fragmentation mechanism may occur several times with typical laser pulses of 6-10 ns and, with sufficient laser power densities, resulting in a total breakdown of the molecule into the atomic particles.

In summary, the MPI technique has great versatility as an ionization source for mass spectrometry in which either soft ionization or very extensive fragmentation

Ladder switching

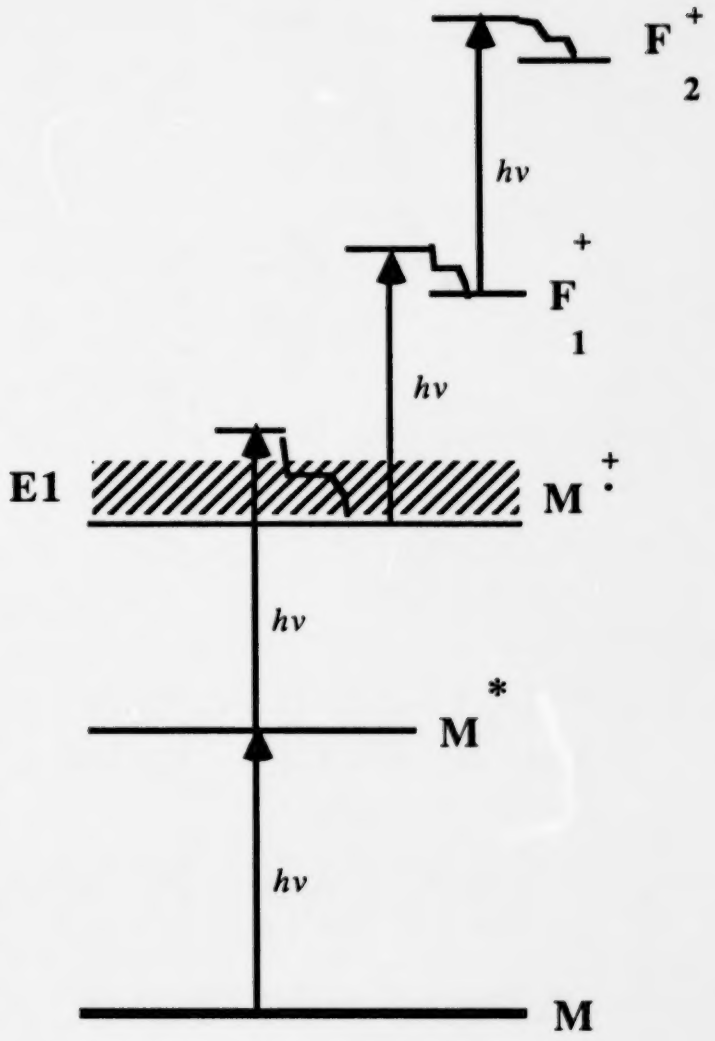

Figure 1.2 Ladder switching mechanism.

through successive up-pumping can be achieved. This can be accomplished by simply changing the laser output power or by varying the laser frequency. More importantly, in either case, ionization occurs with very high efficiency. In addition, the ionization cross-section of MPI reflects the absorption-excitation spectrometry of the intermediate state. This provides the MPI mass spectrometry with a unique feature in mixture analysis, that is, identification and discrimination based on the spectral selection of compounds in mass analysis.

1.2 LC/MS Interfacing

The combination of a chromatographic technique and mass spectrometry offers the analytical chemist a series of powerful analytical techniques for the detection of organic compounds in a variety of complex matrices. Because of its technical simplicity and high performance, and after nearly 30 years of development and application, the combination of high resolution gas chromatography with mass spectrometry (GC/MS) remains unsurpassed for structural determination and quantitative measurement. It is the most powerful tool available at present for the identification of unknown compounds. However, GC/MS is limited by the application domain of GC, other chromatographic techniques such as liquid chromatography (LC) and supercritical fluid chromatography (SFC) have been considered for combination with mass spectrometry.

The application domain of high performance liquid chromatography is nearly boundless, especially for separations of nonvolatile, and thermally labile compounds, and there is no need to emphasize the merits of mass spectrometric detection with regards to universality, high sensitivity and outstanding selectivity. Thus combining liquid chromatography with mass spectrometry (LC/MS) has always attracted great attention, being considered as potentially very important analytical technique.

Unfortunately, coupling LC/MS has been a more challenging task than it was for

GC/MS. The difficulties in coupling LC/MS are well documented [48-51]. These problems are the amount of solvent eluting from the LC column that has to be introduced into the MS vacuum system, the composition of the LC mobile phase, and the nature of the analytes that must be analyzed. To solve these problems, different types of interfaces [52-86] have been developed to be placed between the LC column outlet and the MS high vacuum system.

For interfacing liquid chromatography with mass spectrometry, both LC and MS point-of-view should be considered. In terms of LC operation, the interface must tolerate different solvent systems under different flow conditions, programmed solvent composition gradients, and the possible occurrence of impurities in the solvent. The interface itself should have high sample transfer efficiency so that no or minimum analyte is lost. In order to avoid loss of analyte either as much of the LC column effluent as possible has to be introduced into the MS, or considerable analyte enrichment must be achieved in the LC/MS interface. No additional peak broadening effect by the interface is favorable. More important, the interface should not impose any degradation in resolution of eluted peaks from LC column. The interface must not restrict the operating conditions of the mass spectrometer. The pumping capacity of the mass spectrometer should be high enough to handle large pressure in the source for ionization of analytes. The performance of the interface should also remain the same for the transmission of volatile, nonvolatile, and thermally labile compounds. In addition, the LC/MS system should be simple to operate, able to do quantitation, and have low detection limits.

At present, the mass spectrometer is unique in that it offers a combination of three very important analytical features. These features include sensitivity, selectivity, and nearly universal detection for organic analytes. There is currently no other detector for GC or HPLC that can match these combined benefits of specificity and sensitivity. The other important factor that determines the suitability of particular MS as a detector

for LC work is the scanning rate or in more general term, the rate to collect data from eluted peak. In order to avoid loss in resolution of the eluted peaks, MS should be able to obtain enough data points over the entire LC profile for reconstructing the liquid chromatogram. At present, the most commonly used MS systems in LC/MS are sector and quadrupole instruments [52-55, 63, 65]. For scanning instrument, scanning time depends on scanning mass range. In general, better mass resolution is obtained with longer scanning time but losses of resolution of the eluted peaks are unavoidable [87]. At present, a scan rate up to 1ms per m/z-value is possible [52]. However, when the mass range becomes larger, the limited scan rate will be a problem to obtain a good chromatographic resolution.

The most commonly used ionization techniques [52-55] in LC/MS are electron impact (EI), chemical ionization (CI), fast atom bombardment (FAB), and ion evaporation (IEV). Among these methods, only electron impact is a hard ionization technique that can provide structural information for structural analysis. All the others are considered as soft ionization techniques that can give only molecular weight information. For most of the interfaces developed over the years, only few such as moving-belt [64-66], particle-beam interface [78-80] can access to EI ionization and the rest are subjected to soft ionization techniques.

In 1972, the first coupling technique for LC/MS was reported by Tal'roze et al. [88]. Up to now, over 25 different interface approaches have been described (see Table 1.1). The characteristics of the most widely used LC/MS interfaces are summarized in Table 1.2. Most of the LC/MS interfaces were built in the various research laboratories, while some of them have been adapted by instrument manufacturers and have become commercially available [64-86]. In the development of these LC/MS interfaces, three development lines can be distinguished,which are concerned with efforts (1) to introduce 1 ml/min of aqueous mobile phase into the MS vacuum system, (2) to achieve analyte

Table 1.1 LC/MS interfaces [90]

1972	Stopped-flow
1972	Capillary inlet
1974	Moving-belt
1974	Pneumatic nebulizer in atmospheric pressure ion source
1975	Solvent vapor separator membrane
1976	Liquid ion evaporation
1978	Crossed beam
1978	Jet separator
1979	Vacuum nebulizer
1980	Direct liquid introduction
1981	Conical tip
1981	Continuous sample preconcentrator
1982	Rotating disk
1983	Helium
1983	Thermospray
1984	Monodisperse aerosol generator
1985	Electrospray
1985	Frit-FAB
1986	Continuous-flow FAB
1986	Particle beam
1986	Heated nebulizer
1987	Thermabeam
1987	Gas nebulized
1987	Ionspray
1988	Atmospheric pressure spray
1989	Frit-EI/CI

Table 1.2 Characteristics of the most widely used LC/MS interfaces [52]

Interface	max. flow rate (μL/min)	composition[1]	ionization technique[2]
Moving-belt	2000	NP	EI, CI, FAB
Direct liquid introduction	50	RP, B	LCI
Thermospray	2000	RP, B	LCI, IEV
Continuous-flow FAB	15	RP, B	FAB
Frit-FAB	5	RP	FAB (EI, LCI)
Particle-beam	500	RP, NP, B	EI, CI, FAB
Thermabeam/universal	1000	RP, NP, B	EI, CI, FAB
Electrospray	10	RP, B	IEV, LCI
Ionspray	100	RP, B	IEV, LCI
Heated nebulizer	2000	RP, NP, B	APCI, IEV

Note: [1] NP=normal-phase chromatography with organic solvents;

RP=reversed-phase chromatography with aqueous organic solvent mixtures; B=volatile buffers.

[2] EI=electron impact; CI=conventional chemical ionization;

LCI=solvent-mediated chemical ionization;

IEV=ion evaporation; FAB=fast atom bombardment;

APCI=atmospheric-pressure chemical ionization.

enrichment in the interface, and (3) to develop liquid-based ionization techniques. The details and applications of these interfacing techniques will not be discussed here and can be found in many references [48, 52-55, 65, 73, 84, 89, 90].

In summary, the combination of LC and MS has become a successful analytical tool for analysis of organic mixture. However, various steps in the LC/MS interfacing show the selectivity or discrimination towards certain analytes, especially the inherent properties of the ionization techniques used. No free choice of LC solvent composition is possible. Most favorable solvents in LC/MS are reversed-phase LC solvents containing volatile buffer constituents. This to some extent limits the LC/MS applications. Thermally labile and nonvolatile analytes can be handled in LC/MS especially when soft ionization techniques are applied. The detection limits achievable in LC/MS are not always sufficient, especially in the fields of bioanalysis and environmental analysis. In quantitative analysis, other LC detectors, such as UV, fluorescence and electro-chemical detectors , apparently perform much better than a detector based on LC/MS. However, when the specificity and selectivity of the detector are taken into account, LC/MS comes in much better perspective. Now LC/MS has conquered a place amongst the various applicable analytical techniques.

1.3 Time-of-Flight Mass Spectrometer as a LC Detector

As mentioned before, for most of LC/MS experiments, a sector or quadrupole instrument is used. The main disadvantages of these instruments are limited mass range, lower ion transmission efficiency, and lower scan rate. However, the use of a TOFMS as a LC detector offers several unique advantages over these commonly used scanning mass analyzers: (1) high ion transmission, (2) able to obtain up to ten thousand complete mass spectra per second, (3) no mass limit. Moreover, TOFMS is very simple to construct, and yet inexpensive compared to other scanning mass spectrometers.

TOFMS is well suited for pulsed operation, and detects ions in a discrete form. High ion transmission efficiency is attained by TOFMS since all ions generated in the ionization region are transmitted through a drift tube and subsequently detected by a microchannel plate detector. This higher ion transmission results in increasing the detection sensitivity of TOFMS as a detector for LC.

One of the distinguished advantages of TOFMS as an ideal candidate for LC detector is its ability to obtain up to 10,000 complete mass spectra in a second [84]. This feature is extremely important for fast chromatographic detection. For conventional LC elution, the peak width of a particular chromatographic peak is normally in the range of about 20 seconds. Sufficient number of mass spectra per chromatographic peak must be obtained in order to retain eluted peak shape and resolution. With the use of TOFMS, a sufficient number of spectra can be acquired over the entire elution profile of a peak to reconstruct the chromatographic peak without losing resolution of the eluted peak.

The other important feature of TOFMS is its ability to detect high mass. For most scanning mass spectrometers, mass range up to several thousand Daltons can be obtained. TOFMS on the other hand has no ultimate mass limit. In fact, large proteins with molecular weights up to 300,000 Da. have been detected by TOFMS [91].

Besides all the advantages offered by TOFMS , it also suffers some drawbacks as a LC detector. The most well known weakness of TOFMS is its poor mass resolution. Mass resolution of TOFMS is degraded by initial space, energy variations and the presence of metastable decomposition products in the ion optical path [84]. However, with the use of reflectron TOFMS, mass resolution up to 10,000 has been reported [92, 93].

The duty cycle of TOFMS is another limitation for it to be an effective chromatographic detector. The inability of TOFMS to detect the chromatographic effluent

continuously causes a severe loss in a sample sensitivity. In the light of fact that a TOFMS detects ions in a pulsed form, it is highly desirable to introduce chromatographic effluent into TOFMS in a pulsed form instead of continuous form in order to increase the duty cycle of TOFMS.

By using MPI as the ionization source, TOFMS becomes a more powerful method for LC detection. Some of the most outstanding characteristics of this system are: the ability to obtain both soft and hard ionization mass spectra, higher sensitivity, and higher selectivity.

The goal of our work is to develop an on-line HPLC/TOFMS system that has the following characteristics: (1) Have high sensitivity with low ng or pg detection limit, (2) Have mass resolution up to 2000, (3) Provide qualitative information based on MPI and/or EI mass spectra for reliable molecular identification, (4) Be able to do on-line quantitation with high precision, (5) Be able to detect most compounds of interest in environmental samples, (6) Be reliable and convenient to operate.

In order to accomplish this goal, recently we developed a pulsed sample introduction (PSI) interface [94] specifically suited for TOFMS in our laboratory. Since this PSI interface introduces sample in a pulsed form instead of continuous form, the duty cycle of TOFMS can be enhanced while still maintaining the low system pressure for ionization. This PSI interface can accept LC effluent of up to 1.6 mL/min without splitting and most of organic aqueous or any combination of these solvents can be introduced into the TOFMS system readily. The details of this PSI interface are given in Chapter 2 and successful applications of this PSI interface for on-line HPLC/TOFMS detection of mixture are presented in Chapter 3.

Chapter 2

Experimental

Figure 2.1 shows the schematic diagram of the experimental set-up of on-line HPLC/MPI-TOFMS with a PSI interface. It consists of a liquid chromatography instrument, a PSI interface, a time-of-flight mass spectrometer, and a data system. The details of each part will be discussed next.

2.1 Liquid Chromatography

The LC solvent delivery system consists of a Shimadzu LC-600 programmable liquid pump capable of delivering solvent with variable flow rates ranging from 10 μL/min to 10 mL/min. For chromatographic work, a Waters Nova-Pak C-18 column (Millipore Ltd., Mississauga, On) is used for separation. A Rheodyne Model 7125 syringe loading injector with a 5 μL or 20 μL sample loop is used for sample injection. In between the column and the PSI interface, a Shimadzu SPD-M6A photodiode array detector is used for obtaining a UV chromatogram. All flow lines are connected with the use of 1.58 mm o.d. and 1.00 mm i.d. stainless steel tubings.

2.2 Pulsed Sample Introduction Interface

The schematic diagram of the pulsed sample introduction interface is shown in Figure 2.2. This PSI interface consists of two important parts. One is the heated capillary tube in which the liquid flow is converted into aerosol droplets and/or supersaturated vapor. These aerosols are then expanded into the sample vaporizer for complete desolvation and vaporization. The heated capillary tube is a 5 cm long, 1.58 mm o.d and 0.25 mm i.d. stainless steel tubing wrapped with a Nichrome 60 heating coil (Pelican Wire Co., Naples, FL). The sample vaporizer is part of the nozzle head of a high temperature pulsed nozzle. This nozzle is designed to be used for flow injection

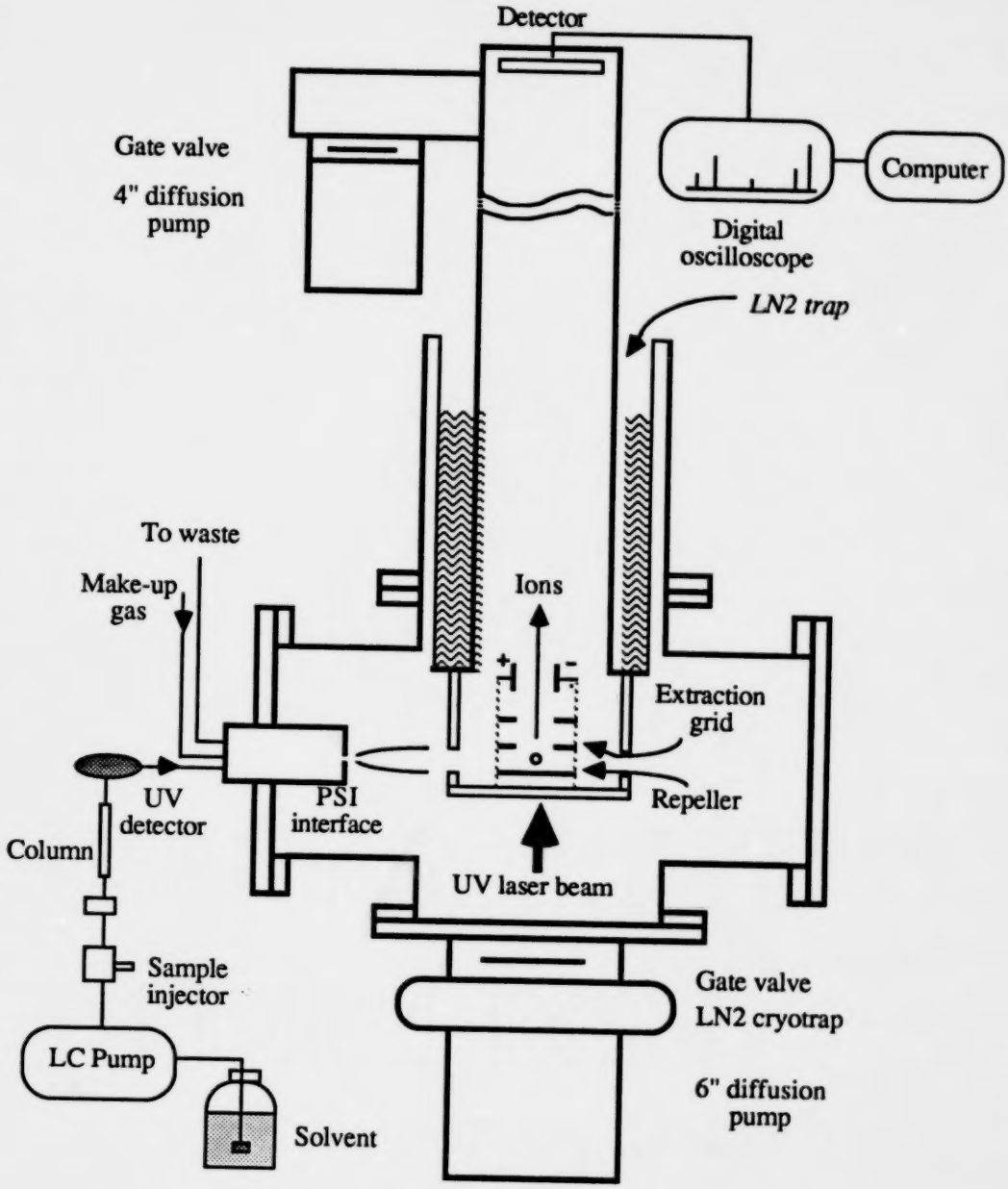

Figure 2.1. Schematic of the experimental set-up of HPLC/TOFMS with a PSI interface.

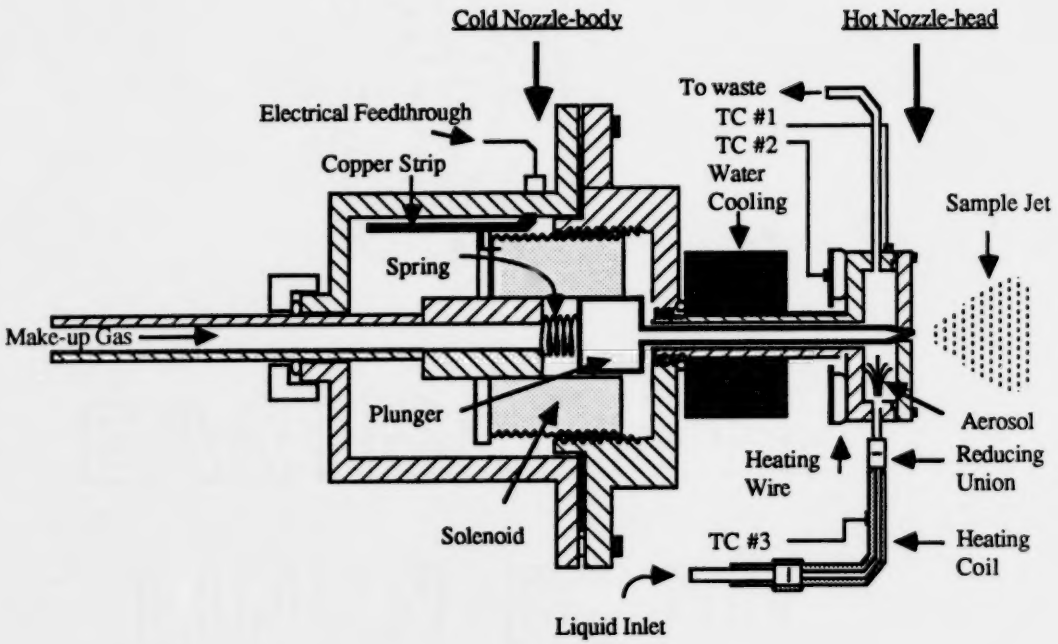

Figure 2.2. Schematic of the design of the pulsed sample introduction interface. Drawing is not to scale. The dimensions of the major components are given in the text.

analysis based on the earlier version of the high temperature pulsed nozzle used for SJS reported by Li and Lubman [95]. It consists of two components, i.e., the nozzle body and the nozzle head, separated by a water cooling system. The cold nozzle-body contains a solenoid, which is used to drive a plunger for introducing the sample vapor to TOFMS in a pulsed form. The nozzle head is heated during the operation for sample vaporization.

The current design of the nozzle body is similar to the one reported by Li and Lubman [95]. It consists of a solenoid, a spring and a plunger (see cold nozzle-body in Figure 2.2). The solenoid is a modified automobile fuel injection valve (Bosch, part number 0280150035, purchased from a local auto-parts' store). The dimensions of the solenoid are 25 mm in diameter and 32 mm in length. The electric feedthrough used to provide the current for driving the solenoid is constructed of Vespel that is threaded so that it screws into the stainless-steel body. A stainless-steel rod is epoxidized into the Vespel using "Torr Seal" (Varian). A copper strip screwed on the rod is used to contact the lead of the solenoid. The power supply for driving this solenoid is similar to that reported [96]. It can generate a 400-V pulse with a duration of about 35 ms. In this experiment, a 100-V pulse is used to drive the solenoid.

The plunger is made of a long stainless-steel needle (1.5 mm in diameter and 55 mm in length) which screws into a steel base for magnetic attraction. The other end of the needle forms a metal-to-metal seal against the orifice. During the operation, a voltage is applied to the solenoid to generate a magnetic field that attracts the plunger away from the orifice to form a jet. When the power is off, the spring pushes the plunger against the orifice to make a seal. The leakage from the seal is negligible compared to the gas emitted per pulse. The sample pulse width is measured to be about 1 ms full-width at half maximum (FWHM) for the current experimental setup. Thus, although sample vapors are continuously generated inside the sample vaporizer, only a small portion of them is pulsed into the mass spectrometer. The pulse repetition rate used for the solenoid is the

same as that of the ionization laser beam.

The hot nozzle-head contains a sample vaporizer, an aerosol inlet, and an outlet to waste. The sample vaporizer is heated by a coil of thermocoax heating wire (Phillips Electronic Instruments, Norcross, GA). A stainless-steel plate with a 500 μm diameter orifice is sealed to the nozzle head using a copper gasket and knife edge seal. The dimensions of the inner area of the nozzle head in which aerosol expansion and vaporization take place are 25 mm in diameter and 8 mm in length.

Three type-K thermocouples (TCs) are used to monitor the temperature of the interface at different regions. In the studies reported here, the temperature of the nozzle front (TC #1 in Figure 2.2) is 480°C. The temperature near the heating wire (TC #2) is 600°C. The temperature of the heating coil (TC #3) is 200°C. The reading of this temperature depends on the position of the TC. In this experiment, TC #3 is located about 5 cm away from the nozzle head. As a matter of fact, the actual temperature of the aerosol is unknown, since a TC cannot be placed inside the sample vaporizer with the current design. Judging from the temperature gradient we observed across the nozzle head, we believe that the temperature of the inner wall of the sample vaporizer and the aerosol is much lower than 480°C.

2.3 Time-of-Flight Mass Spectrometer

A linear time-of-flight mass spectrometer is used for ion detection [94]. It is mounted vertically in a six-port cross pumped by a 6-in. diffusion pump (Varian Associated, Inc., Lexington, MA). The 1-m-long flight tube is differentially pumped by a 4-in. diffusion pump (Varian). A liquid nitrogen (LN_2) trap assembly is used to cool part of the flight tube and the entire acceleration lens assembly. The trap was manufactured by R.M. Jordan Co. (Grass Valley, CA) to our specifications. All other vacuum components were constructed in-house. The pressure of the system during

operation is normally <5.0 10^{-7} torr.

In this study, molecules are ionized by using laser-induced multiphoton ionization [1]. The ionization laser source is a 266 nm laser beam from a frequency-quadrupled Nd:YAG laser (GCR-3, Spectra-Physics, Mountain View, CA). The laser repetition rate can be varied up to 20 Hz, but the laser is normally operated at a repetition rate of 10 Hz. A combination of a concave and a convex lens is generally used to produce a beam 2-3 mm in diameter for ionization. The ions generated by the laser beam are extracted to the acceleration region, and then are accelerated to the drift tube. Voltage up to 15 kV can be applied to both the repeller and the extraction grid through high voltage vacuum feedthrough (Ceramaseal, New Lebanon, NY). The power supplies are from Spellman High Voltage Electronics (Model RH5R20PN60, Plainview, NY). In general, the voltage applied to the extraction grid is about 500-1500 volts less than the repeller voltage. This combination of voltage settings gives optimal sensitivity and mass resolution. The ions are detected by a microchannel plate detector (Galleo Electro-Optics Corp., Sturbridge, MA). The mass spectrum is recorded by a LeCroy 9400A digital oscilloscope. The mass resolution of this system is typically about 300. To establish the ion chromatogram, a boxcar integrator is used for monitoring the ion intensity and the output is recorded on a chart recorder. Alternatively, a data acquisition scheme, based on a General Purpose Interface Bus (GPIB) (National Instruments model AT-GPIB board) for data transfer from a LeCroy oscilloscope to a personal computer (PC), is used for recording and storing transient signals generated by LC/TOFMS. We have developed a software to maximize the speed of data transfer and storage. With our data system, it is possible to record and store mass spectra at a speed ranging from 14 spectra/sec for a transient record length of 20 Kbytes to 50 spectra/sec for a record length of 1 Kbyte. Details of the data system are described next.

2.4 Data System

Hardware A LeCroy 9400A digital osilloscope is used for data acquisition. A one meter cable connects the LeCroy's GPIB port to the National Instruments model AT-GPIB board inside a PC. The board has a transfer speed of 1 Mbyte/sec. The PC is a generic 486DX33 machine with a 210MByte hard drive, 4 MBytes of RAM, a mouse and a high resolution color monitor. A 2MByte cache IDE controller card reduces the disc's seek and latency times to nearly zero. The stored data can be transferred to other machines via ethernet or floppy disc. For off-line data storage, a Hewlett Packard 35470A SCSI DAT drive is currently used to download the data from the hard disk to a tape. A 90 m tape can store 2 gigabytes of data. The drive has reasonable speed (10 Mbytes/min) for data transfer.

Software The application is written in Microsoft Quick C version 2.01 and linked with the LabWindows version 2.2.1 libraries from National Instruments. The LabWindows software was chosen for several reasons. Its graphical user interface is easy to configure and it has many built in functions. Its library of instrument drivers has routines that interface to hundreds of instruments, largely eliminating the usual time consuming task of writing an instrument driver.

Control Panels The control of this application is accomplished with one main menu and three graphical interface panels. The menu can stop the application or select one of the three panels. The panels follow in the chronological sequence of the experiment: setup, run, and analysis. Their actual appearance on the PC monitor are in full color. The main features of the three panels are described below.

A. Setup Panel

The setup panel's sole function (see Figure 2.3) is to configure the digitizer and insure that the computer can acquire data free of errors. The front panel of the LeCroy 9400A is used as a model for the appearance of this panel on the PC. Basic digitizer

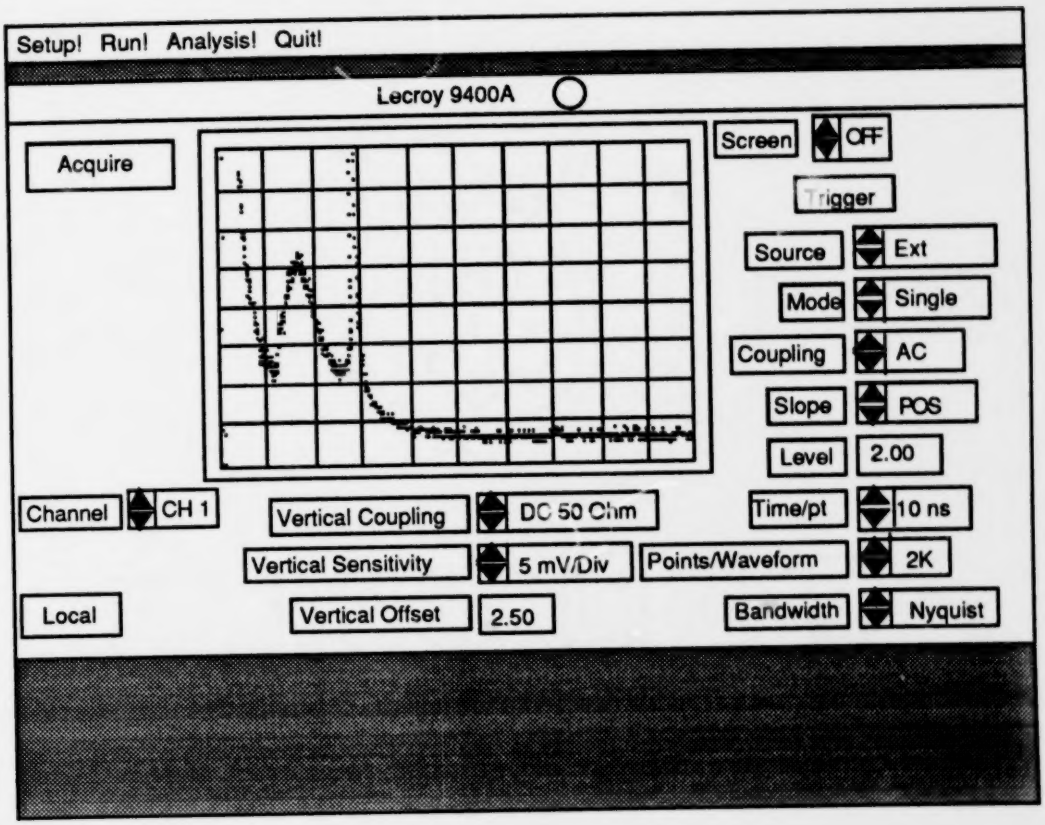

Figure 2.3. The setup panel of the control panels of the data acquisition system.

parameters such as all the triggering, timing and input sensitivities can be set by the click of a mouse button. A few special parameters that are specific to the TOFMS application such as the record length per spectrum and the time resolution are also included in this panel.

There are two push buttons on this panel. The "Acquire" push button sends the complete settings of this panel to the digitizer and displays the captured record on its screen. This thoroughly tests the complete digitizer to computer link and verifies that the parameters have been set correctly and that the desired peaks of the record are observed. The "Local" push button controls the remote function of the digital storage oscilloscopes (DSO). Pushing this button returns the DSO to its local mode.

B. Acquire Panel

Only a toggled "START/STOP" push button is on this panel (Figure 2.4). When the experiment has been set up and the data collection for the chromatogram is to begin the "START" button is pushed. A file name, that is checked for uniqueness, is requested to store the data. The data flowing from the experiment is then triggered, digitized, transferred and stored on the disk until the "STOP" button is pushed. Each record stored increments a counter on the panel.

In developing the software for acquiring the mass spectral data, a detailed study of all aspects of data flow in terms of delay time and transfer rate was first carried out. To achieve rapid data storage, software double buffering is used so that the GPIB board can transfer the data from the digitizer by direct memory access (DMA) to one buffer, while concurrently the contents of the second buffer is transferred to the disk. After the record has been transferred, the buffers are swapped and the sequence repeated. The concurrence of data transfer from the digitizer and simultaneous data to the disk means that the limiting speed of record acquisition is attributed to the slowest operation rather

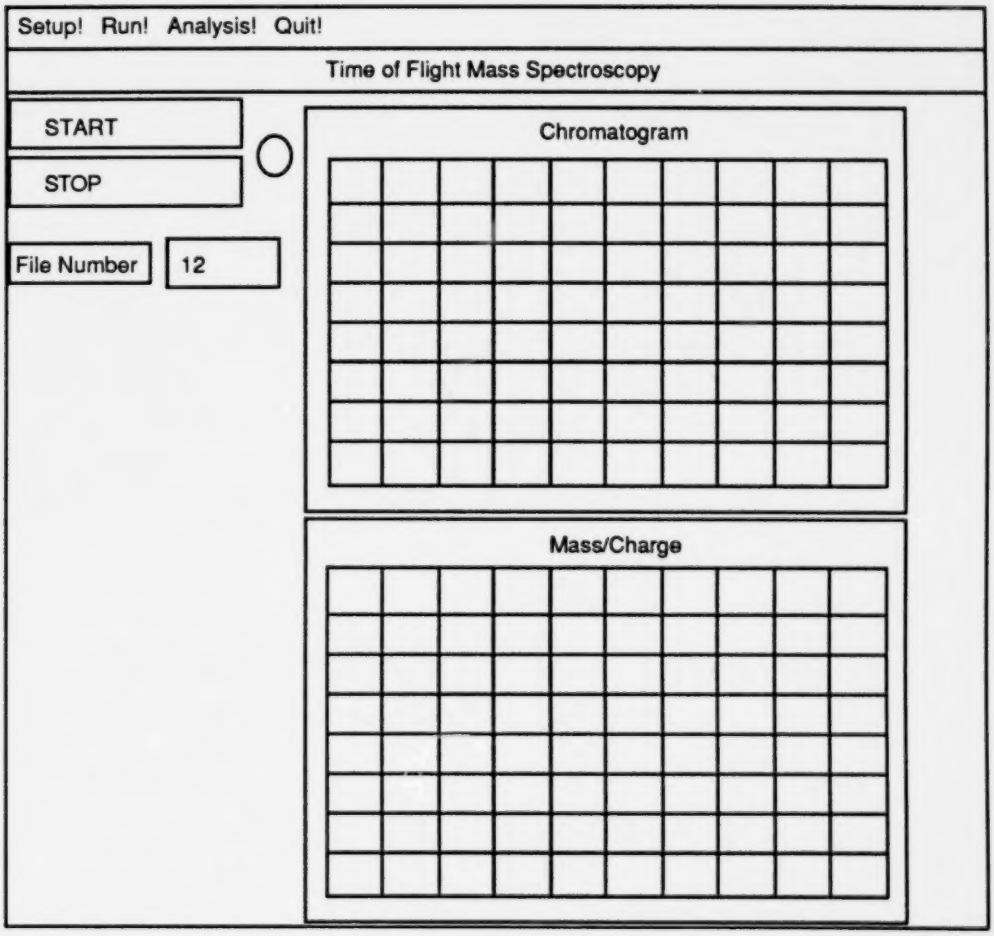

Figure 2.4. The run panel of control panels of the data acquisition system.

than being degraded by both operations. At present, the data transfer step is the major limiting factor. In addition, the latency and seek times for the disk are largely eliminated by buffering the data sent to the disk drive by a cache controller card that allows data to fill its buffer while the heads seek the next track and the disk spins to the correct sector to write on.

An alternative to software double buffering would be to use a large size of RAM to temporarily store the transient signals during the run. After the experiment, the RAM data are then transferred to a disk. However, the method of double buffering eliminates the need of using a large size of RAM.

Delays associated with the LeCroy to decode the commands to arm the trigger and to initiate the transfer of data limit the speed of acquisition for small sized record acquisitions (i.e., record length < 2Kbyte). The data transfer rate from LeCroy to the computer limits the speed of larger sized records. The delays are reduced by using the smallest character combination for a command. The transfer rate is increased by using the fastest GPIB board available and by transferring each point of the record as a byte. A further speed increase for all record sizes is realized by disabling the display on the LeCroy's front panel so LeCroy's internal processor can be freed to deal only with the acquisition and transfer of data, and thus does not have to calculate display information.

The present version of the software does not allow the mass spectrum to be displayed on the computer screen during the experiment. However, as an option defined in the initial setup panel, the DSO screen can be turned on during the run to continuously observe the mass spectrum. Compared with the screen-off mode, running the experiment in the screen-on mode reduces the transfer speed by at least a factor of 2.

C. Analysis Panel

Stored raw data is analyzed in this panel (see Figure 2.5) to produce ion

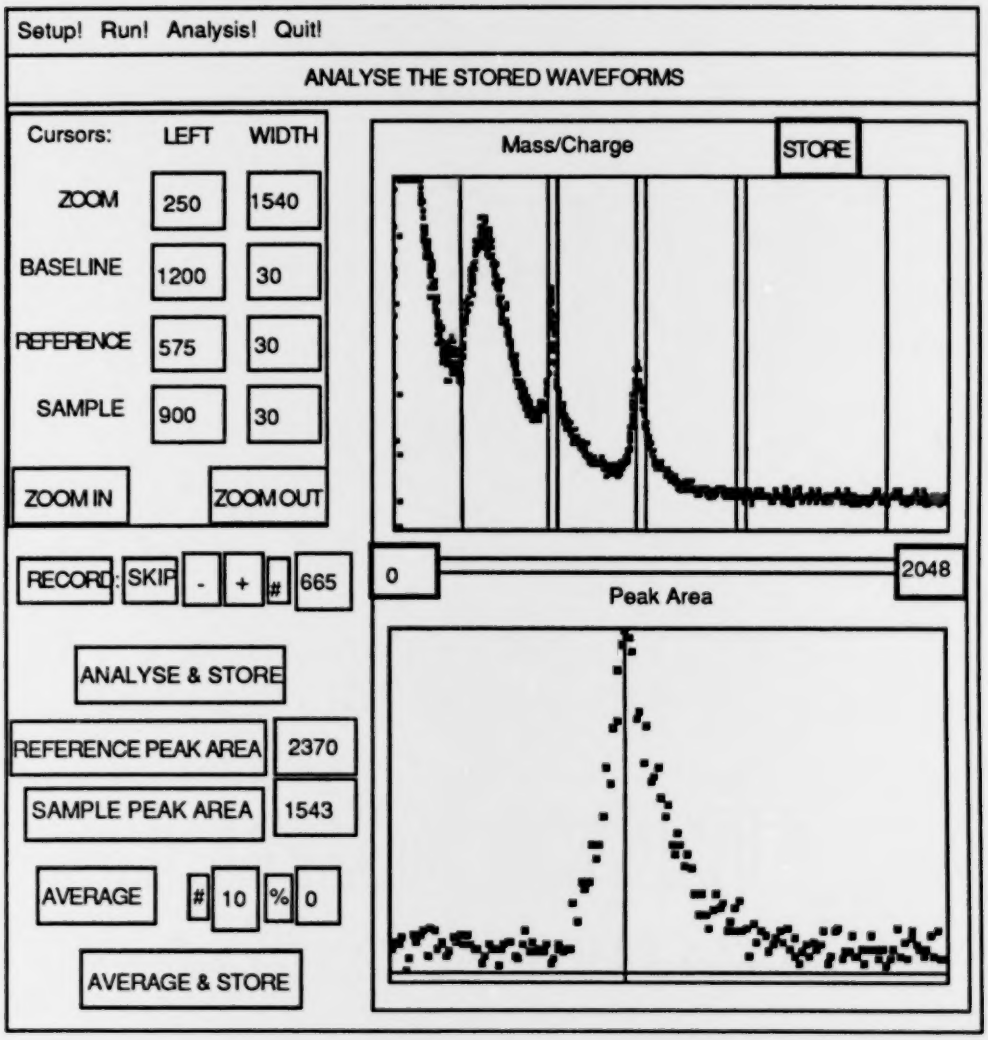

Figure 2.5. The analysis panel of the control panels of the data acquisition system.

chromatograms or plots of ion intensities as a function of record number. The main menu permits the analysis of data directly after launching the application or it can be entered after the Acquire panel has been stopped. A file prompt is provided listing all the raw data files to choose from. The selected raw file is loaded and the first record is displayed. Any record can be viewed either randomly by entering the record number or by skipping sequentially forward or backwards. Several important features in this panel are described as follows.

Cursors and Zooming On the upper graph in Figure 2.5 are four pairs of colored cursors and their corresponding colored indicator boxes. All the cursors can be moved by either entering their left value and width in their indicator boxes or by using the mouse to drag the cursors to a chosen spot on the record. Any mouse movement of a cursor will automatically update that cursor indicator box.

Area Calculations A baseline is selected by using the baseline cursors from a sectional of the transient record that is usually flat and free of all peaks and its width is adjusted to be similar to the width of a peak. The baseline value is calculated by taking a running average between the left and right baseline cursors. If a reference peak is used in the experiment for reasons such as using an internal standard, the reference peak can be selected by a pair of cursors and its value can also be calculated by taking a running integral. The reference peak area is calculated from the running integral of the difference between the reference value and the baseline value. It is displayed in the indicator box below the cursor indicators. Similarly, the sample peak is selected by a pair of cursors. The sample peak area is calculated from running integral of the difference between the sample value and the baseline value and is displayed in the indicator box below the reference peak area indicator box. Any time the baseline, reference or sample cursors are moved or another record is displayed the peak areas are recalculated and displayed in their respective indicator boxes.

After the cursors have been set, the entire set of records can be scanned and stored in a disk file by pushing the button "ANALYSE & STORE". A unique file name is requested and then the entire set of records is analyzed, stored and graphed on the normalized lower graph named "Peak Area". The baseline and reference areas are plotted against record numbers in different colors. The lower graph also displays the ratio of the sample area to the reference area as a normalized chromatogram. In Figure 2.5, only the normalized chromatogram is plotted. In this graph, a vertical cursor can be moved to any part of the chromatogram and displays that record (i.e., the mass spectrum) in the upper graph, the record number, and the areas of the two peaks. At any time the currently displayed record can also be stored in a text disk file by pushing the button labeled "STORE" on the upper right border of the "Mass/Charge" graph.

Averaging The number of records which are averaged is set initially to one. An average of any number of records can be viewed by changing the indicator box labeled "#" with the desired number and pushing the button "AVERAGE". A new chromatogram will be drawn. To store a desired chromatogram with or without record number averaging the button labeled "AVERAGE & STORE" is pushed. A unique file name is requested, the final averaging is performed and each accepted record number, reference peak area, and the sample peak area are stored on a text disk file for use by any other graphing and data analysis software packages which accept text files. In this work, the Igor software (WaveMetrics, Inc., OR) is used.

2.5 Materials and Reagents

In this work, HPLC grade methanol or water is used to prepare the mobile phase. All sample solutions are freshly prepared by using methanol or water as the solvent. All chemicals were purchased from Aldrich Chemical Co., Milwaukee, WI, or Sigma Chemical Co., St. Louis, Mo and used without further purification.

Chapter 3

Results and Discussion

3.1 Applicability of the PSI Interface

Table 3.1 lists the compounds studied by this interface with MPI time-of-flight mass spectrometry. The ionization laser beam is at 266 nm with its power density of 2 x 10^6 W/cm^2. The reason for choosing these compounds to demonstrate the applicability of this interface is mainly because they have been extensively studied by MPI in this laboratory with various vaporization/desorption techniques [94, 97, 98]. Throughout this study the experimental conditions are kept the same. The sample is injected by a sample injector in LC, and directly introduce into the TOFMS system by using the PSI interface without passing through a LC column. Methanol is used as the carrier liquid with a flow rate of 1 mL/min. The temperature of the heated capillary tube is about 200 ^{o}C, and the temperature near the nozzle orifice is about 430 ^{o}C. A make-up gas of CO_2 is used and its flow rate is optimized to be 40 mL/min. The use of the make-up gas prevents sample and liquid carrier condensation which may occur due to their feedback from the nozzle's hot head to its cold body. It also provides a mean of sweeping the sample and liquid carrier vapors out of the sample vaporizer rapidly, resulting in sharp peaks with less tailing.

One of the key results is that molecular ions are observed for most compounds studied in Table 3.1. In general, no thermal-decomposed products are detected. The lack of thermal decomposition in this study can be attributed to the fact that the sample molecules are rapidly vaporized in the sample vaporizer. Moreover, the probability for the sample to make contact with the inner wall of the vaporizer is minimized due to the presence of large quantity of hot methanol vapor, resulting in the reduction of catalysis action of the metal surface [99]. However, for anthranilic acid, as shown in Table 3.1,

Table 3.1 Compounds Studied by MPI Mass Spectrometry with the PSI Interface.

Compounds	M.W.	M.P (°C)	Major Ions [m/z (% rel. int.)
(a) PAHs			
2-Methylanthracene	192	204-206	192(100)
9-Chloroanthracene	212	100-101	212(100), 178(99)
1-Aminoanthracene	193	114-118	193(100), 165(36), 139(10), 63(16), 51(7), 39(13), 27(4)
2-Methylnaphthalene	142	34-36	142(100), 115(7), 63(7), 51(3), 39(5)
Triphenylene	228	197-200	228(100)
Anthranilic acid	137	144-148	93(100)
(b) Pineal Indoles			
Tryptophan	204	289-290	204(100) 130(47)
Harmaline	214	232-234	214(100)
Melatonin	232	116-118	232(100), 174(41), 160(53)
5-Methoxytryptamine	190	121-123	190(100), 160(84), 117(9), 30(22)
Tryptophol	161	59	161(100), 130(43), 103(12), 77(22), 51(77)
5-Hydroxyindole-3-acetic acid	191	161-164	191(100), 146(32)
(c) Catecholamines			
Tyramine	137	161-163	137(100), [illegible]53)
Octopamine[a]	153	169-171	153(69), 123(8), 30(54)
Synephrine	167	187	167(24), 123(8), 44(100)
Metanephrine[a]	197	175	197(21), 153(9), 44(100)
Vanillic acid	168	210-213	168(100)

Table 3.1 (Continued)

Compounds	M.W.	M.P (°C)	Major Ions [m/z (% rel. int.)
4-Hydroxy-3-methoxyphenyl-acetic acid	182	142-145	182(100), 137(33)
4-Hydroxy-3-methoxymandelic acid	198	132-134	198(100), 153(5), 65(9)
(d) Neuroleptic drugs			
Chloropromazine[a]	318	194-196	318(20), 274(3), 86(9), 58(100), 44(9)
Desipramine[a]	266	214	266(100), 208(17), 194(15), 72(20), 58(17), 44(32)
Imipramine[a]	280	174-175	280(100), 236(34), 208(9), 194(6), 86(28), 58(52), 44(7)
Promazine[a]	284	181	284(23), 86(8), 58(100), 44(9)
(e) Volatile molecules			
Phenol	94	43	94(100), 65(10), 39(8)
4-Propylphenol	136	b	136(100), 107(88), 77(10), 27(10)
2-sec-Butylphenol	150	16	150(94), 121(100), 107(3), 91(3), 77(14), 51(10), 39(5), 27(6)
1-Benzylpiperazine	176	b	176(100)
o-Anisidine	123	6	123(100), 108(31), 80(15), 51(8), 39(4), 27(3)
4-Acetaminophenol	151	169-172	151(100), 109(36)
o-Cresol	108	31	108(100), 91(7), 77(10), 27(10)

[a] HCl salt. [b] Liquid.

only the thermally decomposed product is observed. This indicates that for thermally very labile compounds this interface involving rapid heating may still cause decomposition.

It should also be noted from Table 3.1 that this interface is capable of introducing both volatile and nonvolatile sample molecules into a TOFMS. The ability of the system to also detect highly volatile species is an important aspect of this interface technique. For nonvolatile that can be dissolved in methanol, compounds with very high melting points can be transported into the mass spectrometer using the PSI interface. Figure 3.1 shows some typical MPI mass spectra of molecules studied by MPI mass spectrometry with this interface. All peaks shown in Figure 3.1 are from the molecular ions and their fragments.

3.2 Background Reduction

In this PSI interface technique, the sample molecules are vaporized and entrained into the ionization region of the TOFMS. Because only a small portion of the gas phase neutral molecules is ionized, most samples will condense on the wall of the lens assembly of the TOFMS. These molecules and their decomposed products will eventually become the background for the analysis of other samples or the same sample in the next run. Due to the possible overlapping of the molecular ion and fragments with the background signals, the sensitivity for the detection of molecules of interest will be reduced and the structural information obtained from the mass fragmentation pattern will suffer. In the work of interfacing HPLC with TOFMS, this cross-contamination can be quite severe, especially with the limited pumping capacity we have here. Thus the background problems need to be solved.

A method that has been developed for background reduction in our laboratory [100], based on the ion trajectory differences between the sample ions generated from

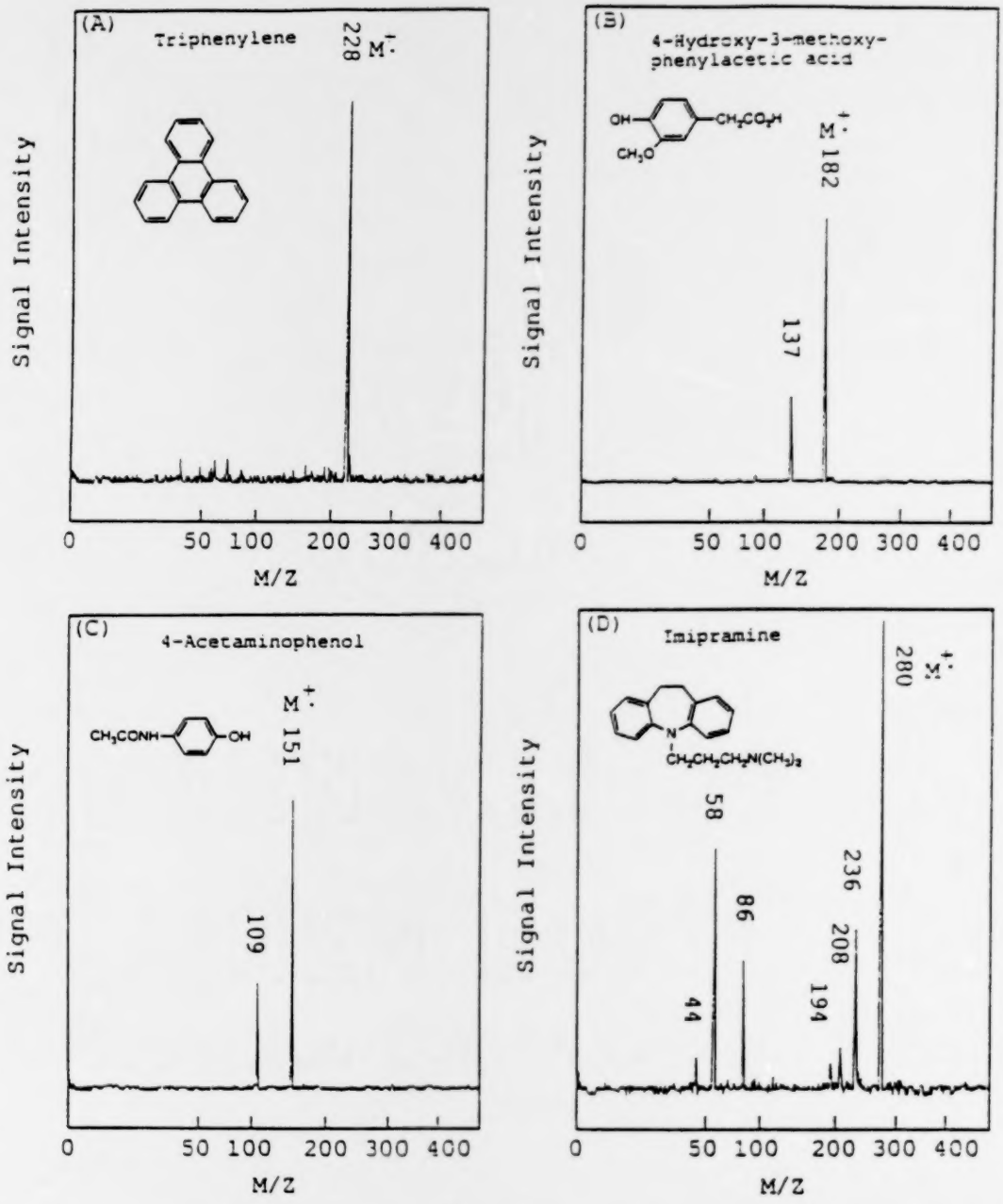

Figure 3.1. MPI mass spectra of (A) triphenylene, (B) 4-hydroxyl-3-methoxyphenylacetic acid, (C) 4-acetaminophenol, and (D) imipramine. The ionization laser beam is at 266 nm with its power density about 1 x 10^6 W/cm^2.

the jet-cooled molecules and the background ions during the flight from the acceleration region to the detector, can only be applied to a reflectron TOFMS. Thus, the method is not suitable for this work in which a linear TOFMS is used. An alternative method is to use a liquid nitrogen (LN_2) trap to condense the background molecules as well as the solvent vapor. A liquid nitrogen trap has been used to reduce the background in a linear TOFMS by Lubman and Jordan [18, 101]. Here we show that the liquid nitrogen trap from Jordan Co. can be used to reduce the back-ground signals very efficiently for this PSI interface.

Figure 3.2 (A) shows the MPI mass spectrum of the background molecules obtained by using the 266-nm laser beam. This represents a typical background spectrum obtained during the LC/TOFMS experiments. It is quite clear that the background signals are very strong. Figure 3.2 (B) shows the MPI mass spectrum of aniline along with the background signals. Note that the relative intensity of the individual peak from the background signals has been changed. This can probably be attributed to the fact that the sample molecules expand into the vacuum and push some background molecules away, resulting in a variation of the background molecule's distribution within the ionization region [100]. Thus, it is difficult to use background subtraction method to eliminate the background peaks. This is particularly true when extensive fragments are produced for structural analysis. Figure 3.2 (C) shows the MPI spectrum of the background with the LN_2 trap filled. All experimental conditions except the vacuum pressure are the same as those in Figure 3.2 (A). As Figure 3.2 (C) illustrates, the background signals are now dramatically reduced. Figure 3.2 (D) is mass spectrum of aniline. This figure illustrates that fragment ions from aniline can be clearly identified.

Besides background reduction, the use of a LN_2 trap can also reduce the vacuum pressure. Without LN_2 being filled in the trap, the pressure is normally at 5×10^{-7} torr in the detector region when the nozzle is off. However, when the nozzle is open, the

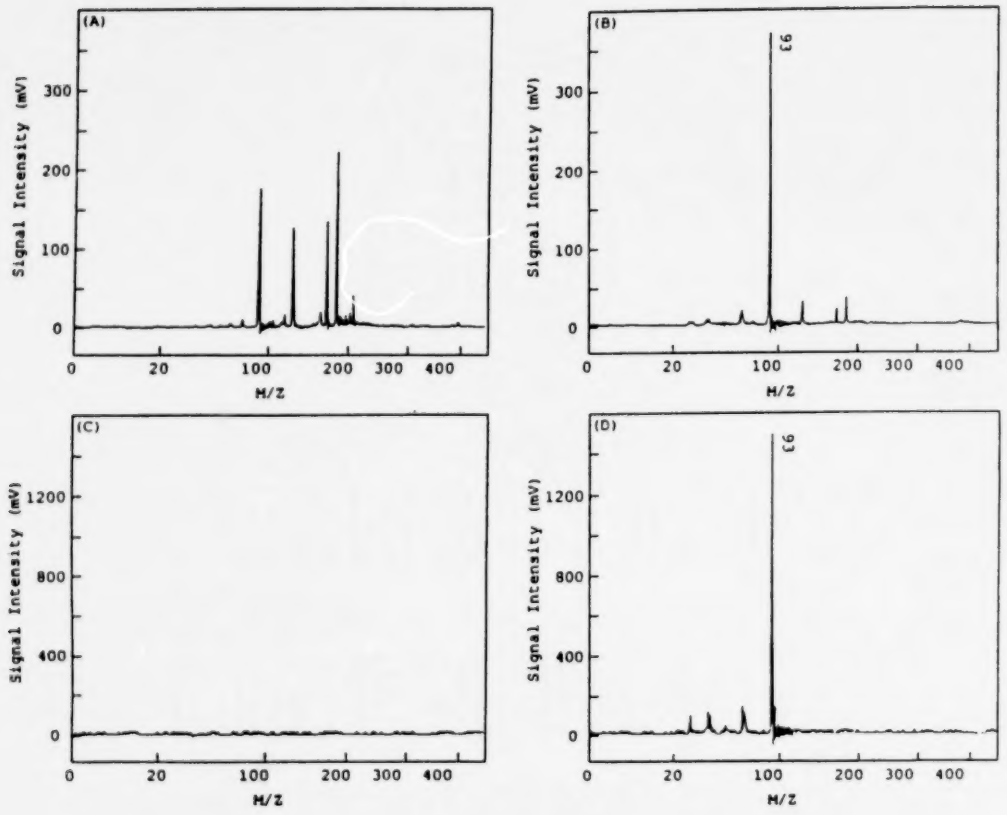

Figure 3.2. MPI mass spectra of (A) background, (B) aniline with background, (C) background with the LN_2 trap filled, and (D) aniline with the LN_2 trap filled. The ionization laser beam is at 266 nm with its power density about $2x10^6$ W/cm^2.

pressure rises to 2 x 10^{-5} torr. After the LN_2 trap is filled with liquid nitrogen, the pressures are 1 x 10^{-7} torr with the nozzle off and 1.5 x 10^{-7} torr with the nozzle on. It is also found that this reduction of the vacuum pressure increases the signal intensity. In addition, it allows us to use higher voltages for ion acceleration without any problems such as arcing. We find that by using 12.5 kV for ion acceleration instead of 5 kV, signals can be generally enhanced about 5-10 times for the compounds studied. It should be noted that when the system is continuously being operated, a full tank of liquid nitrogen in the trap (about 4 liters) can last for about 5 hours without refilling.

3.3 Performance of the on-line LC/TOFMS system

Figure 3.3 shows the chromatograms of two polyaromatic hydrocarbons (PAHs), namely, phenanthrene and 9-bromophenanthrene. A mixtures of these two PAHs at an amount of 100 ng each is separated by using the C-18 column with 95% methanol and 5% water as the mobile phase at a flow rate of 0.8 mL/min. Figure 3.3 (A) is the LC/UV chromatogram recorded at 266 nm from the diode array detector. Peaks 1 and 2 are from phenanthrene and 9-bromophenanthrene, respectively. Laser-induced multiphoton ionization is performed using a wavelength of 266 nm at a repetition rate of 10 Hz. The ionization laser power is estimated to be 5 x 10^6 W/cm^2. The mass spectrum of phenanthrene shows a dominated peak at m/z 178 from the molecular ion, where the most intense peak in the mass spectrum of 9-bromophenanthrene is from the molecular ion with the loss of bromine (m/z 177). The data system is operated at a record length of 2 Kbytes/spectrum and a resolution of 10 ns/point. After the data collection, the peak areas of the dominated ions are integrated individually, and then added together to generate the ion chromatogram shown in Figure 3.3 (B). As Figure 3.3 illustrates, the ion chromatogram is almost the same as the UV chromatogram in terms of peak shapes and retention time. No significant peak broadening and other chromatographic distortions are found. It should be noted that data smoothing can also be performed to

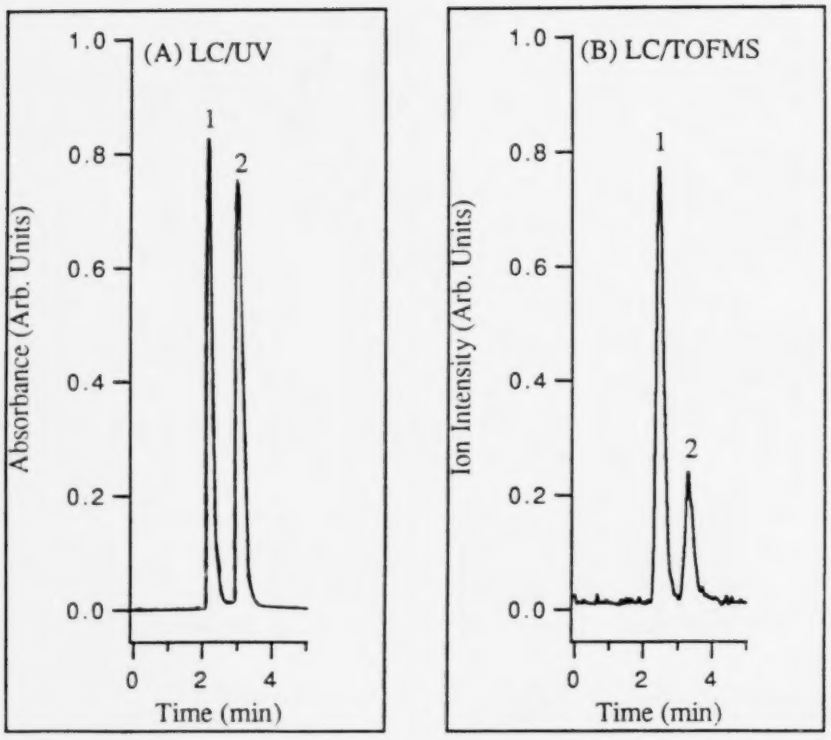

Figure 3.3. (A) LC/UV chromatogram, and (B) total ion chromatogram of a mixture of phenanthrene (peak 1) and 9-bromophenanthrene (peak 2).

improve the signal-to-noise (S/N) ratio without significant degradation of the chromatographic resolution.

Figure 3.4 illustrates a series of repeated injections of different concentrations of caffeine. In this experiment, the molecular ion peak is monitored and integrated to produce a flowgram. As Figure 3.4 shows, for five injections at each concentration, the peak areas are quite reproducible. The relative standard deviation (RSD) for each set of peaks is shown above these peaks in the figure 3.4. We find that reproducible results can also be obtained for other compounds. The average RSD is in the range 4-8%. However, the RSD increases to about 10-20% when the amount of the sample injected is close to the detection limit.

Memory effects of the PSI interface are also investigated. This is studied by making a blank injection after an injection of a sample. Different concentrations of samples are used. In all cases, no peaks are detected in the blank injections, which indicates that there are no memory effects associated with this PSI interface.

3.4 Parameters affecting the LC/TOFMS performance

The above examples demonstrate that the PSI interface is well suited for combining LC with TOFMS. Next we need to study the major parameters affecting the performance of the LC/TOFMS system. These include the flow rate and the composition of the mobile phase, the temperature of the sample vaporizer and the capillary tube, laser power density, laser repetition rate, and the flow rate of the makeup gas which is introduced into the samplevaporizer directly by passing through the solenoid and the long channel used for holding the plunger. Most of these experimental parameters have been investigated [102] in our laboratory.

Figure 3.5 shows the results obtained with a series of injections of 1μg of indole-3-acetic acid into the methanol stream at different flow rates using a C-18 column.

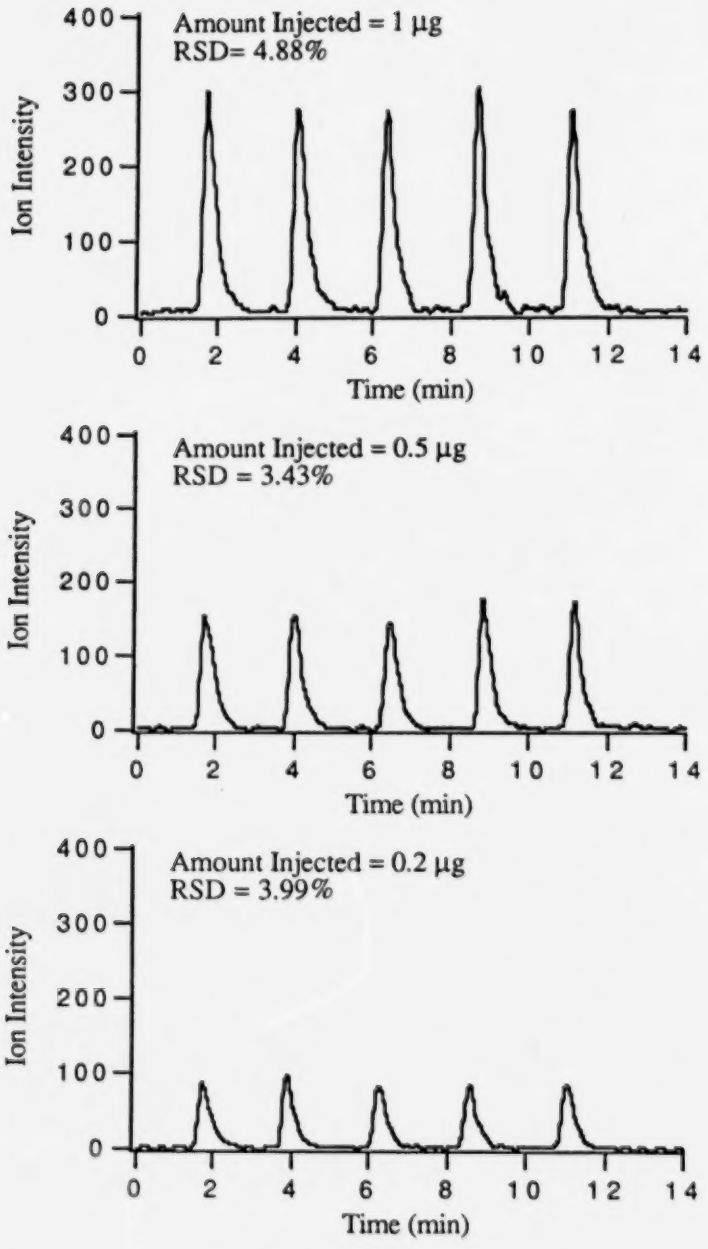

Figure 3.4. Flowgrams for repeated injections of different concentrations of caffeine.

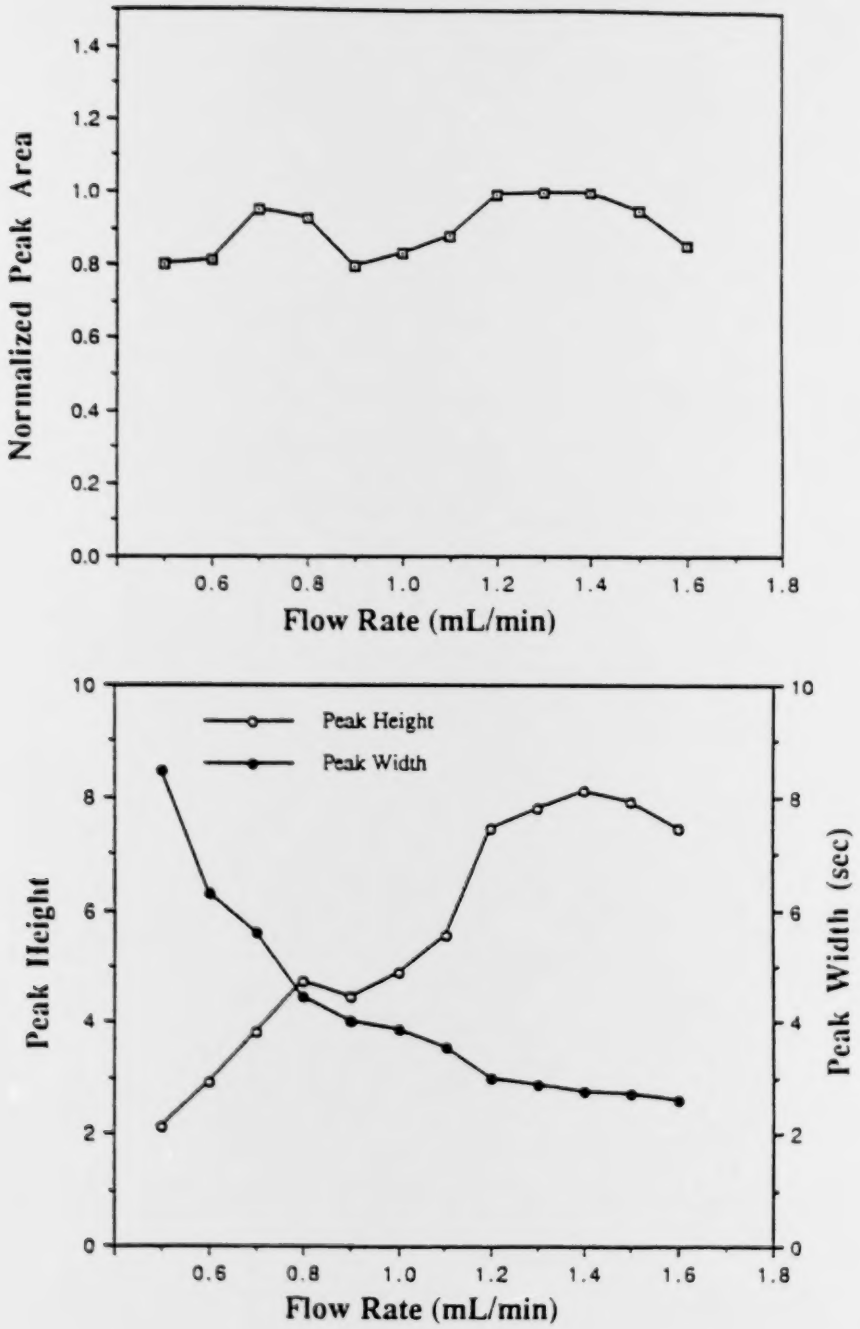

Figure 3.5. Mobile phase flow rate dependence on the performance of the PSI interface. Indole-3-acetic acid (1μg per injection) is used as the test sample. Methanol is used as mobile phase.

All experimental conditions except the flow rate are kept constant. In particular, careful adjustments are made each time when the flow rate is changed to ensure the temperatures of the sample vaporizer and the capillary tube remain constant. As one would expect, a higher flow rate requires more heating power. As Figure 3.5 indicates, the peak height increases and the peak width decreases as the flow rate changes from 0.5 to 1.6 mL/min. However, the peak area, which is related to the amount of the sample injected, does not vary significantly across the entire flow rate range used. In this case, a boxcar integrator combined with a chart recorder is used for recording ion chromatograms. The peak area is measured by cutting out the peak and determining its weight relative to the weight of a known area of the chart recorder paper. This study indicates that the PSI interface is capable of introducing high flow rate LC effluent, comparable to the flow rates used in conventional LC, into the time-of-flight mass spectrometer.

Various organic solvents including methanol, acetonitrile, hexane, and acetone have been tested for suitability for the PSI interface. It is found that these solvents and mixtures with differing proportions can be used without the need to change the interface conditions. Water can also be used as the mobile phase. However, in this case the detection sensitivity generally decreases as the water content increases, as shown in Figure 3.6. Figure 3.6 plots the scaled peak areas for tryptophol, indole-3-acetic acid, and tryptamine, separated by using a C-18 column, as a function of water content in the mobile phase. Here the peak areas of these three compounds are scaled to fit the data into the same figure. Note that, with 100% water used for separation, the peak area for tryptophol is not shown in Figure 3.6. This is because under this condition the peak of tryptophol in the chromatogram becomes too broad to calculate its area.

Several other compounds have also been studied with or without a column. We find that about one order of magnitude reduction in sensitivity generally observed when the mobile phase is changed from an organic solvent to pure water. This sensitivity

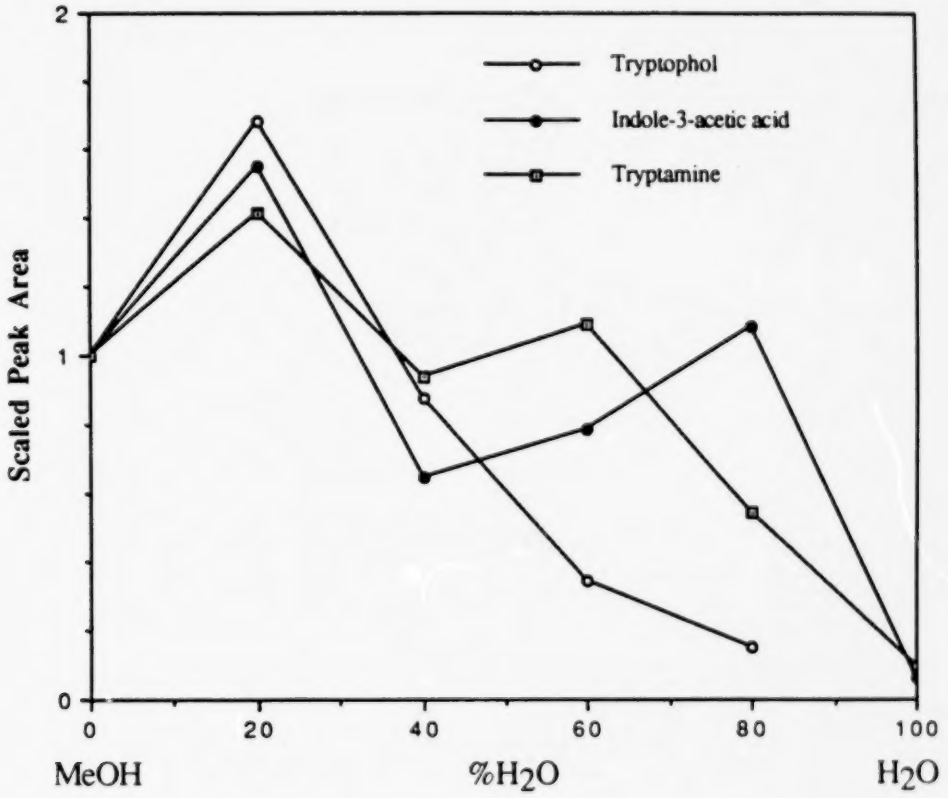

Figure 3.6. Scaled peak area as a function of the water content in the methanol/water mobile phase. The flow rate is kept constant at 1 mL/min.

reduction is mainly due to the pressure increase in the vacuum chamber resulting in lower ion detection sensitivity, although other factors related to the sample introduction process may also play a role. When water is used, the pressure rises from 5×10^{-7} to 5×10^{-6} torr. It is our experience that a 10-fold pressure increase in this mass spectrometer often results in a 5-10 fold signal reduction. It appears that even with the liquid nitrogen trap, the present vacuum pumping system is not capable of removing water very efficiently. A large pump and/or an addition trap may overcome this problem. Nevertheless, our study indicates that most and the common mobile phases used in HPLC can be used for the PSI interface.

For LC separation, solvent modifiers and buffer solutions are often used. We have examined the feasibility of the use of these chemicals in the PSI interface. We find that nonvolatile buffers such as potassium phosphate buffer can clog the capillary tube during the aerosol generation in the interface. However, volatile buffers such as ammonium acetate/acetic acid buffer can be readily used. In addition, it is found that various relatively volatile solvent modifiers such as trifluoroacetic acid can be used with the interface.

To optimize the performance of the interface, The temperature of the sample vaporizer and the capillary tube are found to be critical to enhance the signal stability and the detection sensitivity. Figure 3.7 shows the peak area of indole-3-acetic acid as a function of the sample vaporizer temperature. The temperature is measured near the nozzle front and methanol is used as the mobile phase. As Figure 3.7 indicates, the peak area increases as the temperature rises. A sharp increase in sensitivity is observed when the temperature exceeds about 480 ^{o}C. This sharp rise might be attributed to the fact that a threshold temperature exists and has to be reached for complete desolvation and vaporization. The threshold temperature appears to be compound dependent. Although there is no direct correlation between the threshold temperature and the melting point of

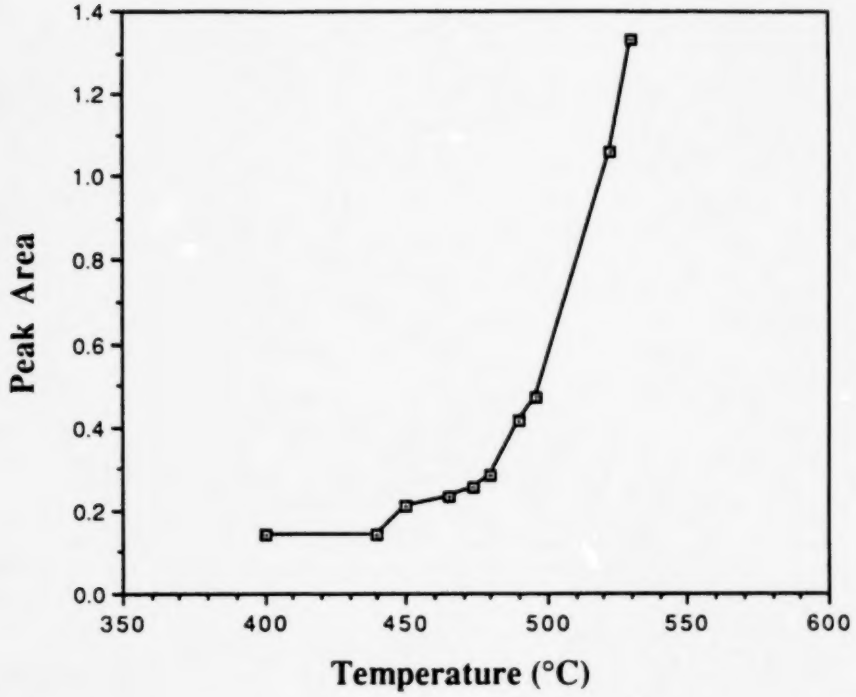

Figure 3.7. Peak area as a function of the temperature of the sample vaporizer. Indole-3-acetic acid is used as the test sample. Methanol is used as the mobile phase at a flow rate of 1mL/min.

the chemical injected, it is found that in general the threshold temperature increases as the compound becomes less volatile. For example, the threshold temperature are about 500°C for vanillic acid (mp=210-213°C) and 510°C for chrysene (mp=252-254°C). Thus, in LC/TOFMS with the PSI interface, the temperature of the sample vaporizer is always kept at maximum. The maximum temperature attained in the present system is limited by heating capacity of the thermal coaxial heating wire. It should be noted that the use of even higher temperatures for sample vaporization will not significantly increase the possibility of thermal decomposition. Recent study in this laboratory [103] finds that once a minimum heating rate is reached for a particular compound, the degree of thermal decomposition is independent of heating temperature used in the range from 200 to 550°C.

Another important parameter is the temperature of the capillary tube where the LC effluent is converted into fine aerosols. Figure 3.8 plots the peak area of indole-3-acetic acid at different tube temperatures. When the temperature reaches above 150°C, peak area does not vary significantly. Other compounds with less volatility such as chrysene display similar temperature dependent behavior as indole-3-acetic acid. Thus the temperature of the capillary tube is normally set at 150-200°C. The use of higher temperatures sometimes resulting in the deposition of the sample inside the tube and thus causes clogging of the tube. Also, it is found that the use of a long capillary tube (>5 cm) is not necessary to generate stable signal. The shorter the tube the less the tube clogging problem. With a 5-cm long capillary tube, tube clogging rarely occurs.

We have also studied the flow rate dependence of the makeup gas on the performance of the interface. Figure 3.9 shows the peak area of indole-3-acetic acid as a function of the CO_2 flow rate. The mobile phase is methanol at a flow rate of 1 mL/min. Similar results are obtained when the mobile phase flow rate is in the range of 0.5 to 1.6 mL/min. It is found that the increase of the flow rate reduces the sensitivity of the

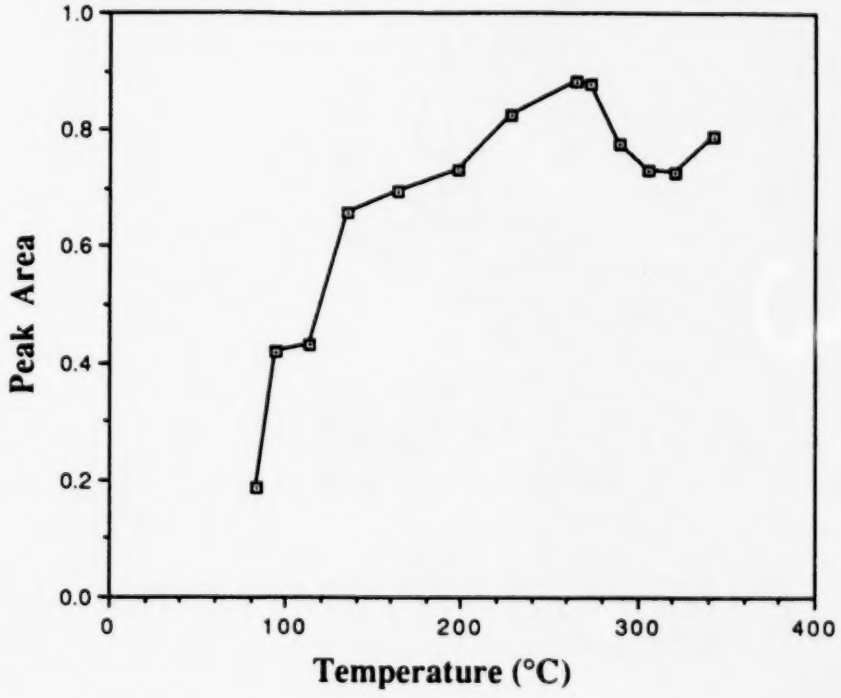

Figure 3.8. Peak area as a function of the temperature of the capillary tube. The LC conditions are the same as those used in Figure 3.7.

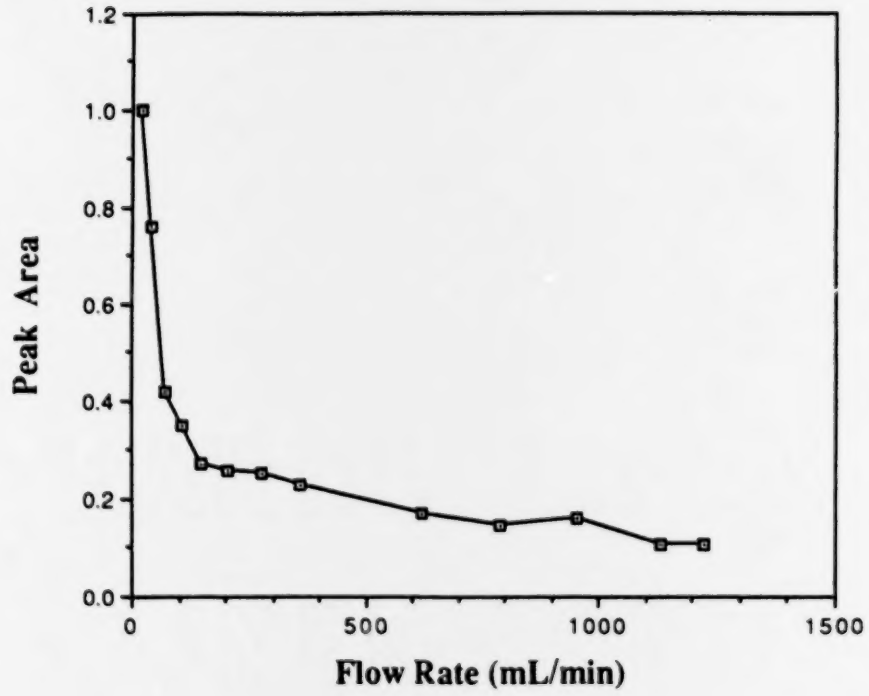

Figure 3.9. Peak area as a function of the makeup gas flow rate. The LC conditions are the same as those used in Figure 3.7.

system. However, the peak width is independent of the makeup gas flow rate in the working range examined. This is also true for other compounds examined including vanillic acid and chrysene. It appears that the main function of the makeup gas in the interface for LC/TOFMS is to prevent the feedback of the hot vapor into the cold solenoid. The minimum flow rate needed to prevent the feedback is dependent on the mobile phase flow rate. It is our experience that when the CO_2 flow rate used is less than 100 mL/min and the mobile phase flow rate is 1 mL/min, hot vapor feedback can sometimes occur during the experiment. Thus, the flow rate of the makeup gas is always kept above 100 mL/min, although the sensitivity may not be at its optimal as shown in Figure 3.9. Other makeup gases such as helium and argon are also tested and similar results are observed. However, CO_2 is chosen here since it can be readily trapped by the liquid nitrogen trap once it is expanded into the vacuum system, resulting in low operational vacuum pressure.

The effect of the experimental repetition rate on the S/N ratio of the ion chromatogram is also studied. If the intensity of the ions generated from one laser pulse remains constant as the repetition rate changes, the use of a high repetition rate would allow one to average many shots to generate one time point, resulting in a high S/N ratio. Figure 3.10 plots the S/N ratios of peak 1 (see Figure 3.3 (B)) in the ion chromatograms obtained at various repetition rates ranging from 2 Hz to 20 Hz. The chromatograms used for calculating the S/N ratio are from the n-point average results of the raw data, where n is the repetition rate. Each data point is the average data of five repeat runs. In the experiment, other than the repetition rate, all other parameters such as the laser power and the interface pulse voltage are kept constant.

As Figure 3.10 indicates, a maximum S/N ratio is reached when the repetition rate is close to 10 Hz and the ratio decreases as the rate further increases. This S/N ratio decrease results from the reduction of the signal intensity of the ions detected from one

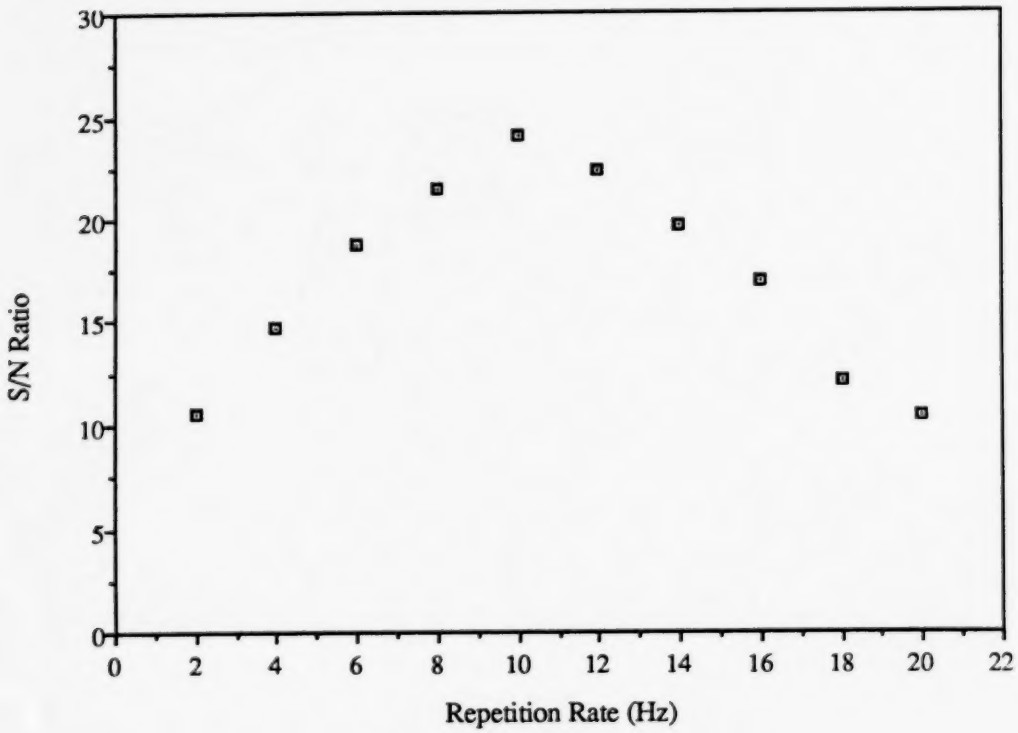

Figure 3.10. Signal-to-noise ratio of the first peak in the ion chromatogram in Figure 3.3 (B) as a function of the repetition rate of the experiment in the PSI-LC/TOFMS.

laser shot. The signal reduction is most likely due to the pressure increase in the system when the pulsed interface is operated at a high repetition rate. We noted previously that a pressure increase of 10 times in our system would result in about 10-fold decrease in the ionization signal intensity mainly due to the reduction of the detection efficiency. In this study, it is found that the vacuum pressure reading does not change when the repetition rate changes from 1 to 10 Hz and remains at about 8×10^{-7} Torr. However, when the repetition rate changes from 10 to 20 Hz, the pressure gradually increases to 2×10^{-6} Torr. This indicates that at higher repetition rate the liquid nitrogen trap used for condensing the solvent in our TOFMS system becomes less effective and cannot completely trap the solvent introduced into the system.

This study indicates that there is an optimal sample introduction rate limited by the capability of the vacuum system. The purpose of using the pulsed sample introduction instead of a continuous sample introduction is to introduce a very large amount of sample in one single pulse without overloading the vacuum system. The vacuum pressure increases as the repetition rate increases and/or the sample throughout per pulse increases. However, as shown in Figure 3.10 with repetition rates less than 10 Hz, the increase of the repetition rate by n times only results in the increase of the S/N ratio by a factor of a square root of n, while the signal intensity increases linearly as the sample throughout increases. Thus, the strategy in designing the PSI interface is to increase the sample throughout per pulse while using a repetition rate sufficient not to degrade the chromatographic resolution.

Clustering. Cluster formation is very likely during the supersonic jet expansion [105]. This is particularly true in the cases where polar solvents are used. Solvents such as methanol and water can interact with sample molecules strongly to form clusters. Cluster formation will reduce the molecular ion peak intensity. In some cases such as the analysis of a mixture, peaks from the cluster ions will also make the

molecular ion peak assignment difficult. Thus, for analytical applications, cluster ions are usually undesirable. Fortunately, in this experimental set-up, we normally do not observe a significant amount of clusters, as illustrated in Figure 3.1. The reason for this is believed to be related to the fact that the temperature of the sample vaporizer of the nozzle is very high. It is known that the reduction of the nozzle temperature energetically favors the formation of clusters while heating the nozzle can reduce the population of clusters [106].

In the cases where we do observe the cluster ions, the variation of the delay time between the nozzle opening and the ionization laser pulse can eliminate the cluster ion peaks in the MPI mass spectrum. An example is shown in Figure 3.11. Figure 3.11 (A) is the MPI mass spectrum of indole-3-acetic acid at 266 nm with the delay time of 660 μs. Figure 3.11 (B) is the mass spectrum of the same compound obtained at the same experimental conditions as in Figure 3.11 (A), but with the delay time of 540 μs. As Figure 3.11 (B) shows the cluster ions are not detected when the delay time is set properly so that the laser beam intersects the front portion of the sample pulse. This portion of the molecular beam does not contain a significant amount of clusters. This finding is consistent with the results reported by Pang and Lubman [107] where a supercritical NH_3 fluid is used for sample delivery.

3.5 Sample transfer efficiency in the PSI interface

Now that the major parameters affecting the performance have been assessed, the next question to be addressed is concerned with the sample transfer efficiency associated with the PSI interface. An ideal interface would introduce all of the sample into the mass spectrometer. With a pulsed ion detection system such as TOFMS, one of the major goals in designing the PSI interface is to introduce a large amount of sample in a number of pulses to allow us to construct a chromatogram with a large peak area. The peak area is ultimately used for the determination of the sample concentration.

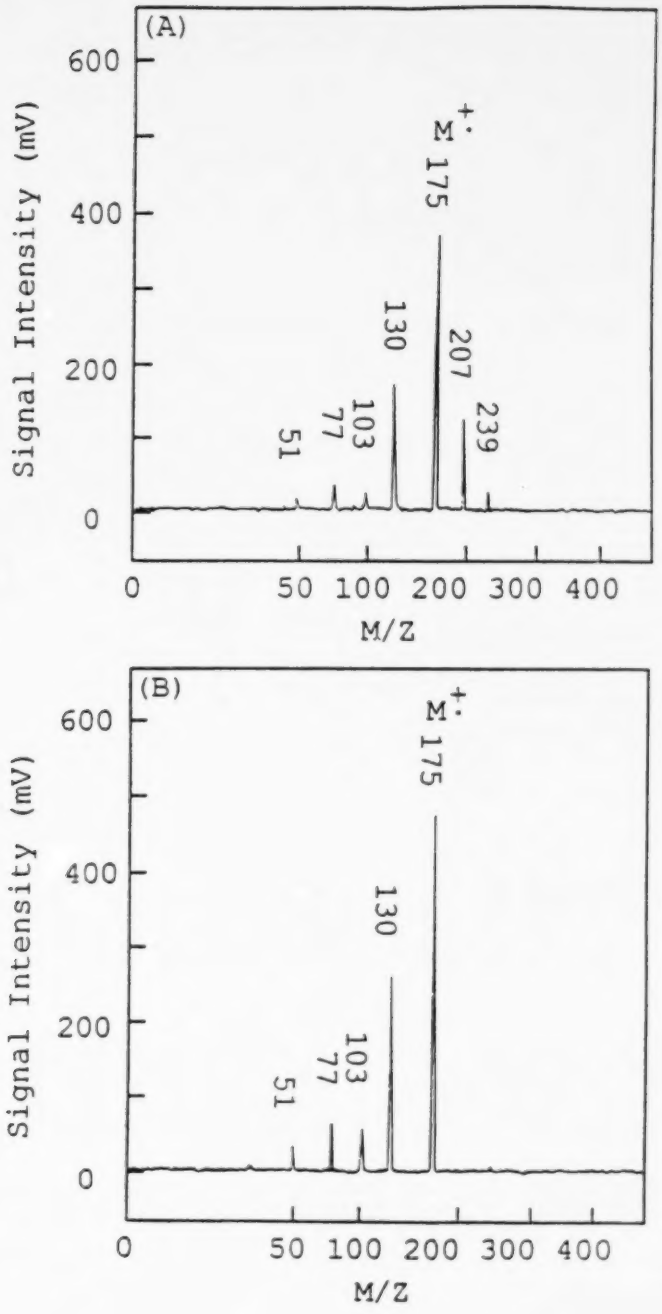

Figure 3.11. MPI mass spectra of Indole-3-acetic acid at different delay time: (A) Δt=660 μs and (B) Δt=540 μs. The ionization laser beam is at 266 nm with its power density about 4×10^6 W/cm^2.

The following experiment was performed to determine the sample transfer efficiency in the PSI interface. A liquid nitrogen cooled sample collector is placed about 2 cm away from the orifice of the PSI interface. A known amount of sample is injected into the interface and vaporized. After the gas phase molecules exit the orifice, they are condensed onto the sample collector. The amount of sample collected is then determined by using HPLC with a UV detector. The results of this measurement for several compounds are listed in Table 3.2. In this table, the sample transfer yield (Y) is defined as the ratio of the amount of the sample collected (N_{col}) to the amount of the sample injected (N_{inj}). It appears that the variation in transfer yield from the compound to compound is relatively small. This small variation could be duo to the differences in vaporization efficiency and the ability to generate a fine aerosol among the compounds examined.

In order to make a direct comparison of the sample transfer efficiency between a continuous sample introduction interface and a pulsed sample introduction interface, we use a term, effective sample transfer efficiency (E), to characterize the interface. Since quantitation in LC is based on the peak area in the chromatogram, we can define E as A_p/A_t, where A_p is the sample peak area of the chromatogram generated from the actual sample introduced by the interface in a continuous or pulsed form to the mass spectrometer, and A_t is the peak area of the chromatogram obtained by assuming the total sample injected is being continuously transferred into the MS system. In a continuous sample introduction interface, the calculation of the effective sample transfer efficiency is quite straightforward. Here, the peak area (A) is directly proportional to the total amount of sample being detected (N). A is equal to kN, where k is a constant related to the properties of the detector and the recorder. The peak area (A_p) from the chromatogram with an injection of N_{inj} moles of sample is equal to kN_{col}, if only N_{col} moles of sample are transported by the interface to the mass spectrometer and collected in the sample collector. However, the peak area (A_t) would be kN_{inj} if all of the sample

Table 3.2 Sample transfer efficiency of the pulsed sample introduction interface.

Compound	m.p. (^{o}C)	Transfer Yield (%)	Effective Transfer Efficiency (%)
Tryptophol	59	0.52	61
Pyrene	149-151	0.38	45
Indole-3-acetic acid	165-169	0.31	37
Acetaminophen	169-172	0.61	72
Triphenylene	197-200	0.53	62
Vanillic acid	210-213	0.44	52
Chrysene	252-254	0.38	45

injected were introduced into the mass spectrometer. Thus, the effective sample transfer efficiency is equal to N_{col}/N_{inj} or the sample transfer yield.

In the PSI interface, the sample introduced into the system is concentrated into a few numbers of pulses. From each sample pulse, an ionization signal or a data point can be generated. In the end, a chromatogram is constructed from these data points. Thus, the size of the peak area in this chromatogram is dependent on the intensity of the individual data points. The intensity of a data point is in turn directly related to the amount of the sample contained in the individual sample pulse. Although the total amount of sample pulsed into the vacuum over the entire peak elution time (N_{col}) is small in the PSI interface, the amount of sample per pulse can be quite high, resulting in a large peak area. Clearly, in the calculation of the effective sample transfer efficiency for the PSI interface, A_p is not equal to kN_{col}. However, A_t is still equal to kN_{inj} as defined above. Thus, $E=A_p/(kN_{inj})$. In reality, A_p (in arbitrary units) can be easily calculated from the chromatogram and Ninj is known.

To find out the k value, we need to examine carefully how we construct the chromatogram. From the experiment, we know that the individual sample pulse profile is close to a rectangular shape with a width of about 1 ms. Now if we assume that a chromatogram was constructed using a continuous ion detection technique, then the peak in the chromatogram would consist of a series of rectangles with equal widths, but different heights. The area of an individual rectangle (A_i) can be readily estimated by multiplying the height (H_i) by 1 ms and it should be equal to kN_i, where N_i is the amount of sample contained in the sample pulse. Thus, $N_i=A_i/k=(H_i \times 1)/k$. Since the sum of the amount of sample under all individual sample pulses should be the total amount of sample introduced into the mass spectrometer, we have $N_{col} = \Sigma N_i = \Sigma A_i/k$ or $k = \Sigma A_i/N_{col}$. Thus, $E = A_p/(kN_{inj}) = A_p/(\Sigma A_i/N_{col} \times N_{inj}) = A_p/\Sigma A_i \times N_{col}/N_{inj} = Y \times A_p/\Sigma A_i$.

To calculate the peak area, a curve fitting method is used. Figure 3.12 shows a typical flow injection peak (dot line) obtained by injecting indole-3 acetic acid into the LC/TOFMS system without the use of a column. The solid line is generated from a curve fitting program, Matlab (The Mathworks, Inc., Natick, MA). The experimental data fits well to an exponentially modified Gaussian function [108,109]. This function is used to determine the peak area as well as the peak height. The peak height is then used to calculate the area of an individual sample pulse at a given elution time according to the equation, $A_i = H_i \times 1$. The ratio between the peak area (Ap) in Figure 3.12 obtained by fitting function and the area sum of all individual sample pulses ($\sum A_i$) is determined to be 118. Thus, for indole-3-acetic acid, the effective sample transfer efficiency is 0.31% X 118 or 37%. This simply means that although only 0.31% of the sample or LC effluent is introduced into the vacuum system with the PSI interface, it would be equivalent to transfer 37% of the sample into the mass of the spectrometer with a continuous sample introduction interface. However, without a sample enrichment device, it is difficult to introduce 37% of the LC effluent into the vacuum without overloading the pumping system.

Since other compounds examined give similar peak profiles as shown in Figure 3.12, the E values listed in Table 3.2 are simply calculated by multiplying Y and 118. Table 3.2 shows that the effective sample transfer efficiency ranges from 37% to 72% for the compounds examined. This demonstrates that the PSI interface provides an efficient means of introducing LC effluent into the mass spectrometer without overloading the vacuum pumping system. Combined with a pulsed ion detection system, it should provide high detection sensitivity. However, the overall sensitivity of the LC/TOFMS system is related not only to the sample transfer efficiency but also to other factors such as the background noise level, the ionization efficiency, and the ion detection efficiency. Currently the detection limit of the system is compound dependent, ranging from pg to ng. For example, the detection limits for aniline and tryptamine are

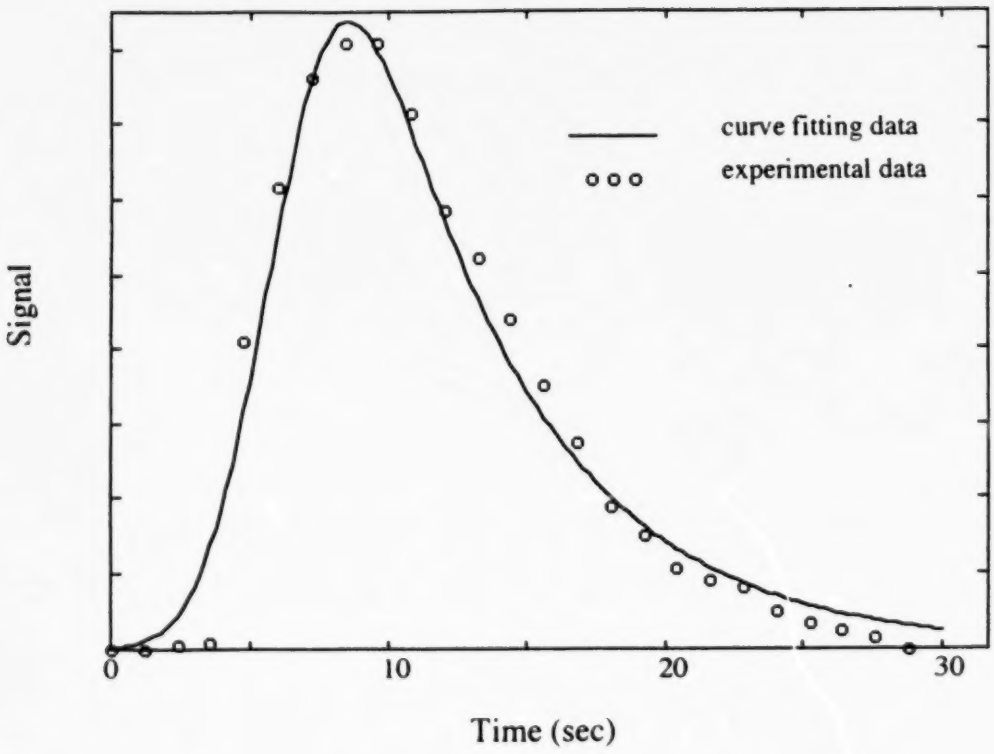

Figure 3.12. A typical peak obtained by the LC/TOFMS system. The dot line is the experimental result from the injection of indole-3-acetic acid. The solid line is generated from the curve fitting program.

about 10 pg and 100 pg, respectively. Figure 3.13 shows the mass spectrum of aniline obtained by using the PSI interface with a total injection of 20 pg of the sample (i.e., 1 pg/μL). In Figure 3.13, the peak at m/z 93 is from the molecular ion of aniline. The peak at m/z 45 is from the background molecules.

3.6 Applications of LC/TOFMS with the PSI interface

The final goal of the development of the PSI interface with LC/TOFMS is to apply this technique for real sample analysis such as the analysis of residues from drugs, antibiotics, and pesticides. In order to highlight the inherent capabilities of our PSI-HPLC/TOFMS, a few examples will be presented next. It is hoped that these applications will emphasize the analytical utility of our technique by means of real examples.

Pineal Indoles Figure 3.14 shows the UV and ion chromatograms of four indole derivatives, namely, 5-hydroxytryptamine (serotonin), tryptamine, melatonin, and tryptophol, with an injection of a mixture of 10 ng each in methanol. The separation is carried out under the isocratic condition with a mobile phase containing 40% methanol and 60% 0.3M acetic acid at a flow rate of 0.8 mL/min. Figure 3.14 (A) is the UV chromatogram recorded at 283 nm from the diode array detector. After the data collection, the peak areas of the molecular ions are integrated individually and then added together to generate the ion chromatogram shown in Figure 3.14 (B). As Figure 3.14 illustrates, the ion chromatogram is almost the same as the UV chromatogram in terms of peak shapes and retention times. No significant peak broadening and other chromatographic distortions are found. A representative mass spectrum (single shot) of each peak is shown in Figure 3.15. In our data system, these mass spectra are easily obtained by moving the cursor along the chromatogram, while simultaneously viewing the mass spectra in the upper graph named "Mass/Charge" (see Figure 2.3 (C)). All peaks shown in Figure 3.15 are from the molecular ions and their fragments. These

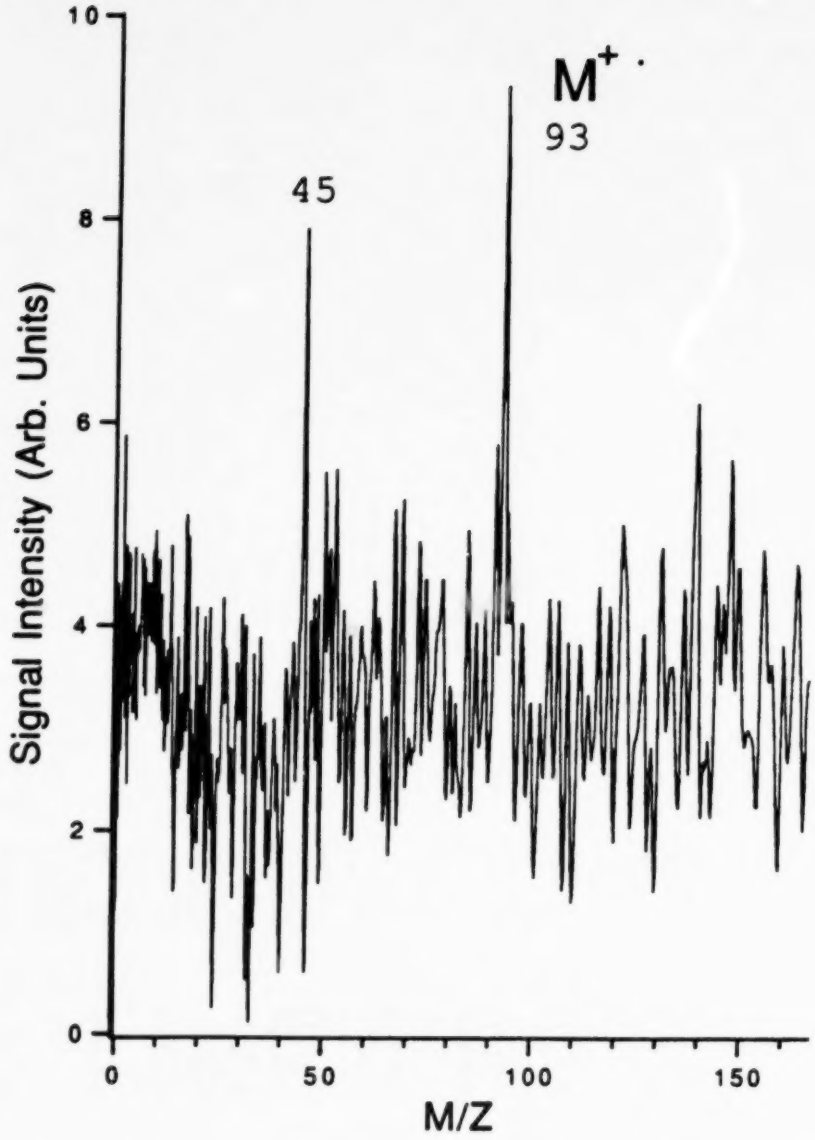

Figure 3.13 Multiphoton ionization mass spectrum of aniline obtained by using the PSI interface with a total injection of 20 pg of the sample. Methanol is used as the mobile phase at a flow rate of 1 mL/min. Laser ionization is performed at 266 nm with a laser power density of ~ 5 x 10^6 W/cm^2.

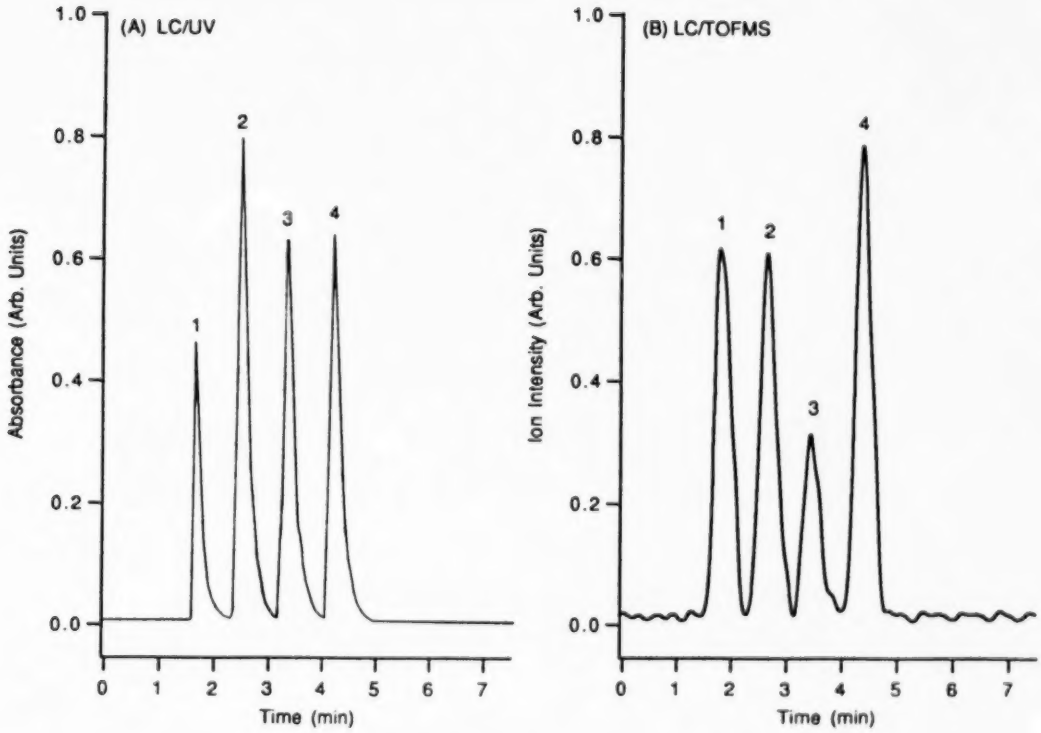

Figure 3.14. (A) LC/UV chromatogram, and (B) LC/TOFMS ion chromatogram of a mixture of indoles (10ng each): (1) 5-hydroxytryptamine (serotonine), (2) tryptamine, (3) melatonin, and (4) tryptophol.

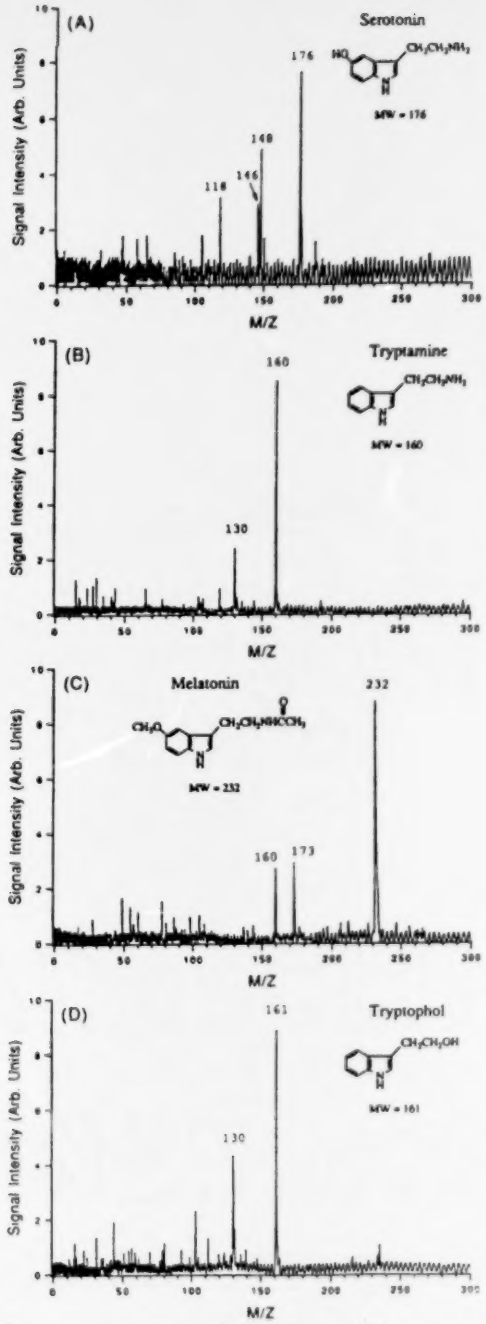

Figure 3.15. MPI mass spectra of indoles at the peaks corresponding to the ion chromatogram shown in Figure 3.14 (B): (A) 5-hydroxytryptamine (serotonin), (B) tryptamine, (C) melatonin, and (D) tryptophol. The laser ionization is performed at 266 nm with a laser power density of about 5 x 10^6 W/cm^2.

is determined to be about 300 ($t/(2\partial t)$). With this resolution, the isotope ratios can be readily revealed by expanding the peaks (figures not shown).

Dipeptides Peptides are important biological molecules and have been extensively investigated by using the existing LC/MS interfaces. Among these techniques that can handle the high flow rate used in the conventional LC system, thermospray has been demonstrated to be able to introduce small peptides into a MS [110, 111]. However, thermospray normally does not generate fragmentation or structural information of the peptide without the use of tandem mass spectrometry. On the other hand, the particle beam interface can provide structural information by obtaining the EI spectrum of the sample molecule. But it is known that nonvolatile species such as small peptides are difficult to be detected with this interface [77, 112, 113]. Similar to the particle beam interface, the PSI interface used here also generates gas phase neutral species prior to molecular ionization. However, the sample transport and vaporization processes between the two techniques are significantly different. Here, we show that small peptides can be introduced into the TOFMS by the PSI interface. Moreover, with MPI, it is possible to obtain hard ionization mass spectrum with extensive fragments for structural analysis.

Figure 3.16 shows the UV chromatogram (A) and the ion chromatogram (B) of four dipeptides. These dipeptides (in order of elution) are Tyr-Gly (MW=238), Gly-Trp (MW=261), Leu-Trp (MW=317), and Trp-Leu (MW=317). The mixture of these four dipeptides contains 400 ng of Tyr-Gly, and 200 ng each of other compounds, respectively. The mixture is separated under the isocratic condition with a mobile phase containing 48% methanol and 52% 0.1%-trifluoroacetic acid aqueous solution at a flow rate of 0.8 mL/min. It should be noted that because of the nonvolatile dipeptides, the temperature of the heated capillary tube is about 280^{o}C. Typical mass spectra of the four dipeptides are shown in Figure 3.17. The mass spectrum of each species is obtained by using the 266 nm laser beam with a power density of about 5 x 10^{6} W/cm^{2}.

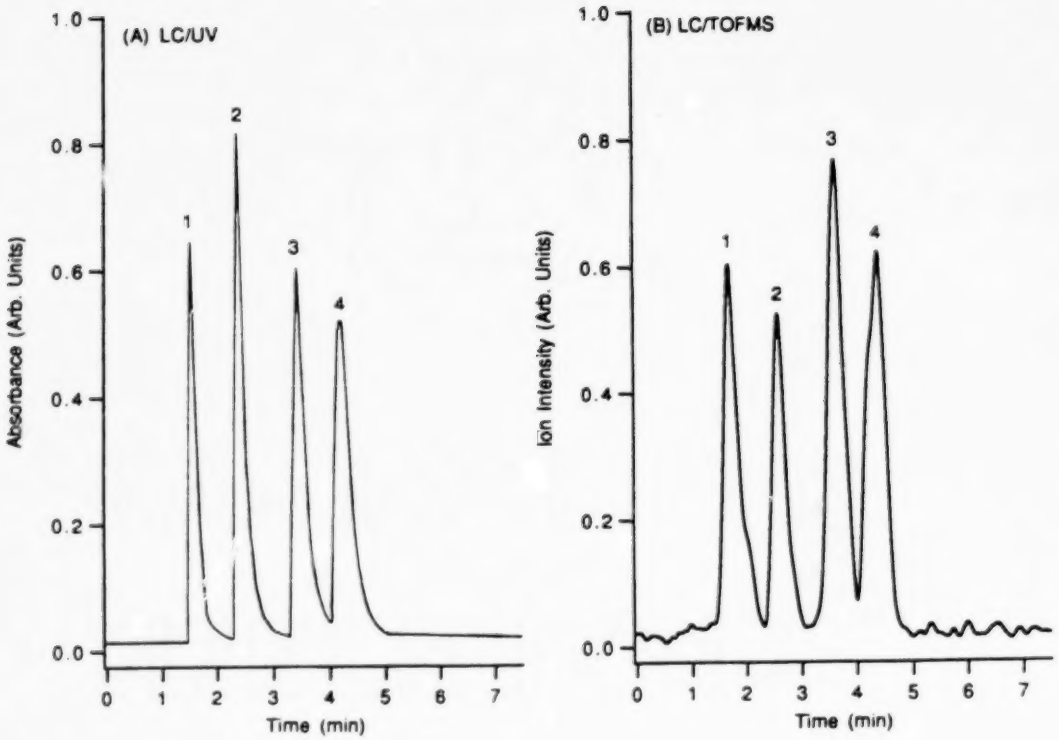

Figure 3.16. (A) LC/UV chromatogram, and (B) LC/TOFMS ion chromatogram of a mixture of four dipeptides: (1) Tyr-Gly (400 ng), (2) Gly-Trp (200 ng), (3) Leu-Trp (200 ng), and (4) Trp-Leu (200 ng).

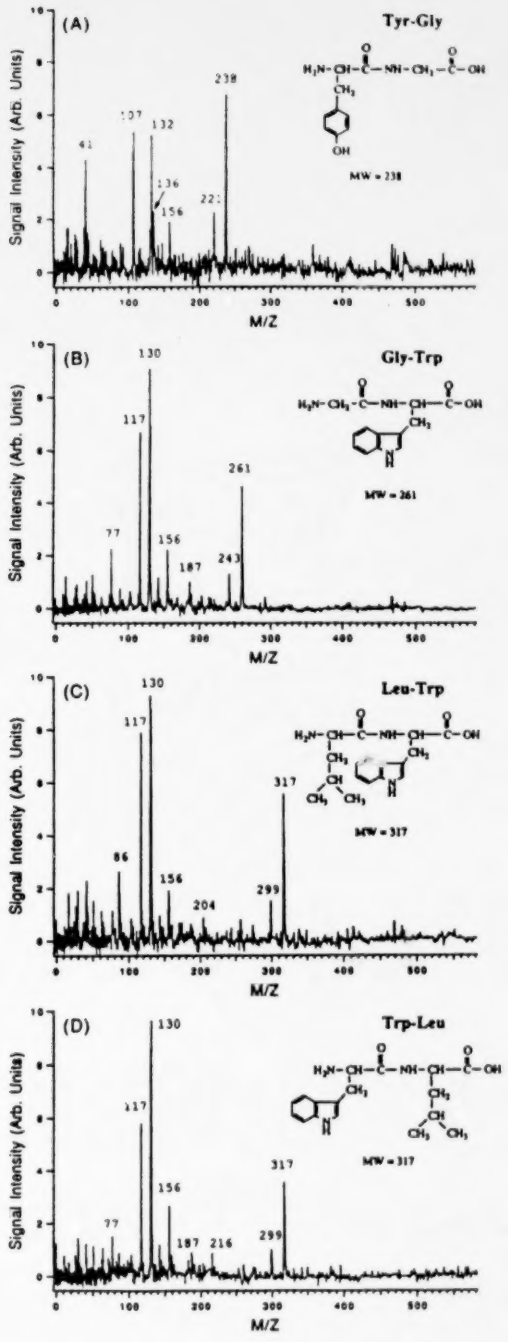

Figure 3.17. MPI mass spectra of (A) Tyr-Gly (MW=238), (B) Gly-Trp (MW=261), (C) Leu-Trp (MW=317), and (D) Trp-Leu (MW=317). The ionization laser beam was at 266 nm with its power density of about 7×10^6 W/cm^2.

As Figure 3.17 illustrates, an intense molecular ion peak along with a M-18 peak is observed for each dipeptide. This M-18 peak is believed that to be from the thermal decomposition product, cyclodipeptide, formed by the elimination of a water molecule from the original linear dipeptide [114-116]. This peak can also found in MPI mass spectra of dipeptides with laser desorption [114-116], pulsed FAB [117], and pulsed rapid heating [114, 98] for sample vaporization.

Except M-18, all other peaks in Figure 3.17 appear to belong to the fragments from the dissociation of the molecular ion. These fragments are quite informative for structural analysis. For example, the proposed fragmentation pattern for Gly-Trp (see Figure 3.17 (B)) is shown in Scheme I. This shows that the ability of generating fragments from this technique should be very useful for positive identification or structural confirmation of the molecule of interest.

PAHs Chromatography techniques have been widely used for analysis of environmental pollutants. However, for the analysis of organic pollutants, one of the most challenging problems is isomer discrimination [118]. The identification of different isomers in a mixture is very important. This is particularly true for the identification of polycyclic aromatic hydrocarbons (PAHs), since mutagenic or carcinopenic properties of PAHs depend strongly on isomeric structure and substitution. Although chromatography techniques can be used for the separation of isomers, the separation of isomers in a complicated matrix is often incomplete. Thus a selective detection method such as LC/MS is needed.

Figure 3.18 shows the chromatograms of a mixture of seven PAHs. These seven PAHs (in order of elution) are naphthalene, 1-methylnaphthalene, acenaphthene, fluorene, phenanthrene, 1-methylphenanthrene, and 9-bromophenanthrene. The mixture of these chemicals at amount of 10 ng each is separated under a solvent gradient condition. Initially, The mobile phase containing 70% CH_3OH and 30% H_2O is kept at

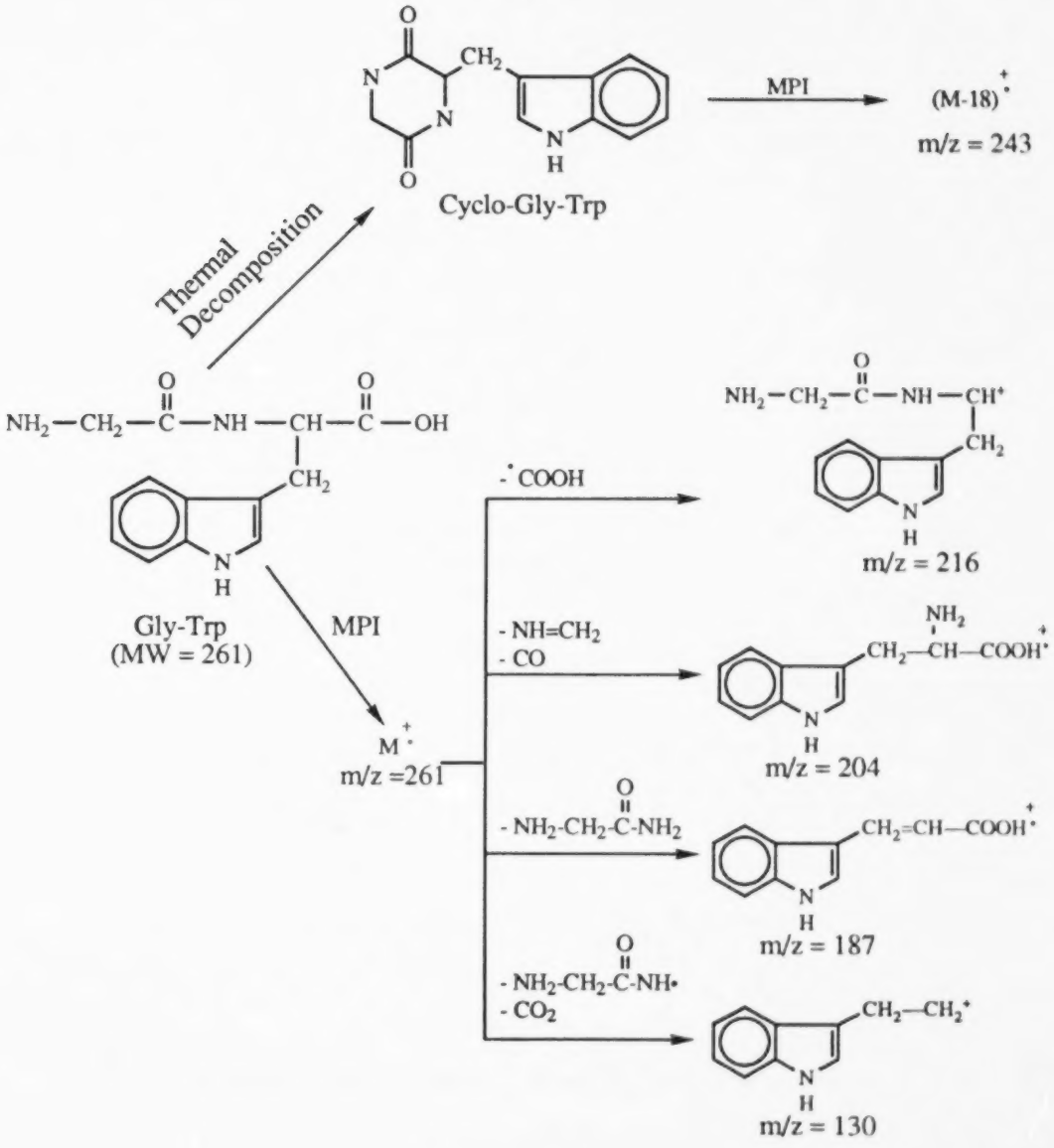
Cyclo-Gly-Trp
MPI
(M-18)+·
m/z = 243
Thermal Decomposition
Gly-Trp
(MW = 261)
MPI
M+·
m/z =261
-·COOH
m/z = 216
- NH=CH2
- CO
m/z = 204
- NH2-CH2-C-NH2
m/z = 187
- NH2-CH2-C-NH·
- CO2
m/z = 130

Scheme I

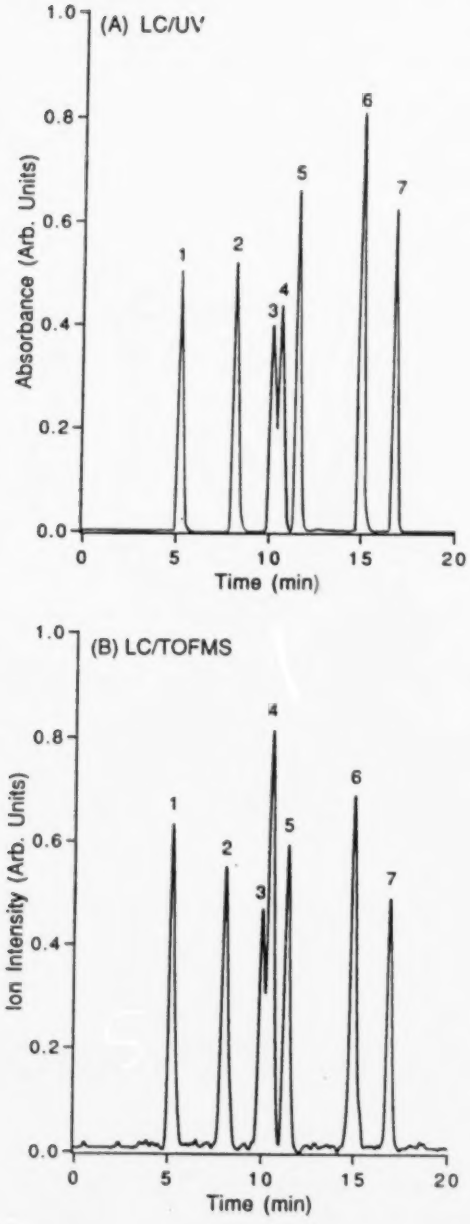

Figure 3.18. (A) LC/UV chromatogram, and (B) LC/TOFMS chromatogram of a mixture of seven PAHs.

a flow rate of 1mL/min for six minutes. Then the composition of the mobile phase is gradually changed from 70% CH_3OH to 100% CH_3OH in 20 min minutes. Figure 3.18 (A) is the LC/UV chromatogram recorded at 283 nm from diode array detector. Figure 3.18 (B) shows the ion chromatogram of these seven PAHs obtained by using LC/TOFMS with the PSI interface. The GPIB-based data system is used for recording and storing all the mass spectra during the experiment, followed by mass spectra data processing for generating the ion chromatogram. As Figure 3.18 illustrates, the LC/TOFMS ion chromatogram is almost the same as the UV chromatogram in terms of peak shapes and retention time. No significant peak broadening or other chromatographic distortions are found. Clearly, under the experimental conditions used, the separation of acenaphthene (peak 3) and fluorene (peak 4) in Figure 3.18 (B) is incomplete. However, by integrating the peak areas of the individual molecular ion, a selected ion chromatogram can be obtained. Figure 3.19 (A) and (B) are the selected ion chromatograms for acenaphthene and fluorene, respectively. Their MPI mass spectra are shown in Figure 3.20. It is obvious that TOFMS is superior for the detection of coelutes for LC, compared with a UV detector.

Quantitative Analysis of Caffeine in Instant Coffee The present LC/TOFMS technique can also be used to provide quantitative information. As example, we haveperformed quantitation of caffeine in instant coffee. A brand name of instant coffee purchased from a local store is dissolved in water and injected into a C-18 column for separation. The mobile phase is 50% methanol and 50% water at flow rate of 1 mL/min. Figure 3.21 shows the chromatograms of a brand name of instant coffee. Figure 3.21 (A) is the LC/UV chromatogram recorded at 274 mn from the diode array detector. Peak 1 is the peak of at least three nonseparated unknown components in the instant coffee. Peak 2 is the peak of caffeine in instant coffee. Clearly, under the experimental conditions used, the separation of caffeine and other components in instant coffee is incomplete. It should be noted that we can completely separated caffeine from other

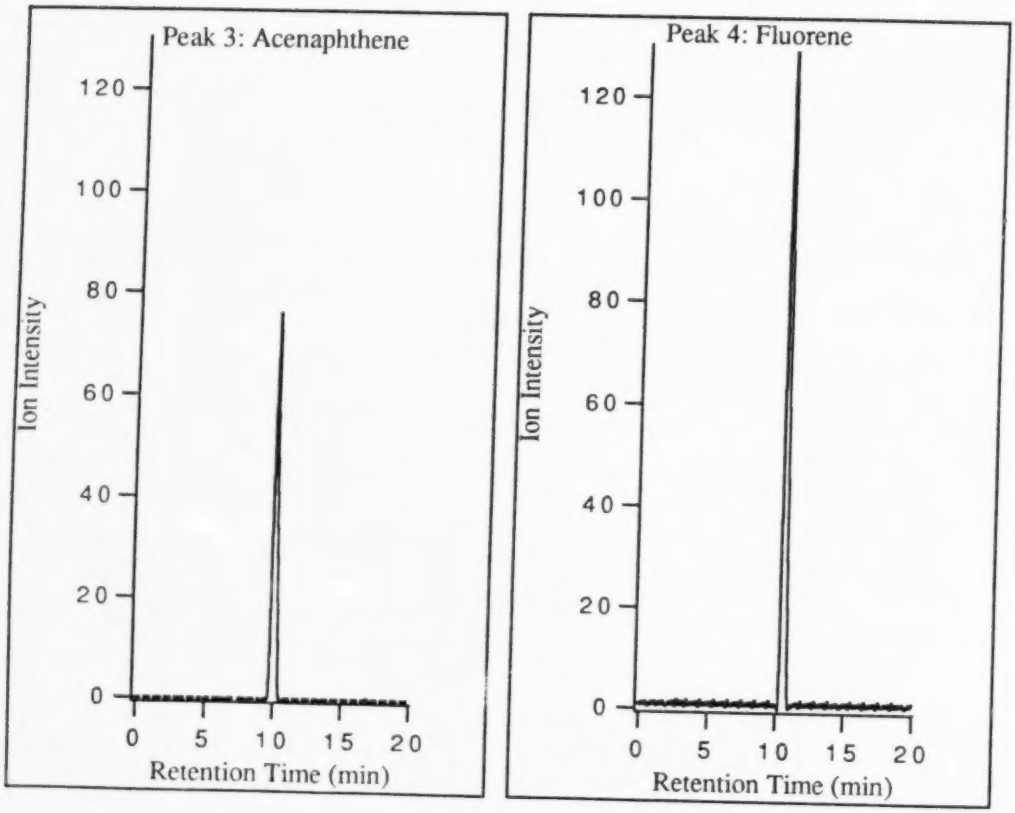

Figure 3.19. (A) the selected ion chromatogram of acenaphthene, and (B) the selected ion chromatogram of fluorene.

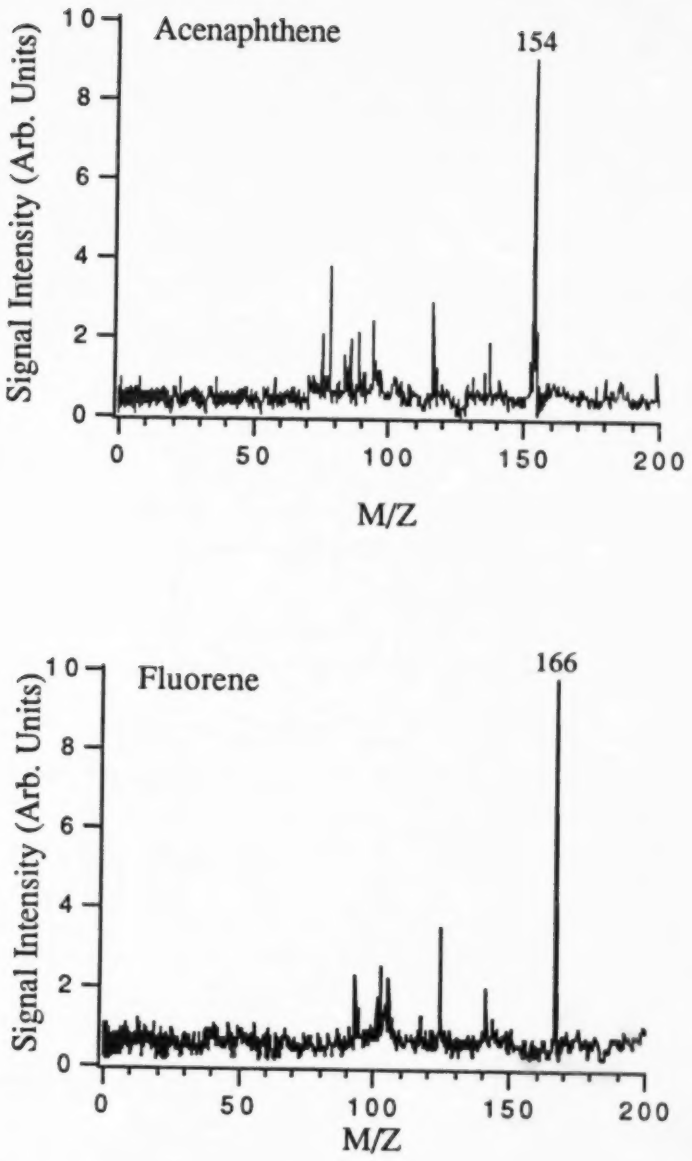

Figure 3.20. MPI mass spectra of acenaphthene and fluorene.

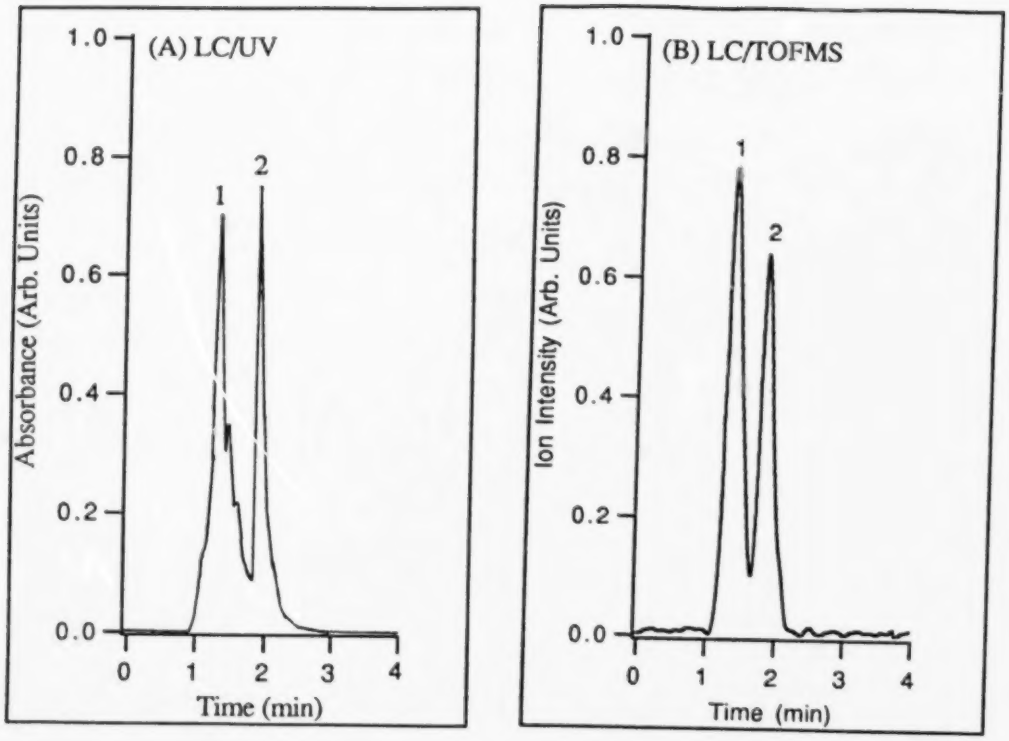

Figure 3.21. (A) LC/UV chromatogram of instant coffee; (B) LC/TOFMS chromatogram of instant coffee.

components in instant coffee by using high percentage water in mobile phase composition. However, our pumping system can not remove a large amount of water very efficiently. The detection sensitivity also decreases as the water content increases. Figure 3.21 (B) is the ion chromatogram of caffeine in instant coffee. The selected ion chromatogram is obtained by integrating the peak areas of caffeine molecular ion (M^+=194). The mass spectrum of caffeine is shown in Figure 3.22.

Figure 3.23 is the LC/UV calibration curve. The data of the peak areas (in arbitrary units) are expressed as an average of five sample injections. The peak areas are directly obtained from the printout of the HPLC integrator. As Figure 3.23 shows, an excellent linearity (R^2 = 1.00) is obtained from the calibration curve. By injecting the 1: 100 dilution of instant coffee into the LC column, the peak area of caffeine in instant coffee is obtained. Using the LC/UV calibration curve, we find that the weight percentage of caffeine in instant coffee is 2.31 ± 0.02%.

Figure 3.24 shows the LC/TOFMS calibration curve of caffeine. The data of the peak area (in arbitrary units) are also expressed as an average of five sample injections. The peak areas are obtained by integrating the molecular ion peak of caffeine. The calibration curve also has a very good linearity (R^2 = 0.993). From the calibration curve, we find that the weight percentage of caffeine in instant coffee is 2.37% ± 0.14%.

Comparing the LC/UV result with the result of LC/TOFMS, there is an excellent agreement between the two methods. This study indicates that our LC/TOFMS with a PSI interface is suitable for quantitative analysis. The results obtained by the technique is comparable with that by LC/UV.

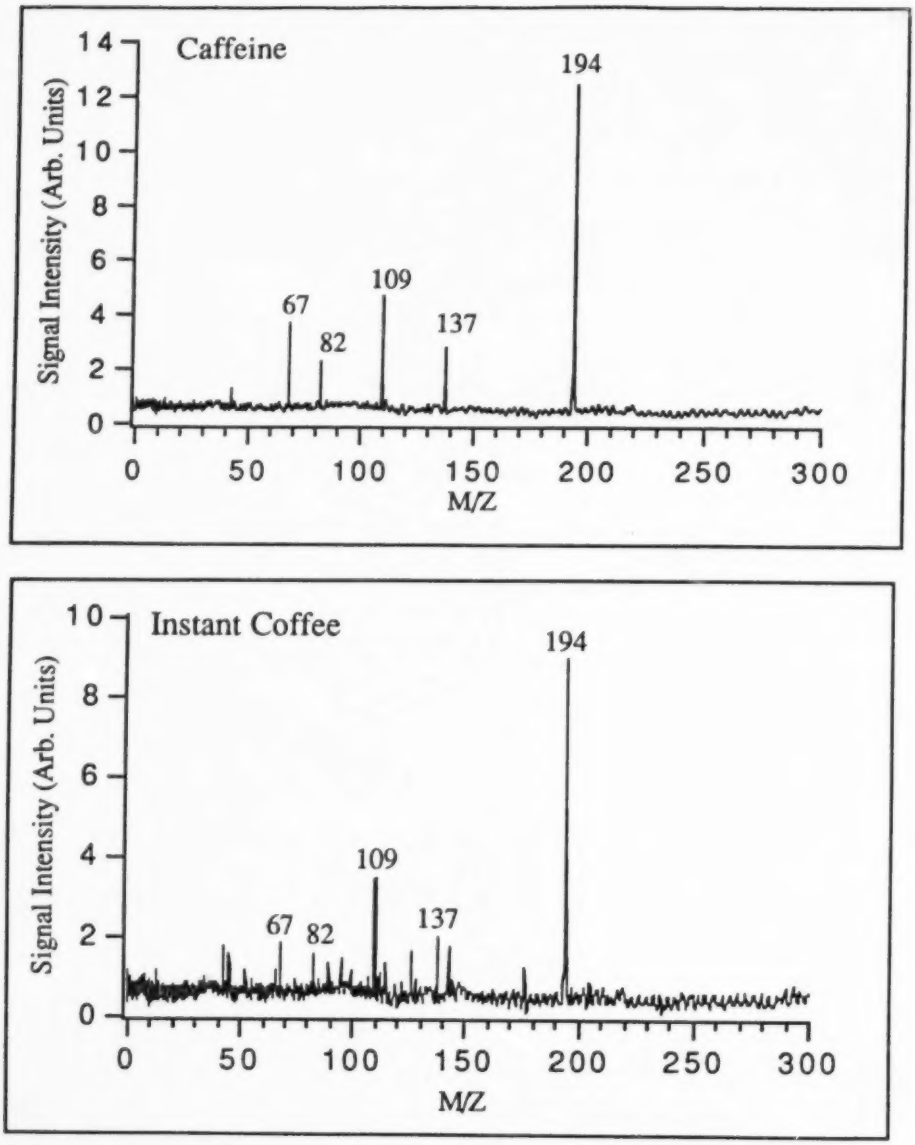

Figure 3.22. MPI mass spectra of pure caffeine, and caffeine in instant coffee.

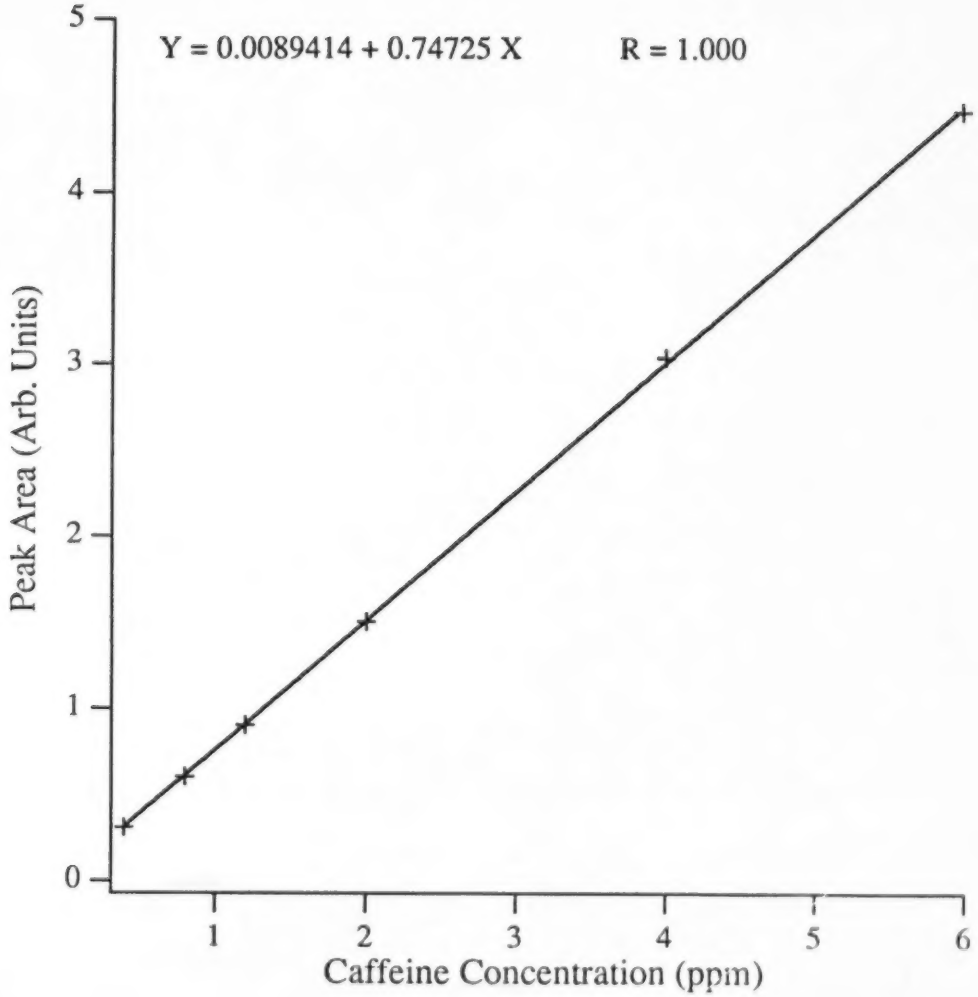

The LC/UV result: 2.31% ± 0.02%

Figure. 3.23. The calibration curve of caffeine by LC/UV.

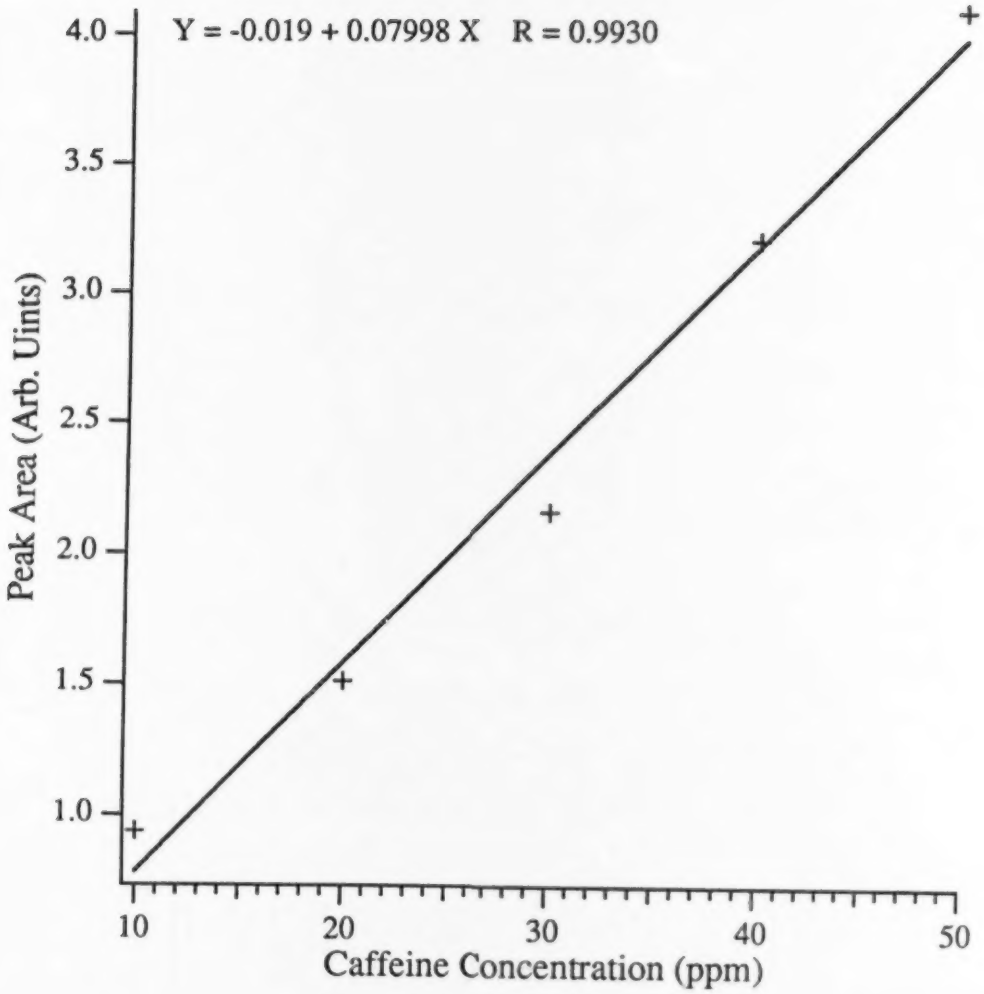

The LC/TOFMS result: 2.37% ± 0.14%

Figure. 3.24. The calibration curve of caffeine by LC/TOFMS.

Chapter 4

Conclusion and Future work

Comparing the present LC/TOFMS system with existing LC/MS techniques, we note the following strengths associated with the PSI interface. The PSI interface, in principle, provides an alternative means for interfacing LC to any type of mass spectrometer that is capable of detecting ions in a pulsed form. The PSI interface described here is simple to operate and inexpensive to construct. Unlike other interfaces, the PSI interface does not require additional pumping systems in the interfacing region. The interface also provides high sampling efficiency as illustrated above.

The PSI interface bears some resemblance to the particle beam interface [77,79] and the atmosphere-pressure spray with electron ionization (APEI) [119]. In all cases, samples are thermally vaporized, followed by ionization. In the case of the particle beam interface, a solute enrichment device is also used to reduce the solvent content prior to sample introduction into a mass spectrometer. In light of the fact that there are many different experimental parameters used, a direct comparison between these techniques is difficult. However, we note that there are reports of studies on sampling efficiency in the particle beam interface. The sampling efficiency is strongly dependent on the experimental conditions such as the solvent type and the amount of the sample injected [80,120]. Transfer efficiencies, determined by comparing the signal level obtained by using the interface with that obtained by an insertion probe, are reported to be between 2% to 15% [80, 120-122] and as high as 70% efficiency for chrysene is reported for the universal interface, a technique closely related to the particle beam interface [123]. We also note that the sampling efficiencies determined by a technique similar to that used in

our study (i.e., using a cold sample collector to condense the sample and measure the actual amount of sample transported) are reported to be less than 2% in a commercial particle beam instrument [124]. In the case of APEI, we are not aware of any reports of studies on sampling efficiency. However, in terms of detection sensitivity, it has been reported that APEI provides comparable sensitivity to that of the particle beam interface for the detection of naphthalene and anthrancene [119]. One recent report of determination of PAHs by using particle beam LC/MS with a ultrasonic nebulizer illustrated low nanogram detection limits [125]. The results obtained with our PSI interface appear to be better in detection sensitivity for the PAH molecules studied. Several factors including the sampling efficiency and the ionization efficiency (laser MPI vs. EI) may contribute to this difference. It should also be noted that the results obtained for quantitation of caffeine content in instant coffee are quite comparable to that reported by using isotope dilution particle beam LC/MS [126]. However, in the PSI interface, a linear calibration curve is obtained, which averts the necessity of using isotopically substituted compounds for quantitation.

Compared to the particle beam and APEILC/MS system, one major limitation with the present PSI LC/TOFMS system is related to the ionization technique used. While MPI can be very selective and sensitive for the ionization of certain types of molecules such as aromatic compounds, it is not universal technique for molecular ionization [1]. For future development, we plan to add an electron beam to this system for obtaining EI spectra. This will enable us to generate classical EI spectra for molecular identification and extend the applicability of the current system to a much broader range of biological and environmental chemicals. Then, a direct comparison between theses interfaces may become possible. It should be noted that the sensitivity of the PSI interface could be further increased by combining a particle beam interface or a universal interface to it. In this case, the aerosol generation tube in the PSI interface would be replaced by a solute enrichment device. This would increase the amount of solute per

pulse being introduced into the mass spectrometer. Another potential drawback of the present PSI interface is related to the use of thermal heating for sample vaporization. Due to possible thermal decomposition, the technique would have limited applicability for ionic and very polar chemicals such as sulfated azo dyes. While molecules such as small peptides and a number of thermally labile aromatic acids that are not amenable to GC/MS can be studied as illustrated above and in the previous paper [94], it appears that the present PSI interface is best suited for the detection of nonpolar compounds or polar compounds with some volatility. To increase its applicability, techniques currently being developed for sample vaporization and/or ionization [128,129], could be adapted for the PSI interface. An alternative method of enhancing its general applicability is to generate ions directly from the LC effluent, followed by pulsing the ions into the mass spectrometer. This will take full advantages of several very powerful atmospheric ionization techniques such as APCI and electrospray. These techniques have been shown to be very effective for the detection of polar and ionic species. In these techniques, ions, not the neutrals, are generated at a high pressure and subsequently introduced into a mass spectrometer. Conceptually, ions generated at a high pressure can also be mechanically pulsed into the mass spectrometer. We are currently in the process of developing a nozzle to introduce the ions generated from APCI and electrospray into a time-of-flight mass spectrometer in a pulsed form.

In summary, the pulsed sample introduction method provides an alternative means for interfacing LC with mass spectrometer. The PSI interface involving single stage pumping provides high sampling efficiency. The interface does not introduce significant peak distortion in LC/TOFMS. Further improvement in instrumentation such as the addition of an EI source and a solute enrichment device prior to sample introduction could enhance the utility of the PSI LC/TOFMS system. The present PSI system uses a heated capillary tube to generate aerosol, followed by thermal vaporization of the samples. Thus, the technique would be best suited for the analysis of nonpolar

compounds or polar compounds with some volatility. To extend the pulsed sample introduction method for the analysis of ionic and very polar compounds, we are developing a technique based on the current work to mechanically pulse the ions generated at a high pressure using APCI and electrospray into a TOFMS for detection. It is our hope that the combination of several modes of operation (i.e., MPI, EI, CI, and electrospray) in a PSI interface would enable us to analyze a wide variety of compounds from nonpolar chemicals to ionic species in LC/TOFMS.

Part II

Analytical Applicability of Laser-Induced Photoelectric Effects in Teflon Membrane

Chapter 5

Introduction

The development of highly sensitive, selective, and widely applicable analytical methods is one of the most important goals in analytical chemistry. With the advent of powerful lasers, new detection systems in solutions based on laser-induced effects have provided a quantum leap for trace analysis in terms of sensitivity and sensitivity [129, 130]. These detection systems include laser-induced fluorescence spectrometry [131, 132], laser adsorption spectrophotometry such as photoacoustic and thermal lens [133, 134] techniques, and laser photoionization spectrometry [135-137]. Of these, laser fluorescence spectrometry may be the most sensitive but can be applied only to fluorescent molecules. Other techniques also have a limited applicability [129]. For example the photoacoustic methods are not particularly sensitive for liquids. Laser photoionization detection based on the photoconductance technique can not be used in ionic solutions. In this work, we introduce a new detection system based on laser-induced photoeffects in bilayer membranes. We hope this technique will be complementary to the existing methods in the future.

5.1. Laser Ionization in Solution

The laser multiphoton ionization (MPI) technique has been widely used in gas phase (see 1.1. Multiphoton Ionization). In the gas phase, the recombination of ion-electron pairs is insignificant and amplification of the initial charge carriers is efficient by using a proportional counter. However, in the liquid phase, solvent molecules interact not only with ground and intermediate states of the molecule but also with charged species produced by photoionization. The threshold (I_{th}) for photoionization in the

solution becomes considerably lower than the ionization potential (I_p) in the gas phase because of the solvent interaction as is given by

$$I_{th} = I_p + V_0 + P^+ \qquad (1)$$

where P^+ is the polarization energy of the positive ion and is always negative, and V_0 is the electron affinity of the solvent [140, 141]. The conductivity signal measured as a function of the excitation wavelength can be used to determine I_{th}. The one-photon ionization threshold using synchrotron radiation [140, 141] and the two-photon ionization threshold using lasers [142, 143] have recently been determined for several aromatic molecules in nonpolar solvents. The values of I_{th} are 1-2 eV lower in the former (~ 6 eV) and 2-3 eV lower in the latter (~4- ~5 eV) as compared with the corresponding values of I_p. Accordingly, UV-visible lasers with modest peak power (~MW/cm^2) can induce two-photon ionization of organic molecules. Meanwhile, the solvent interaction induces a substantial difference in the fate of charged species as compared with those in the gas phase. The recombination of ion-electron pairs occurs quickly and the apparent ionization yield will be lower than that in the gas phase.

5.2. Photo-Electric Effects

Photo-electric effects in bilayer membranes were first studied by Tien in 1968 [144]. Due to its relevance to biological processes, the study of photo-electric effects in membranes has been an active area since then [145-155]. Several reviews have been appeared in the literature [156-159].

In the study of photo-electric effects, a bilayer lipid membrane is used to separate an ionic solution (e.g. 1mM NaCl) into two parts (see Figure 5.1.). Molecules of interest are added into one side of the membrane. Electric charges produced by molecules absorbed on one side of membrane surface when irradiated displace either into the

adjacent aqueous solution or across the core of the membrane. This charge displacement gives rise to a photovoltage which can be detected by an electrometer. Photoelectric effects in membranes are define as transmembrane voltage or current fluctuations resulting from illumination.

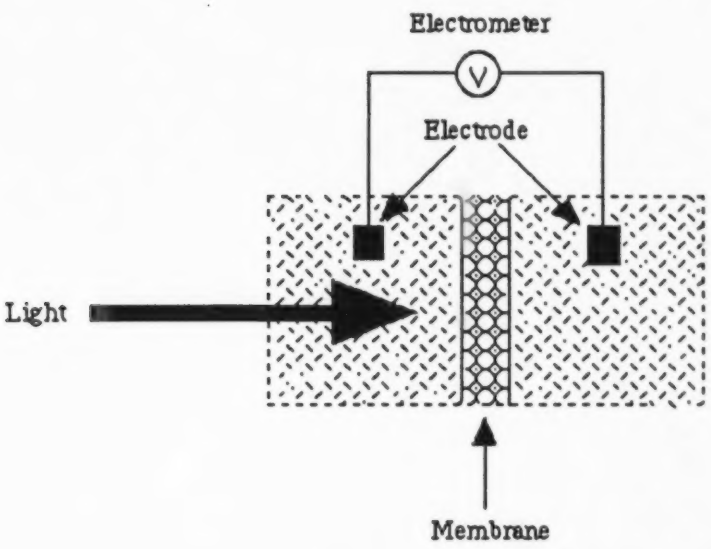

Figure 5.1. Photoelectric effects in membranes.

The simplest physical model of a bilayer membrane is a parallel plate in which the aqueous solutions form conductor plates and the lipid bilayer forms the dielectric. In the usual arrangement, the outside solution connects to electrical ground while the inside solution connects to the active (positive) electrometer input. The movement of electric charges across the capacitor dielectric results in transmembrane voltage variations, as illustrated by the following example. If positive charges leave the outside

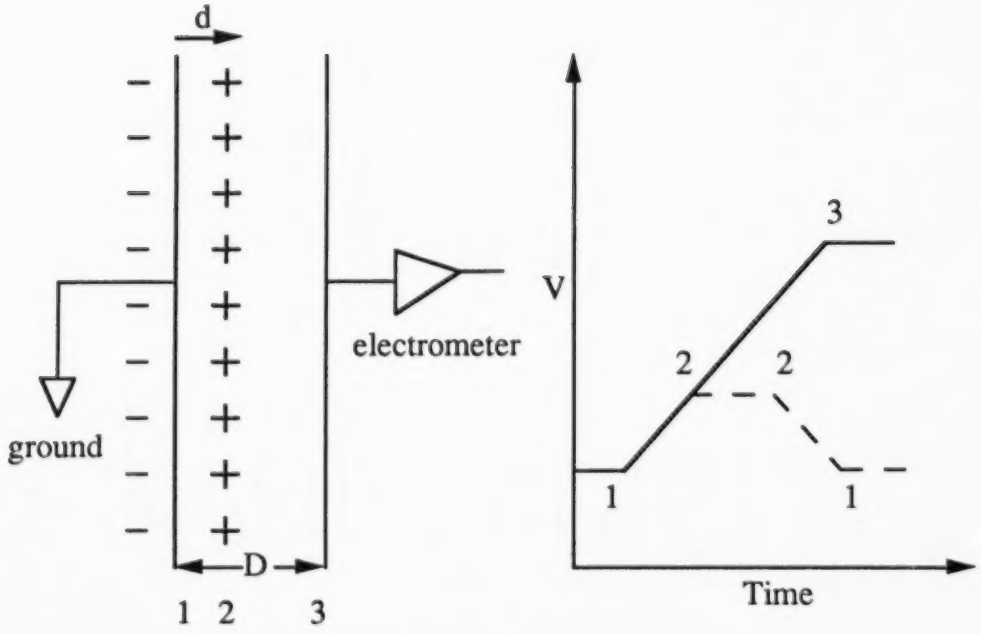

Figure 5.2. A simple parallel-plate capacitor model of a bilayer membrane, in which electric charges displaced within the dielectric alter the transmembrane voltage. These voltage variations are detected by an electrometer. The positive charge movements illustrated here, from point #1 to 2, and either on to 3 or back to 1, produce the voltage variations illustrated, which are also discussed in the text.

membrane surface (#1 in the Figure 5.2.) and move with constant velocity across the dielectric,then a linear voltage ramp will be generated, as illustrated on the right, reaching a peak voltage when the charges reach position #3. The membrane voltage is given by

$$V(t) = nqd(t)/CD \qquad (2)$$

where n is the number of charges q that have moved a distance d(t) across a membrane of capacitance C and thickness D. On the other hand, if the positive charge in Figure 5.2. stops moving at position #2, and then after a time moves back to #1, the membrane voltage will stop rising, and then fall back to zero, as illustrated by the dashed trace. It is assumed in this discussion that charge movements are initiated by flash illumination, so the resulting membrane voltage variations are referred to as photovoltages.

It is useful to think of bilayer membranes as ordered structures that tend to order absorbed chromophores in space so that charge displacements, synchronized by light flashes, may be detected. The following points summarize important details of the relation between charge displacement and the observed photovoltages [160-161] :

(1) The photovoltage amplitudes are proportional to the number of charges moving times the distance of their displacement. Since bilayer membranes are essentially two lipid molecules thick, the photovoltages are the result of charge displacements over molecular dimensions.

(2) The photovoltage waveforms closely follow the kinetics of charge displacement within the limits of the electrometer and oscilloscope slewing rates, the flash duration, and resistance-capacitance (RC) time constants.

(3) The photovoltage observed when several different mechanisms independently displace charges is the linear sum of the photovoltage resulting from each mechanism

separately.

(4) The production and/or reorientation of dipoles should also contribute to the photovoltages, although signals known to ocurr by this mechanism have not been described.

Experimentally, there are two general types of bilayer membrances that can be employed in photoelectric effects. These are the black lipid membranes (BLM) and the liposomes. The major problems with these membranes are their lack of reproducible stability over long periods of time, and the small surface area. It would obviously be of great experimental value to see if one could construct a model membrane system which would have an indefinitely long lifetime, larger surface area, and greater stability to both chemical and mechanical disturbances. In this work, we plan to use Teflon membrane which has superior stability, longer lifetime and larger surface area to conduct the photoelectric effects experiment. Note that Teflon membrane has been used previously for the measurement of photo-induced effects in solution [155, 159].

5.3. Research Goal

Extensive studies have been performed by a variety of laboratories in an effort to understand the charge transport mechanism. However, to the best of our knowledge, photoelectric effects have not previously been used for analytical purposes. Therefore we are interested in studying the analytical applicability of this technique.

The main aim of this study is to develop a technique for trace analysis of biological molecules and PAHs in ionic solution.Specially, this technique will involve a novel and convenient method for detecting charged intermediates of organic molecules based on laser induced photoelectric effects in a membrane. The technique developed here may offer several advantages. First of all, it may provide a detection method of high sensitivity. The photovoltage generated by a monochromatic light pulse is a function of

light intensity, the number of molecules absorbed in the membrane before the light pulse, and the molecular absorption cross section [134]. It is reasonable to say that the saturation of photoelectric effects is possible with a high power laser beam as the light source. Thus we may achieve high sensitivity with a high power Nd:YAG laser. Another important parameter determining the sensitivity of this technique is the quantum efficiency of the photoelectric process. It has been shown that the quantum efficiency is very high, typically above 10% [153]. This suggests that with sensitive charge detection technique, trace analysis is possible based on photoelectric effects.

Another important feature of this technique may be the high selectivity. Only molecules which absorb laser radiation and initiate a charge displacement in membranes will generate a photovoltage. This will eliminate background noise from the solvent. Selectivity can also be achieved based on the absorption cross section and ionization potential if photoelectric effects are induced by photoionization process. In addition, ionic solutions are used so that biological molecules can be directly studied without the need for sample preparation.

In this work, the experimental set-up of the photoelectric effects in Teflon membrane will be presented next. The preliminary results of our experiment will be also reported. Finally, the conclusion and future work will be given.

Chapter 6

Experimental

Figure 6.1 shows a schematic diagram of the experimental set-up used to obtain the photoelectric effects from the Teflon membrane. The main components of this apparatus include a laser light source, a membrane cell, and a photoelectric detection system.

The light source is a frequency quadrupled Nd:YAG laser (GCR-3, spectra-physics, Mountain View, CA). The laser repetition rate can be varied up to 20 Hz, but the laser is normally operated at a repetition rate of 10 Hz. The fourth harmonic (266 nm) laser beam from the pulsed laser will be used throughout the experiments.

The membrane cells used in the experiments are made of quartz. The external membrane cell has a snug fit for the inside membrane cell in which there is a 0.5 cm hole in the middle of the cell. The commercial 4.7 μm thick Teflon membrane film is used to produce the photoelectric signal across the teflon membrane. The Teflon film is type C, Chemical Fabrics Corp. (West Palm Beach, FL). The Teflon film is mounted on the 0.5 cm hole of the internal cell with Elmer's superfast Epoxy adhesive (TM the Borden Company). Before the experiments, the assembled membrane cells are rinsed with the desired aqueous electrolyte solution such as a certain concentration of NaCl solution, and then filled the external membrane cell with the same aqueous electrolyte solution. The internal membrane cell is also filled with aqueous sample solution prepared with the same concentration of the aqueous electrolyte solution in the external membrane cell.

The agar electrodes are prepared by filling the lower portion of disposable micropippet tips (Uni-Tip 250 μl, Fisher Scientific Limited) with 5% agar in 0.1 M NaCl

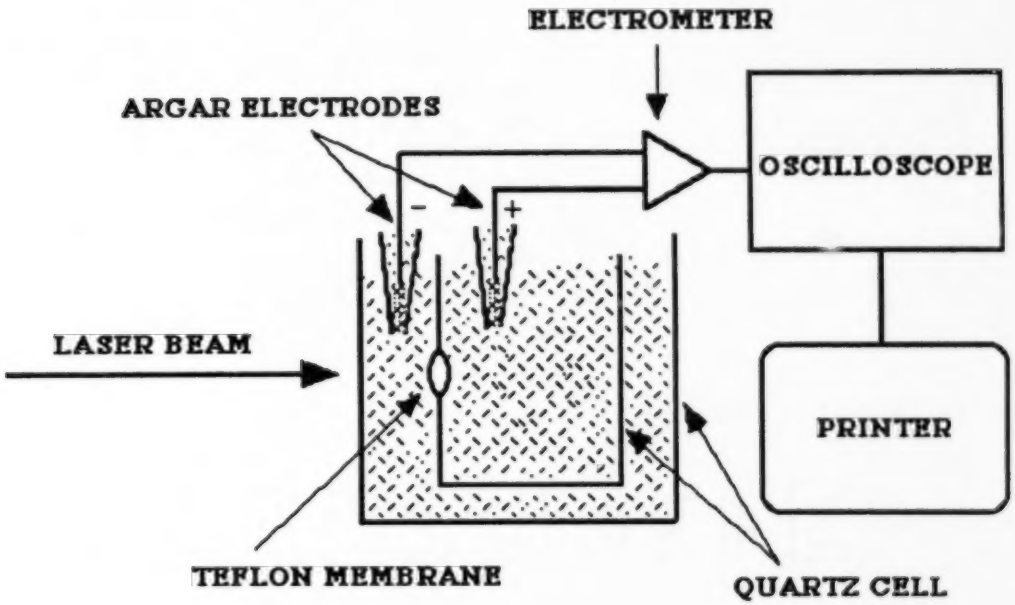

Figure 6.1. The schematic of the experimental set-up used to obtain photoelectric effects from the Teflon membrane.

solution. The lower ~ 8 mm of the micropippet tips are cut off after the agar become hardened. The electrode elements are 10 cm of silver wire, electrodeposited with AgCl, coiled and wrapped with black cotton cloth, and then packed inside the micropippet tips while wet with saturated NaCl solution.

The electrometer is positioned over the membrane cells inside a metal box. The photoelectric signal produced across the teflon membrane is recorded by a LeCroy 9400A digital oscilloscope. The photoelectric signal of a sample solution (V_s) is obtained by averaging over 100 laser pulses. The blank signal or noise trace (V_b) is measured under the same condition. The true photoelectric signal of a sample (V_c) can be obtained as $V_c = V_s - V_b$ directly from the oscilloscope. The final results are printed by HP Color Pro Graphic plotter (Hewlett-Packard Co.). The laser intensity is measured by using OPHIR laser power meter (Diamond Ophir Optica, Inc.).

The DL-tryptophan was obtained from Sigma Chemical Co. (St. Louis, MO). L-Tyrosine, 2-Naphanol, $K_4Fe(CN)_6$ and $K_3Fe(CN)_6$were obtained from Fisher Scientific Company. Sodium chloride was purchased from BDH Inc.. All sample solutions are prepared with the same concentration of NaCl solution as the reference solution in external cell.

Chapter 7

Results and Discussion

7.1 Teflon Membrane Generated Waveforms

Laser light flashes induce voltage transients across Teflon membrane with aromatic amino acids such as tryptophan (Trp) or related compounds adsorbed to one side of the membrane. Typical photovoltage waveforms obtained from the Teflon membrane with tryptophan, tyrosine are shown in Figure 7.1. In our experimental conditions, each of the chemicals produces a negative photovoltage transient with a similar waveform shape as illustrated in Figure 7.1.

Tryptophan is known to be photoionized by ~ 280 nm light in aqueous solutions [162]. The initial negative voltage excursion results from absorbed tryptophan ejecting electrons, which move toward the inside aqueous solution. The photovoltage amplitude and rise time are defined, respectively, as the maximum voltage excursion following the light flash, the time required after the flash onset for the voltage to reach 80% of the amplitude. The rise time of the negative transients induced Trp is ~ 6 μs. The negative photovoltage transients observed with Teflon membrane in the presence of Trp may be compared to those observed with lipid bilayer membranes [152] and are consistent with the primary process being photoionization of Trp [155].

7.2 Important Factors affecting the photovoltage in Teflon Membrane

Concentration Effects of NaCl Solutions In the Teflon membrane experiments, NaCl solutions are used as an reference solution and also used to prepare the sample solution. Figure 7.2 shows the photovoltage amplitude variations of 10 mM Trp in

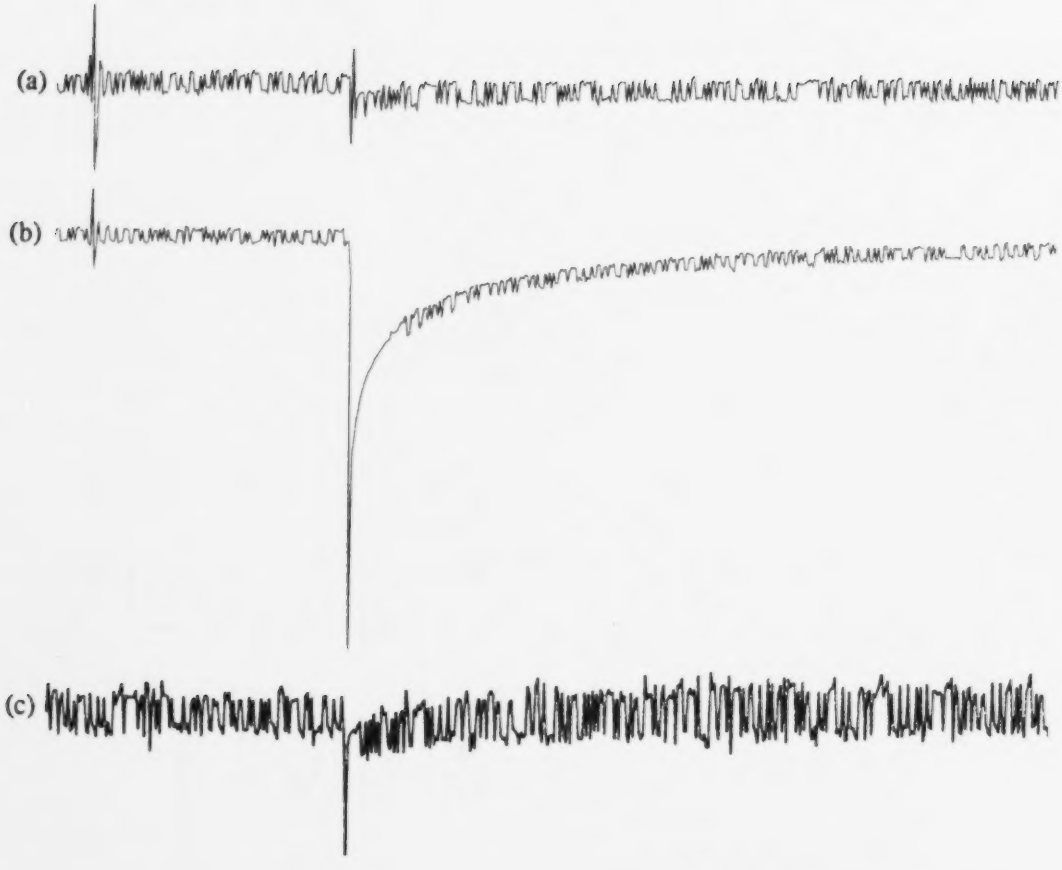

Figure 7.1. Typical photovoltage waveforms induced by Tryptophan, Tyrosine and UV light flashes on Teflon membrane. (a) 10 mM NaCl noise trace. (osilloscope was set at 1.0 mV/0.1 ms per division). (b) 10 mM tryptophan. (c) 20 mM tyrosine.

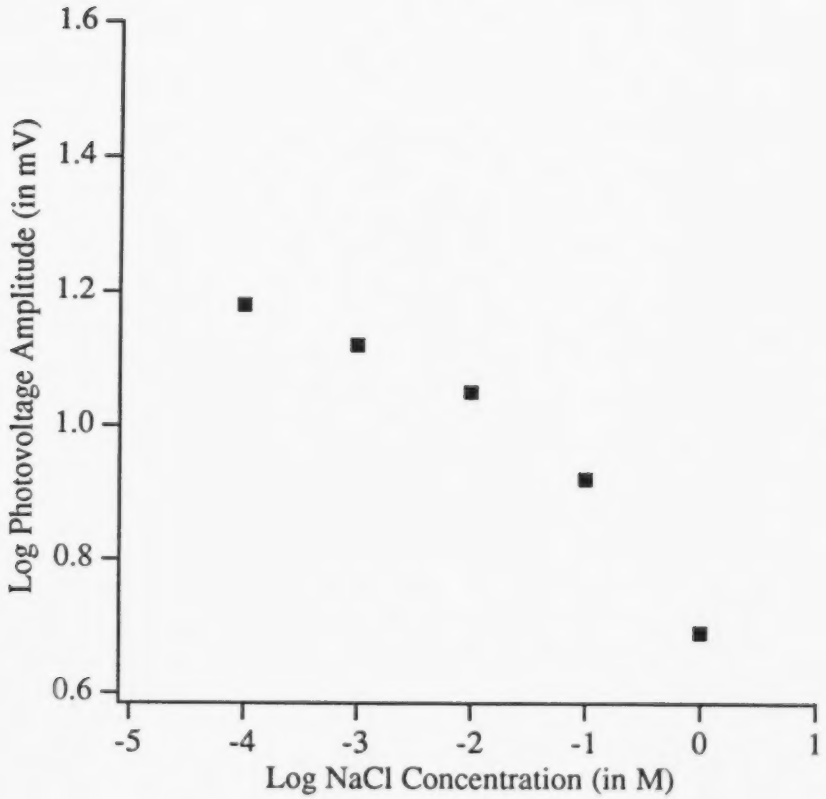

Figure 7.2. A log-log plot of the photovoltage amplitude (mV) vs salt concentration for the teflon membrane with 10 mM Trp.

different concentrations of NaCl. If the molecules absorb at the edge of the oily layer of the membrane, then the maximum value of d(t)/D (see equation (2)) will vary with the solution debye length. Assuming that the number of molecules absorbed in the membrane before the light flash does not vary with salt concentration, the photovoltage amplitude should vary with the inverse square root of the ionic strength on the tryptophan side of the membrane. The dashed line in Figure 7.2 is in approximate agreement with the data presented for > 1mM NaCl concentrations. The photovoltage amplitude is expected to fall below this line at low salt concentrations because (a) the amplitude is limited by low solution conductances for < 1 mM NaCl concentrations, and (b) the debye length variations with NaCl concentration deviate from the dashed line when the hydrogen ion concentration makes a measurable contribution to the solution ionic strength. Variations in the number of molecules absorbed in the membrane and the membrane capacitance may also make minor contributions to the variations shown in Figure 7.2.

Experiments with salt gradients show that the salt concentration on the Trp side of the membrane influences the photovoltage amplitude, while the salt concentration on the other side does not (see Figure 7.3.).

Concentration Effects of Sample Solution Variations in the photovoltage amplitude with sample concentration are illustrated in Figure 7.4. The increased photovoltage amplitude with increased tryptophan concentration in solution apparently follows as a consequence of increased Trp absorption to the Teflon membrane. As Figure 7.4 shows, a very good linearity over more than 2 orders of magnitude (Trp concentration from 0.4 mM to 40 mM) is obtained. This suggests that a chemical method can be used to measure the concentration of a sample solution that may induce the photoelectric signal across the Teflon membrane the photoelectric signal across the Teflon membrane.

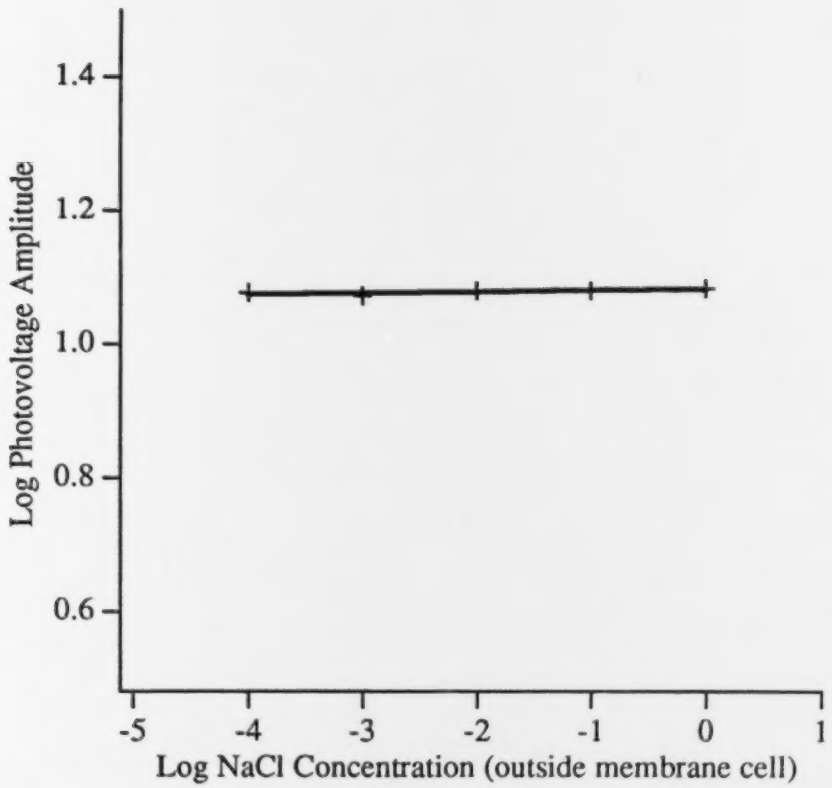

Figure 7.3. The log-log plot of photovoltage amplitude of 10 mM Trp in 0.1 mM NaCl inside cell vs the NaCl concentration outside the membrane cell.

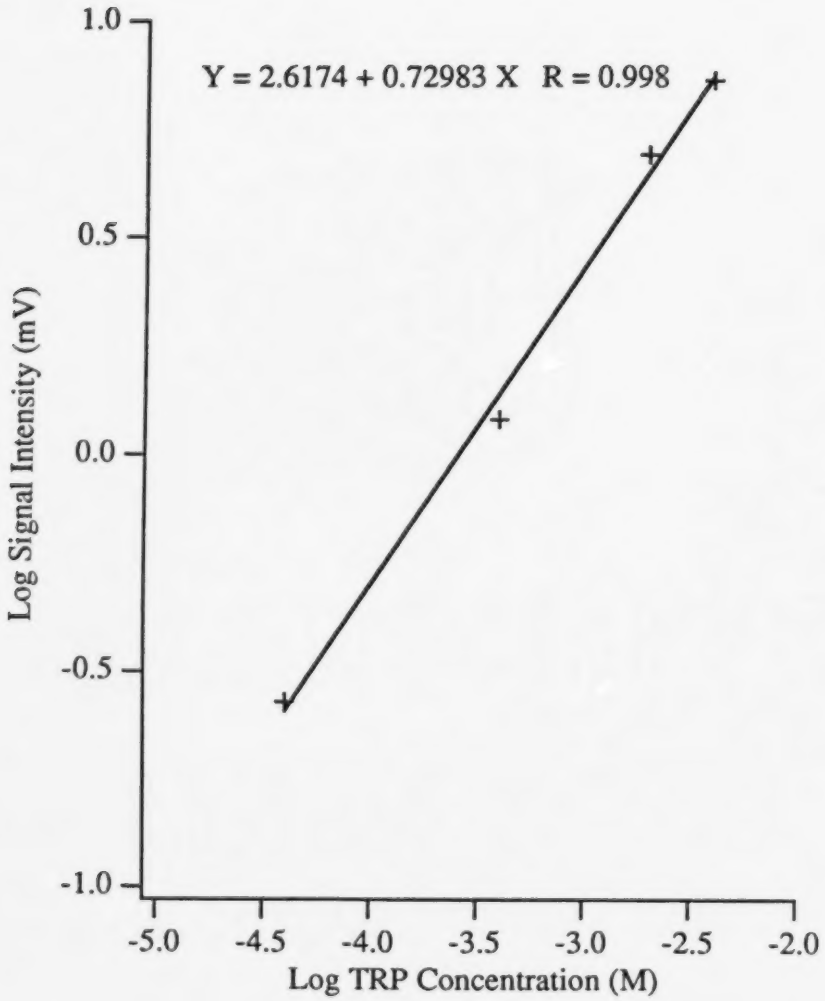

Figure 7.4. A log-log plot of the photovoltage amplitude vs Trp concentration in 10 mM NaCl.

However, the detection limit of this method is about 10 μM for tryptophan. This limit is much higher than we expect to be. Since the photovoltage amplitudes are proportional to the number of charges moving times the distance of their displacement, Tryptophan that is in the aqueous surface layer as well as any adsorbed Trp molecules would contribute to the photovoltage amplitude. It has been suggested that approximately 80% of the photovoltage amplitude occurs from the photoionization of Trp adsorbed on Teflon [155]. Clearly, under our experimental conditions, the limited number of Trp molecules adsorbed to the Teflon membrane is the main reason resulting in the low detection limit. The low ionization yield might be another reason due to the solvent interaction and the recombination of ion-electron pairs. The present system of the Teflon membrane experiment also needs to be fully optimized.

Laser Power Figure 7.5 shows the plot of the photovoltage amplitude vs the laser power for 20 μM Trp in 10 mM NaCl solution for the Teflon membrane experiment. Here the laser power unit is in mega Watts per cm^2. As shown in Figure 7.5, the photovoltage amplitude of Trp gradually increases with the laser power. However, it almost does not change at all at high laser power. Thus the phenomenon of saturation is clearly observed at high laser intensity. Similar results are also obtained for tyrosine, 2-Naphanol, $K_4Fe(CN)_6$ sample solutions. The experimental result indicates that the proper laser power should be used in the Teflon membrane experiments.

In the Teflon membrane experiments, the laser wavelength is at 266 nm. From the experimental results, we find that the photoionization of tryptophan, tyrosine and $K_4Fe(CN)_6$ in aqueous solution proceeds through a monophotonic mechanism (see Figure 7.6, Figure 7.7, and Figure 7.8). Similar results are given by other workers [162, 163].

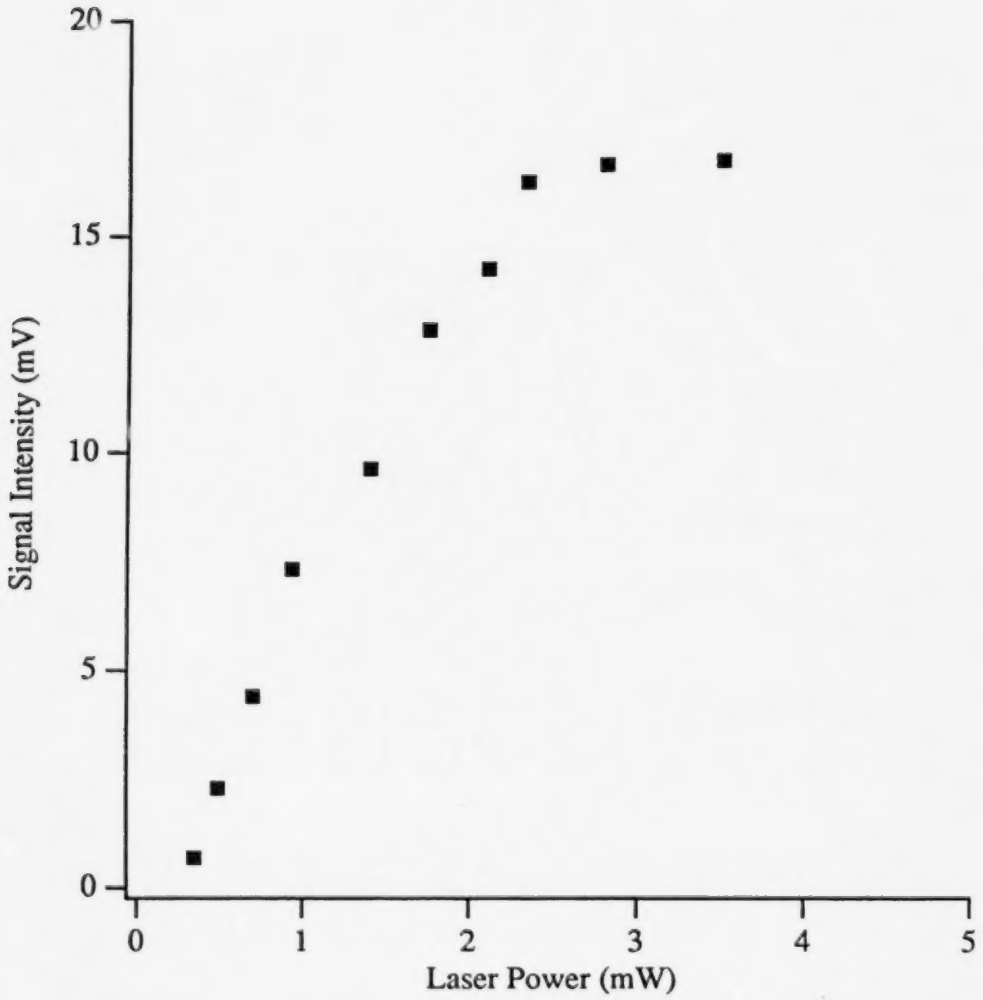

Figure 7.5. A log-log plot of the photovoltage amplitude (mV) vs laser power (mW) for 20 μM Trp in 10 mM NaCl.

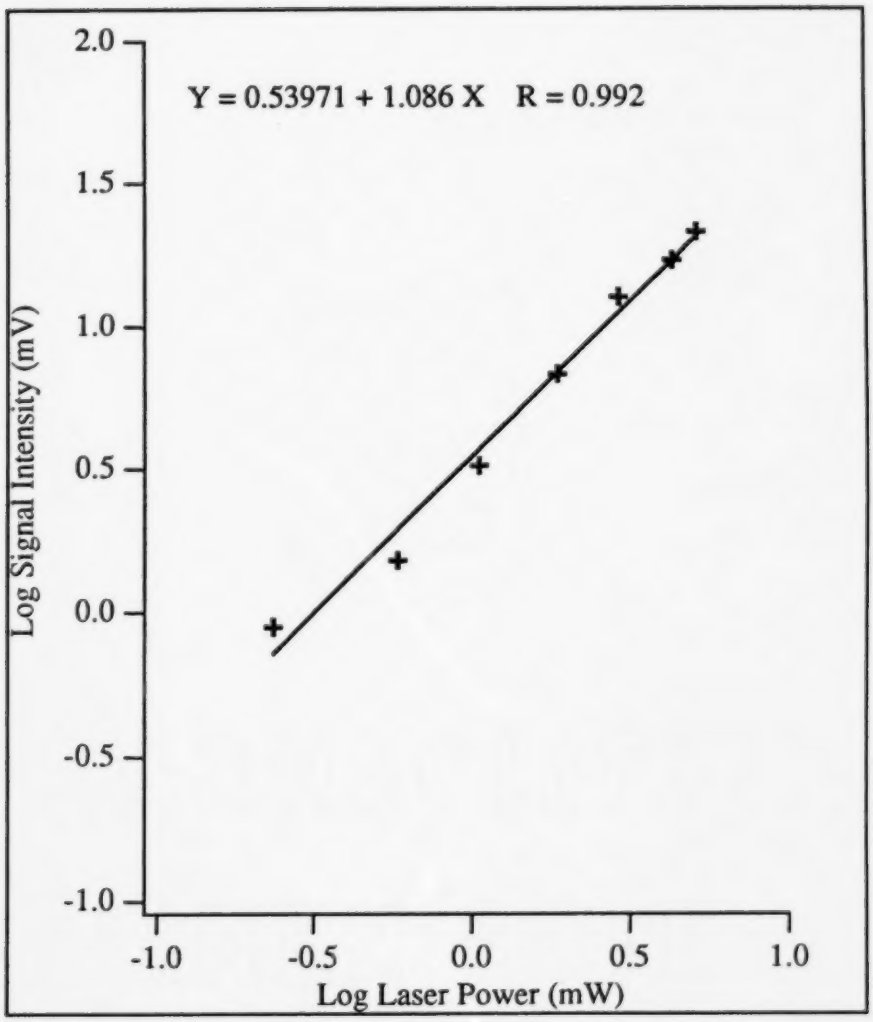

Figure 7.6. A log-log plot of the signal intensity vs the laser intensity (mW) for 20 mM Trp in 10 mM NaCl solution.

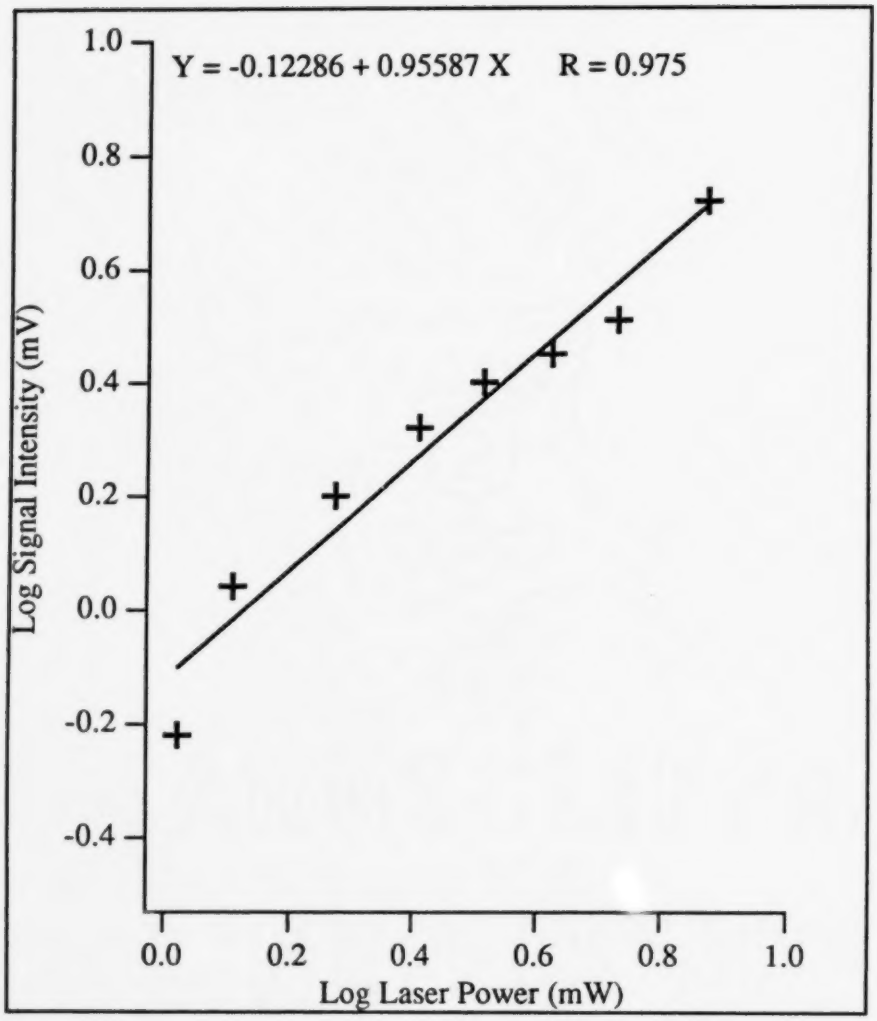

Figure 7.7. A log-log plot of the signal intensity vs the laser intensity (mW) for saturated tyrosine in 10 mM NaCl solution.

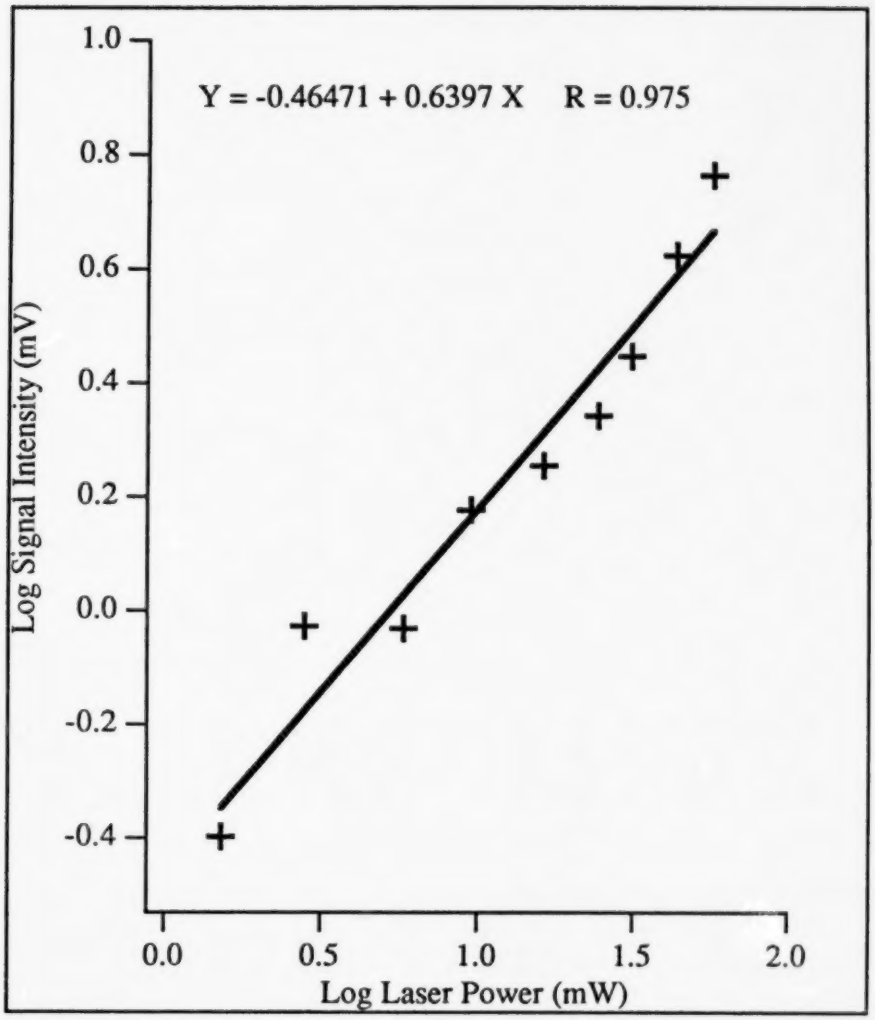

Figure 7.8. A log-log plot of the signal intensity vs the laser intensity (mW) for 0.1 M $K_4Fe(CN)_6$ in 10 mM NaCl solution.

Chapter 8

Conclusion and Future work

In our preliminary membrane experiments, we have shown that photoelectric effects in membrane can be used for analytical purpose. It is found that UV light flashes induce voltage transients across Teflon membrane by ionizing absorbed molecules such as aromatic amino acids. The photovoltage waveforms obtained from the Teflon membrane have very similar shape for the chemicals we studied. With Trp, the photovoltage amplitude varies with the aqueous solution debye length on the chromophore side of the membrane, while the salt concentration on the other side of the membrane does not. It is found that a very good logarithmic linearity can be obtained over a two orders of the magnitude analytical range for Trp. In our laser power and intensity dependence experiments, we found that high laser power can result in the saturation for the photoelectric process. The photoionization of tryptophon, tyrosine and $K_4Fe(CN)_6$ in aqueous solution proceeds through a monophotonic mechanism.

Although Teflon membrane has superior stability, longer life-times, and large areas, the high detection limit (10 μM for Trp) is the major drawback for this technique. The future improvement of this technique will involve three stages. In the first stage, the sensitivity of our current system will be fully addressed. They will include (1) the use of chemically modified Teflon membrane to increase its adsorbed ability, (2) the studies of photoelectric effects in other membranes, (3) the use of faster electrometer with higher resolution.

In the second stage, we will investigate the factors related to the optimization of the detection process for photoelectric effects. Some of the important factors are laser wavelength, laser pulse repetition, and matrix effects.

In the third stage, we will apply the technique to a variety of chemicals, such as PAHs, dyes, catecholamines, and drugs. In the future, this technique could be used as a detector for HPLC analysis.

Bibliography

1. D.M. Lubman and L.Li, In Lasrs and Mass Spectrometry; D.M. Lubman, Ed; Oxford: New York, 1990, Chapter 16, pp 353-382 (and references cited therein).
2. G. Klimack and J.E. Wessel, Anal. Chem., 52 (1980) 1233.
3. G. Rhodes, R.B. Opsal, J.T. Meek, J.P. Reilly, Anal. Chem., 55 (1983) 280.
4. R.L.M. Dobson, A.P. D'Silva, S.J. Weeks, V.A. Fassel, Anal. Chem., 58 (1986) 2196.
5. N. Winogrard, J.P. Baxter and F.M. Kimock, Chem. Phys. Lett., 88 (1982) 581.
6. C.H. Becker and K.T. Gillen, Anal. Chem., 56 (1984) 1671.
7. R. Tembreull and D.M. Lubman, Anal. Chem., 58 (1986) 1299.
8. F. Engelke, J.H. Hahn, W. Henke and R.N. Zare, Anal. Chem., 59 (1987) 909.
9. J. Grotemeyer, U.Boesl, K. Walter, E.W. Schlag, Org. Mass Spectrom., 21(1986) 595.
10. M.P. Irion, W.D. Bowers, R.L. Hunter, F.S. Rowland and R.T. Mclver, Jr., Chem. Phys. Lett., 93 (1982) 375.
11. T.J. Carlin and B.S. Frieser, Anal. Chem., 55 (1983) 571.
12. T.M. Sack, E.A. McCrery and M.L. Gross, Anal. Chem., 57 (1985) 1290.
13. G.H. Kuo, C.G. Beggs, P.R. Kemper, M.T. Bowers, D.J. Leahy and R.N. Zare, Chem. Phys. Lett., 163 (1989) 291.
14. J.A. Zimmerman, C.H. Watson and J.R. Eyler, Anal. Chem., 63 (1991) 361.
15. D. S. Nagra, J.Y. Zhang and L.Li, Anal. Chem., 63 (1991) 2188.
16. L. Li, A.M. Hogg, A.P.L. Wang, J.Y. Zhang, D.S. Nagra, Anal. Chem., 63 (1991) 974.
17. R. Tembreull, D.M. Lubman, Anal. Chem., 59 (1987) 1003.
18. R. Tembreull, D.M. Lubman, Anal. Chem., 59 (1987) 1082.

19. R. Tembreull, D.M. Lubman, Appl. Spectros., 41 (1987) 431.

20. J.H. Hahn, R. Zenoba, R.N. Zare, J. Am. Chem. Soc., 109 (1987) 2842.

21. J. Grotemeyer, U.Boesl, K. Walter, E.W. Schlag, Org. Mass Spectrom., 21 (1986) 595; Org. Mass Spectrom., 23 (1988) 388.

22. J.W. Hager, S.C.Wallace, Anal. Chem., 60 (1988) 5.

23. D.A. Gobeli, J.J. Yang, and M.A. El-Sayed, Chem. Rev., 85 (1985) 529.

24. T.G. Dietz, M.A. Duncan, M.G. Liverman and R. E. Smalley, Chem. Phys. Lett., 70 (1980) 246; Chem. Phys. Lett., 73 (1980) 4816.

25. C.T. Rettner; J.H. Brophy, Chem. Phys., 25 (1981) 53.

26. U. Bosel, H.J. Neusser and E.W Schlag, Chem. Phys., 55 (1981) 193.

27. D.M. Lubman, M.N. Kronick, Anal. Chem., 54 (1982) 660.

28. D.M. Lubman, Anal. Chem., 59 (1986) 31A.

29. J.M. Hayes, Chem. Rev., 87 (1987) 745.

30. J. Grotemeyer and E.W. Angew. Schlag, Chem Int. Ed. Engl., 27 (1988) 447.

31. L. Zandee, R.B. Bernstein, D.A. Lichrin, J. Chem. Phys., 69 (1978) 3427.

32. L. Zandee, R.B. Bernstein, J. Chem. Phys., 70 (1979) 2574.

33. L. Zandee, R.B. Bernstein, J. Chem. Phys., 71 (1979) 1359.

34. R.B. Bernstein, J. Phys. Chem., 86 (1982) 1178.

35. D.M. Lubman, R. Naaman, and R.N. Zare, J. Chem. Phys., 72 (1980) 3034.

36. J.P. Reilly, and K.L. Kompa, J. Chem. Phys., 73 (1980) 5468.

37. R.Trembreull, C.H. Sin, P. Li, H.M. Pang, D.M. Lubman, Anal. Chem., 57 (1985) 1084.

38. G. Rhodes, R.B. Opsal, J.T. Meek, J.P. Reilly, Anal. Chem., 55 (1983) 280.

39. G.J. Fisanick, T.S. Eichelberger, B.A. Heath, M.B. Robin, J. Chem. Phys., 72 (1980) 5571.

40. D.H. Parker, R.B. Bernstein, J. Phys. Chem., 86 (1982) 60.

41. J. Silberstein, N. Ohmici, and R.D. Levine, J. Phys. Chem., 89 (1985) 5606.

42. F. Rebentrost, K.L. Kompa, and A. Ben-Shaul, Chem. Phys. Lett., 77 (1981) 394.

43. J.E. Wessel, D.E. Cooper, and C.M. Klimack, In Laser Spectrometry for Sensitive Detection, J.A. Gelbwach, Ed., Proc. Society of Photo-Optical Instrumentation Engineering: Bellingham, WA, 1981, p 286.

44. F. Rebentrost, and A. Ben-Shaul, J. Phys. Chem., 74 (1981) 3255.

45. U. Boesl, H.J. Neusser, E.W. Schlag, J. Chem. Phys., 72 (1980) 4327.

46. U. Boesl, H.J. Neusser, E.W. Schlag, Chem. Phys. Lett., 87 (1982) 1.

47. W. Dietz, U Boesl, H.J. Neusser, E.W. Schlag, S.H. Lin, Chem. Phys., 66 (1982) 105.

48. P.J. Arpino, and G. Guiochon, Anal. Chem., 51 (1979) 682A.

49. G. Guiochon, and P.J. Arpino, J. Chromatogr., 271 (1983) 13.

50. S.P. Markey, Anal. Chem., 42 (1970) 306.

51. D.E. Games, Adv. Chromatogr., 21 (1983) 1.

52. W.M.A. Niessen, and J. van der Greef, In Liquid Chromatography-Mass Spectrometry, J. Cazes (Ed.), Marcel Dekker, New York, 1992.

53. R.M. Caprioli, T. Fan, and J.S. Cottrell, Anal. Chem., 58 (1986) 2949.

54. D.E. Games, in: J.C. Giddings, E. Grushka, J. Cazes, and P.R. Brown (Ed.), Advances in Chromatography, Vol. 21, 1983, Marcel Dekker, New York, pp1-39.

55. A.L. Yergey, C.G. Edmonds, I.A.S. Lewis, and M.L. Vestal, in Liquid Chromatography/Mass Spectrometry Techniques and Applications, D. Hercules (Ed.), Plenum Press, New York, 1990.

56. C.G. Edmonds, J.A. Mccloskey, and V.A. Edmonds, Biomed. Mass Spectrom., 10 (1983) 237.

57. D.M. Desiderio, G.H. Fridland, and C.B. Stout, J. Liq. Chromatogr., 7 (1984) 31.

58. P.J. Arpino, J. Chromatogr., 323 (1985) 3.

59. B.L. Karger, and P. Vouros, J. Chromatogr., 323 (1985) 13.

60. A.P. Bruins, J. Chromatogr., 323 (1985) 99.

61. K. Vekey, D. Edwards, and L.F. Zerilli, J. Chromatogr., 488 (1989) 73.

62. K.B. Tomer, and C.E. Parker, J. Chromatogr., 492 (1989) 189.

63. T.R. Covey, E.D. Lee, A.P. Bruins, and J.D. Henion, Anal. Chem., 58 (1986) 1451A.

64. N.J. Alcock, C. Eckers, D.E. Games, M.P.L. Games, M.S. Lant, M.A. Mcdowall, M. Rossiter, R.W. Smith, S.A. Wetswood, and H. Wong, J. Chromatogr., 251 (1982) 165.

65. P.J. Arpino, Mass Spectrom. Rev., 8 (1989) 35.

66. D.S. Millington, D.A. Yorke, and P. Burns, Adv. Mass Spectrom., 8 (1980) 1819.

67. A. Melera, Adv. Mass Spectrom., 8B (1980) 1579.

68. P.J. Arpino, P. Krien, S. Vajta, and G. Devant, J. Chromatogr., 203 (1981) 117.

69. J.S.M. de Wit, C.E. Parker, K.B. Tomer, and J.W. Jorgenson, Anal. Chem., 59 (1987) 2400.

70. J.S.M. de Wit, K.B. Tomer, and J.W. Jorgenson, J. Chromatogr., 462 (1989) 365.

71. M.L. Vestal, G.J. Fergusson, Anal. Chem., 57 (1985) 2373.

72. C.H. Vestal, G.J. Fergusson, and M.L. Vestal, Int. J. Mass Spectrom. Ion. Proc., 70 (1986) 185.

73. P.J. Arpino, Mass Spectrom. Rev., 9 (1990) 631.

74. Y. Ito, T. Takeuchi, D. Ishii, and M. Goto, J. Chromatogr., 346 (1985) 161.

75. R.M. Caprioli, T. Fan, and J.S. Cottrell, Anal. Chem., 58 (1986) 2949.

76. P. Kokkonen, W.M.A. Niessen, U.R. Tjaden, and J. van der Greef, J. Chromatogr., 474 (1989) 59.

77. R.C. Willoughby, and R.F. Browner, Anal. Chem., 56 (1984) 2626.

78. L. Baczynskyj, J. Chromatogr., 562 (1991) 13.

79. P.C. Winkler, D.B. Perkins, W.K. Williams, and R.F. Browner, Anal. Chem., 60 (1988) 489.

80. T.A. Bellar, T.D. Behymer, W.L. Budde, J. Am. Soc. Mass Spectrom., 1 (1990) 92.

81. J.V. Iribarne, P.J. Dziedzic, and B.A. Thomson, Int. J. Mass Spectrom. Ion Phys., 50 (1983) 331.

82. R.D. Smith, J.A. Olivares, N.T. Nguyen, and H.R. Udseth, Anal. Chem., 60 (1988) 436.

83. R.D. Smith, C.J. Barinaga, and H.R. Udseth, Anal. Chem., 60 (1988) 1948.

84. J.B. Fenn, M. Mann, C.K. Meng, S.F. Wong, and C.M. Whitehouse, Mass Spectrom. Rev., 9 (1990) 37.

85. R.D. Smith, J.A. Loo, C.G. Edmonds, C.J. Barinaga, and H.R. Udseth, Anal. Chem., 62 (1990) 882.

86. M. Mann, Org. Mass Spectrom., 25 (1990) 575.

87. J. Allison, J.F. Holland, C.G. Enke, J.T. Watson, Anal. Instrum., 16 (1987) 207.

88. V.L. Tal'roze, V.E. Skurat, I.G. Gorodetskii, and N.B. Zolotai, Russ. J. Phys. Chem. 46 (1972) 456.

89. P.J. Arpino, Fresenius J. Anal. Chem., 337 (1990) 667.

90. W.M.A. Niessen, U.R. Tjaden, and J. van der Greef, J. Chromatogr., 554 (1991) 3.

91. M. Karas, and U. Bahr, Trends Anal. Chem., 9 (1990) 321.

92. K. Walter, U. Boesl, and E.W. Schlag, Int. J. Mass Spectrom. Ion. Proc., 71 (1986) 309.

93. M. Yang, and J.P. Reilly, Anal. Instrum., 16 (1987) 133.

94. A.P.L. Wang, and L. Li, Anal. Chem., 64 (1992) 769.

95. L. Li, and D.M. Lubman, Rev. Sci. Instrum., 60 (1989) 499.

96. C.H. Sin, H.M. Pang, and D.M. Lubman, Anal. Instrum., 17 (1988) 87.

97. D.S. Nagra, J.Y. Zhang, and L. Li, Anal. Chem., 63 (1991) 2188.

98. J.Y. Zhang, D.S Nagra, A.P.L. Wang, and L. Li, Int. J. Mass Spectrom. Ion. Proc., 110 (1991) 103.

99. R.J. Beuhler, E. Flanigan, L.J. Greene, and L. Friedman, Biochem. Biophys. Res. Commun., 46 (1972) 1082.

100. A.P.L. Wang, and L. Li, Appl. Spectrosc., 45 (1990) 969.

101. D.M. Lubman, and R.M. Jordan, Rev. Sci. Instrum., 56 (1985) 373.

102. A.P.L. Wang, X.J. Guo, and L. Li, manuscript in preparation.

103. D.S. Nagra, J.Y. Zhang, and L. Li, manuscript in preparation.

104. B.J. Chien, S.M. Michael, and D.M. Lubman, Anal. Chem., 65 (1993) 1916.

105. D.H. Levy, L. Wharton, and R.E. Smalley, In Chemical and Biochemical Applications of Lasers, C.B. Moore (Ed.), Academic: 1977, New York., Vol II, p1-41.

106. L.S. Bartell, J. Phys. Chem., 94 (1990) 5102.

107. H.M. Pang, and D.M. Lubman, Rev. Sci. Instrum., 59 (1988) 2460.

108. E. Groshka, Anal. Chem., 44 (1972) 1733.

109. J.P. Foley, J. Chromatogr., 22 (1984) 40.

110. C.R. Blakley, M.L. Vestal, Anal. Chem., 55 (1983) 750.

111. K. Stachowiak, C. Wilder, M.L. Vestal, D.F. Dyckes, J. Am. Chem. Soc., 110 (1988) 1758.

112. R. Voyksner, T. Pack, C. Smith, H. Swaisgood, D. Chen, in Liquid Chromatography/Mass Spectrometry, Applications in Agricultural, Pharmaceutical, and Environmental Chemistry; M.A. Brown, Ed.; American Chemical Society: 1990, Washington, DC.; Chapter 2, pp14-39.

113. P. Levi, Analusis 1988, 16, XLVII-L.

114. R.C. Beavis, J. Linder, J. Grotemeyer, E.W. Schlag, Chem. Phys. Lett., 146 (1988) 310.

115. L. Li, D.M. Lubman, Rapid Commun. Mass Spectrom., 3 (1989) 12 and Appl. Spectrosc., 43 (1989) 543.

116. D.S. Nagra, J.Y. Zhang, A.P.L. Wang, L. Li, "Multiphoton Ionization Study of Water and Ammonia Elimination from Dipeptides with Pulsed Rapid Heating and Laser Desorption for Sample Vaporization", Int. J. Mass Spectrom. Ion Processes, submitted for publication.

117. L. Li, A.M. Hogg, A.P.L. Wang, J.Y. Zhang, D.S. Nagra, Anal. Chem., 63 (1991) 974.

118. R.A. Hites, in V.-D. Tuan (Ed.), Chemical Analysis of Polycyclic Aromatic Compounds, Wiley, New York, 1989, Chapter 8, pp219-261.

119. M. Sakairi, A.L. Rap., Comm. Mass Spectrom., 5 (1990) 354.

120. J.S. Ho, T.D. Behymer, W.L. Budde, T.A. Bellar, J. Am. Soc. Mass Spectrom., 3 (1992) 662.

121. K.R. Edman, J.D. Kirk, R.F. Browner, in Processings of the 37th ASMS Conference on Mass Spectrometry and allied Topics, Miami Beach, FL., May 21-26, 1989, p130.

122. Jr.W.V. Ligon, S.B. Dorn, Anal. Chem., 62 (1990) 2573.

123. M.L. Vestal, in Liquid Chromatography/Mass Spectrometry, Applications in Agricultural, Pharmaceutical, and Environmental Chemistry; M.A. Brown, Ed.; American Chemical Society: 1990, Washington, DC.

124. A.P. Tinke, R.A.M. Van der Hoeven, W.M.A. Niessen, U.R. Tjaden, J. Van der Greef, J. Chromatogr., 554 (1991) 119.

125. R.P. Singh, I.D. Brindle, T.R.B. Jones, J.M. Miller, M. Chiba, J. Am. Soc. Mass Spectroc., 4 (1993) 898.

126. D.R. Doerge, M.W. Burger, S. Bajic, Anal. Chem., 64 (1992) 1212.

127. J.D. Kirk, R.F. Browner, Biomed. Environ. Mass Spectrom., 18 (1989) 355.

128. (a) V. Lanyon, A.B. Schilling, in Processings of the 41st ASMS conference on Mass Spectrometry and allied Topics, San Francisco, CA, May 30-June 4, 1993.; p214. (b) J.C. Richardson, R.F. Browner, ibid, p663. (c). A.P. Tinke, R.A.M. Van der Hoeven, W.M.A. Niessen, U.R. Tjaden, J. Van der Greef, ibid, p761.

129. T.D. Harris, Anal. Chem., 54 (1982) 741A.

130. E.S. Yeung, LC&GC, 7 (1989) 118.

131. G.J. Diebold, R.N. Zare, Science 196 (1977) 1439.

132. N.J. Dovichi, Trends in Anal. Chem., 3 (1984) 55.

133. A. Rosencwaig, "Photoacoustics and Photoacoustic Spectroscopy"; Wiley; New York, 1980.

134. N.J. Dovichi, CRC Crit. Rev. Anal. Chem., 17 (1987) 357.

135. E. Voigtman, J.D. Winefordner, Anal. Chem., 54 (1982) 1834.

136. S. Yamada, A. Hino, K, Kano, T. Ogawa, Anal. Chem., 55 (1983) 1914.

137. S. Yamada, Anal. Chem., 61 (1989) 612.

138. R.A. Holroyd, J.M. Preses and N. Zevos, J. Chem. Phys., 79 (1983) 483.

139. R.A. Holroyd, J.M. Preses, E.H. Bottcher and W.F. Schmidt, J. Phys. Chem., 88 (1984) 744.

140. K. Siomos and L.G. Christophorou, Chem. Phys. Lett., 72 (1980) 43.

141. K. Siomos, G. Kourouklis, J.D. Christophorou, Chem. Phys. Lett., 80 (1981) 504.

142. H.T. Tien, Nature, 219 (1968) 272.

143. J. Kutnik, H.T. Tien, Photochem. Photobiol., 46 (1987) 1009.

144. R.T. Arrieta, I.C. Arrieta, P.M. Pachori, A.E. Popp, J.S. Huebner, Photochem. Photobiol., 42 (1985) 1.

145. H.W. Trissl, Biophys. J. 33 (1981) 233.

146. G. Varo, L. Keszthelyi, Biochim. Biophys. Acta, 934 (1988) 247.

147. N.K. Packham, P. Mueller, P.L. Dutton, Biochim. Biophys. Acta, 933 (1988) 70.

148. J.S. Huebner, Photochem. Photobiol. 30 (1979) 233.

149. J.A. Baker, J.R. Duchek, R.L. Hooper, R.J. Koftan, and J.S. Huebner, Biochim. Biophys. Acta, 553 (1979) 1.

150. J.S. Huebner, R.T. Arrieta, D.B. Millar, Photochem. Photobiol., 35 (1982) 467.

151. J.S. Huebner, W.E. Varnadore Jr., Photochem. Photobiol., 35 (1982) 141.

152. J.S. Huebner, R.T. Arrieta, I.C. Arrieta, and P.M. Pachori, Photochem. Photobiol., 39 (1984) 191.

153. D.H. Tallmadge, J.S. Huebner, and R.F. Borkman, Photochem. Photobiol., 49 (1989) 381.

154. H.T. Tien, "Bilayer Lipid Membranes (BLM): Theory and Practice"; Dekker: New York, 1974.

155. D.S. Berns, Photochem. Photobiol., 24 (1976) 117.

156. H.T. Tien, Photochem. Photobiol., 24 (1976) 97.

157. J.S. Huebner, A.E. Popp, K.R. Williams, J. Chem. Educ., 65 (1988) 102.

158. J.S. Huebner, Biochim. Biophys. Acta, 406 (1979) 178.

159. J.S. Huebner, J. Membrane Biol., 39 (1978) 97.

160. L. Grossweiner, A.M. Brendzel, A. Blum, Chem. Phys., 57(1981) 147.

161. U. Lachish, A. Shafferman, and G. Stein, J. Chem. Phys., 64(1976) 4205.